JAEA-Research
2010-035

JAEA-Research

Groundwater/Porewater Hydrochemistry at Horonobe URL: Data Freeze I

- Preliminary Data Quality Evaluation for Boreholes HDB-9, 10 and 11 -

Takanori KUNIMARU, Kunio OTA
W. Russell Alexander and Hajime YAMAMOTO

Geological Isolation Research and Development Directorate

November 2010

Japan Atomic Energy Agency

日本原子力研究開発機構

本レポートは独立行政法人日本原子力研究開発機構が不定期に発行する成果報告書です。
本レポートの入手並びに著作権利用に関するお問い合わせは、下記あてにお問い合わせ下さい。
なお、本レポートの全文は日本原子力研究開発機構ホームページ（http://www.jaea.go.jp）
より発信されています。

独立行政法人日本原子力研究開発機構　研究技術情報部　研究技術情報課
〒319-1195　茨城県那珂郡東海村白方白根 2 番地 4
電話 029-282-6387, Fax 029-282-5920, E-mail:ird-support@jaea.go.jp

This report is issued irregularly by Japan Atomic Energy Agency
Inquiries about availability and/or copyright of this report should be addressed to
Intellectual Resources Section, Intellectual Resources Department,
Japan Atomic Energy Agency
2-4 Shirakata Shirane, Tokai-mura, Naka-gun, Ibaraki-ken 319-1195 Japan
Tel +81-29-282-6387, Fax +81-29-282-5920, E-mail:ird-support@jaea.go.jp

JAEA-Research 2010-035

Groundwater/Porewater Hydrochemistry at Horonobe URL: Data Freeze I - Preliminary Data Quality Evaluation for Boreholes HDB-9, 10 and 11 -

Takanori KUNIMARU[+1], Kunio OTA[+2], W. Russell Alexander[*1] and Hajime YAMAMOTO[*2]

Geological Isolation Research and Development Directorate
Japan Atomic Energy Agency
Tokai-mura, Naka-gun, Ibaraki-ken

(Received August 16, 2010)

Characterisation of the geological environment within host sedimentary formations is currently ongoing at the site of the Horonobe Underground Research Laboratory in northern Hokkaido, Japan, with the main aim of establishing and testing the relevant techniques for future repository site characterisation. One facet of this is one of the first use of rock matrix porewater data in Japan, in conjunction with the site groundwater data, as part of characterisation of the site hydrochemistry. Surface-based investigations have been largely completed and one of the remaining issues is the development of an appropriate quality assurance (QA) system which is applicable to all aspects of the site characterisation process.

A QA audit of hydrochemical datasets for boreholes HDB-9 – 11 has been carried out by the application of a formal QA analysis which is based on the methodology previously employed for groundwaters during the recent site characterisation programme in Sweden. To set this novel approach specifically for rock matrix porewater data in context, several guidelines for assigning the QA categories of the porewater data are proposed. Discussion on the quality level of both the groundwater and porewater data is presented as is a preliminary description of the site hydrochemistry. This exercise has indicated areas where additional information would be of value and further improvement of work would be required to the ongoing hydrochemical characterisation at Horonobe.

Overall, it is emphasised that an appropriate QA system, which is among the first such tools required for repository site characterisation, will save on effort by reducing errors and the requirement to re-sample and re-analysis – but this can only be guaranteed by continuously assessing if the system is truly fit-for-purpose and amending it as necessary based on the practical experience of the end-users on-site.

Keywords: Horonobe URL Project, Groundwater, Porewater, Quality Assurance, Category

---

+1 Tono Geoscientific Research Unit
+2 Research and Development Integration Unit
*1 Bedrock Geosciences
*2 Technology Center, Taisei Corporation

JAEA-Research 2010-035

幌延深地層研究計画における地下水・間隙水の地球化学的特性調査
－HDB-9，10，11 孔の地球化学データセットの品質評価－

日本原子力研究開発機構　地層処分研究開発部門

國丸　貴紀[+1]，太田　久仁雄[+2]，W. Russell Alexander[*1]，山本　肇[*2]

（2010 年 8 月 16 日受理）

幌延深地層研究計画では，北海道幌延町に分布する堆積岩を事例とした調査・評価を通じて，候補サイトの地質環境特性を体系的に調査・評価するための技術の整備を進めている。このうち地下水の地球化学的特性の評価においては，地下水とともに堆積岩から抽出した間隙水の地球化学データを用いており，このような取り組みは日本では他に例を見ないものである。これまでに地上からの調査研究（第 1 段階）は終了し，その残された課題の一つとして，候補サイトの地質環境調査の様々な段階において適用可能な品質保証システムを整備することがある。

地質環境の調査・評価における適切な品質保証システムは，候補サイトの地質環境調査において最初に必要とされる重要なツールの一つであり，それを整備し適用することによって調査・評価を効果的・効率的に実施することが可能となる。ただし，このためには整備する品質保証システムが目標に適合していることが継続的に確認されるとともに，その適用した結果に基づき継続的に改善されることが求められる。

以上のような背景を踏まえ，近年，スウェーデンのサイト特性調査において適用された地下水水質の品質保証の手法を用いて，HDB-9～11 孔の地下水および間隙水の地球化学データセットの品質評価を実施した。この際，既存の手法を間隙水に適用するために，間隙水の地球化学データの品質を評価し区分するための新たな指針を提案した。本報告書では，HDB-9～11 孔の地下水および間隙水の地球化学データの品質について論じるとともに，その結果に基づき地下水の地球化学的特性について予察的に評価した結果を示す。また，この品質評価を通じて明確になった，地下水の地球化学特性の評価において，今後，取得すべき情報や改善すべき項目などについても述べる。

核燃料サイクル工学研究所（駐在）：〒319-1194　茨城県那珂郡東海村村松 4-33
+1　東濃地科学研究ユニット
+2　研究開発統括ユニット
*1　Bedrock Geosciences
*2　大成建設株式会社　技術センター

Contents

目　次

1. Introduction

The Horonobe Underground Research Laboratory (URL) Project is a comprehensive research and development (R&D) project aimed at studying the sedimentary formations in the region of Horonobe Town in Hokkaido, northern Japan. This Horonobe URL project is one of two in Japan (the other is at Mizunami in central Japan – see Figures 1.1 and 1.2) which are run by the Japan Atomic Energy Agency (JAEA) as part of the national R&D programme for the geological disposal of high-level radioactive waste (HLW) in Japan.

The choice of a site was prescribed by several factors:

- presence of the target geological formation and groundwater conditions (geological environment factors);
- feasibility of safe construction of the URL (safety factors) as being of prime importance;
- ease of obtaining the permits required for the investigations (societal factors);
- advantages for layout and construction of the URL (geographical factors);
- aspects of site accessibility and land use planning.

Based on a stepwise selection approach, the candidate area was narrowed down and, finally, the Hokushin area of Horonobe town was selected.

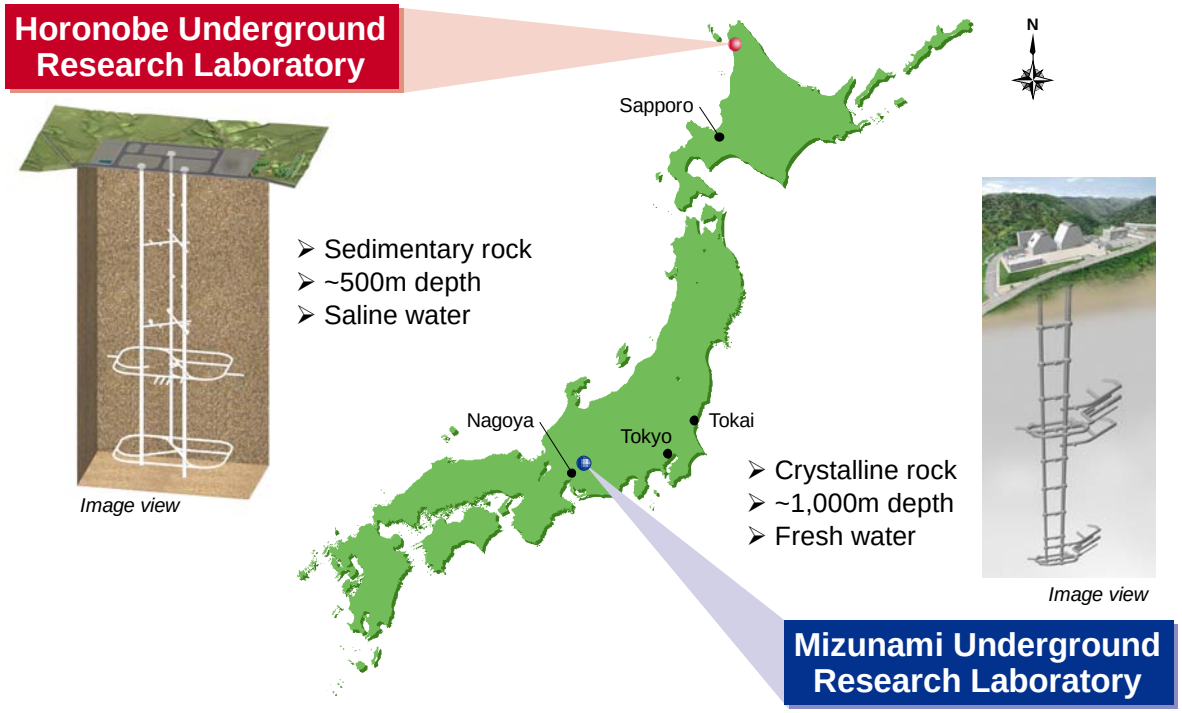

Figure 1.1: Location of both JAEA URLs in Japan[1)]

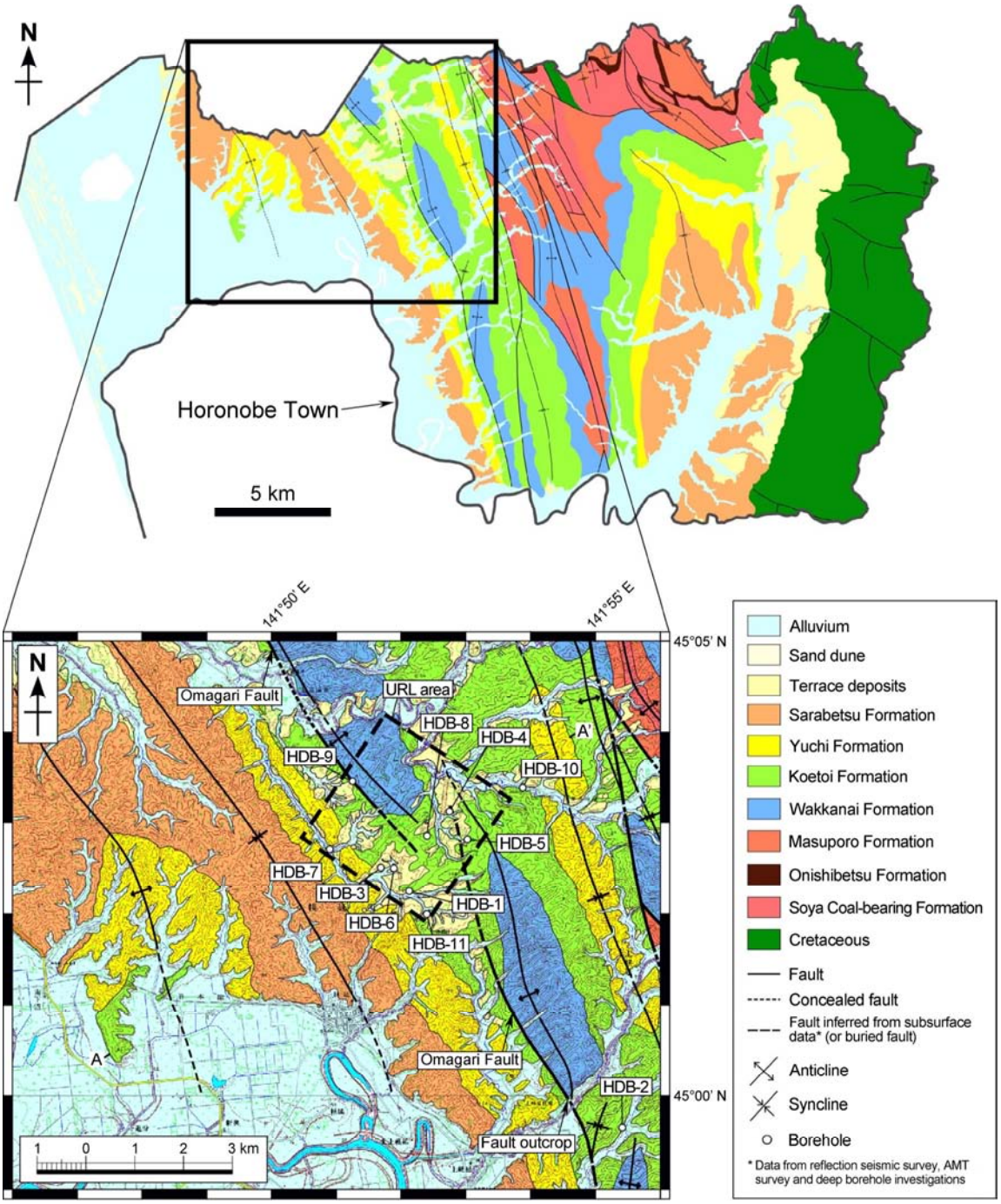

Figure 1.2: Overview of the geology of the Horonobe URL area[1)]. Line A-A' refers to the geological cross section shown in Figure 2.1

The Horonobe URL project consists of two research areas[1)]:

- Geoscientific research: *to establish the basis for technologies for characterising the deep geological environment and to develop engineering technologies for application deep underground;*
- R&D on geological disposal technology: *to confirm the applicability of geological disposal technologies in specific.*

These areas are addressed in three, partially overlapping, phases extending over around 20 years:

- Phase I: surface-based investigation;
- Phase II: construction;
- Phase III: operation.

Phase I of the Horonobe URL project began in March 2001 and is now complete and stage II is currently ongoing with two of the three shafts being driven in parallel (Figures 1.3 and 1.4). Phase III experiments, which are to be carried out in the galleries of the URL, are currently being planned.

In Phase I, surface-based techniques[2)] were used in these investigations to characterise the geological environment mainly in and around the selected URL area (Figure 1.2). A vast amount of information on the geological environment was acquired throughout the surface-based investigations involving a range of geophysical surveys, surface geological and hydrological investigations and borehole investigations. Hydrogeological and hydrochemical investigations were also carried out using data obtained from a series of deep boreholes that were drilled in and around the URL area. These data include detailed geological and geophysical borehole logs, chemical and mineralogical properties of drillcore samples, hydraulic parameters derived from fluid logging and hydraulic tests, chemical, isotopic and microbiological compositions of groundwaters and porewaters and gas compositions. Such information have been reported not only in the Phase I synthesis report[1)] but also in a wide range of papers and individual reports[3) – 10)].

Now, in Phase II, in parallel to the ongoing URL construction work (Figure 1.3), additional geoscientific research to address key issues remained in the Phase I is ongoing and this report represents part of this effort. The data examined here were collected during the drilling and testing campaign and, as such, represent the initial, low category data which are of use in building a primary conceptual model of the site. This preliminary hydrochemical dataset for boreholes HDB-9 – 11 is described in detail, but the first priority is an analysis of the data quality. This is carried out by the application of a formal quality assurance (QA) analysis which is based on the system currently being applied by SKB in their Laxemar and Forsmark site assessments[11), 12)]. This methodology has been successfully applied to the groundwaters of the Fennoscandian Shield and has been applied here to the groundwaters of the Horonobe site, boreholes HDB-9 – 11. In addition, the methodology has been extended to cover the HDB-9 – 11 porewaters, a first in any site characterisation worldwide. Finally, a preliminary QA audit of the groundwater and porewater data from boreholes HDB-1 – 8 has also been carried out as a preliminary basis for a fully formal QA of the data in Data Freeze II.

Figure 1.3: East Access Shaft (green highlighted building in the foreground) and the Ventilation Shaft (pink highlights in the background) are currently under construction

Figure 1.4: Inside the Ventilation Shaft, looking down to the shaft bottom

Finally, it should be noted that producing a quality-based dataset is, by necessity, an ongoing, dynamic process with changes occurring in the previous dataset with each new data freeze as new or modified data are reported. Thus, data currently judged to be representative, may be downgraded and/or data considered inadequate (e.g. lacking isotopes or incomplete sampling) may be upgraded. This report, Data Freeze I, is thus only the first step in the production of a fully quality assured (QAd) dataset for the Horonobe URL project.

Following a short overview of the site geology in Chapter 2, the most significant areas of data uncertainty, namely sampling, handling and analytical methods, will be examined to lay the groundwork for the detailed assessment of the dataset quality. This will be presented in Chapter 3, while in Chapter 4 the multi-level QA scheme which will be employed here is laid out and explained.

In Chapter 5, the QAd data will then be presented and described, supported by an examination of the stable isotope data for these boreholes. The main aim is to provide a statement of the quality level of the existing data and, in parallel, provide a preliminary description of the site hydrochemistry. This will allow identification of areas to prioritise in future borehole sampling and data interpretation.

Finally, in Chapter 6, the report conclusions will be presented as will recommendations for future application of the QA process to the site hydrochemistry data, both that existing from the Phase I and likely to be produced in the Phases II and III.

From the viewpoint of the site hydrochemistry, this report should be seen as a comment on the status as of the end of the preliminary, drilling programme related, data analysis. After this, higher quality samples, taken without the constraints (and contaminants) of on-going drilling operations will be available and these can be placed in the context of the existing, lower quality data. The final use of all hydrochemistry data (both existing and those produced in the future) will vary with the use foreseen for the data. For example, only samples which show no disturbance to their redox couples will be used in prime level calculations of the redox state of the groundwaters. If necessary (for example, to provide reasonable statistics), secondary level samples (i.e. those which show explicable deviations in the redox parameters) will be utilised. This will not only allow more detailed assessments of the redox state of the system (for example), but also the development of a more detailed site palaeohydrogeological conceptual model of the site.

Much weight is laid here on QA methods and approaches, but this is fully justified as this is the basis of any full repository site characterisation. As such, what is being practiced here now is exactly what will be required later in the Japanese national programme as stakeholders look towards implementing and regulatory organizations for clear indications that their confidence in them and their site characterisation programme is justified. Only then can they have full confidence in the final outcome of the characterisation work which will be ongoing in their community.

2. Site description and geological setting

The geology of the Horonobe area based on results of the Phase I is summarised in Figures 1.2 and 2.1.

Horonobe is situated on the western coastal plain of Hokkaido where Quaternary alluvium and terrace deposits (Figure 2.2) overlie Tertiary and Cretaceous sedimentary rock that were deposited in the Mesozoic Tenpoku Basin[13]. The Tenpoku Basin is an on-shore basin that is elongated in the Horonobe area along a north-south axis.

The Cretaceous sequence includes the Yezo and Hakobuchi Groups. The Upper Yezo Group consists of marine mudstones, sandstones and tuffs. The overlying Hakobuchi Group is represented by a fluviodeltaic sequence of sandstones, mudstones and thin coals. The Cretaceous rocks are unconformably overlain by a Palaeogene sequence consisting of the Haboro Formation, which is coal bearing and includes sandstones, mudstones and tuffs. It is unconformably overlain by the Magaribuchi Formation, which includes mudstones and tuffs deposited in a marine environment.

The Palaeogene rocks are unconformably overlain by the marine sequences of the Miocene Onishibetsu, Masuporo and Wakkanai Formations, the Miocene-Pliocene Koetoi Formation and the Pliocene-Pleistocene Yuchi and Sarabetsu Formations[10), 14]. The Onishibetsu Formation contains alternating mudstones and sandstones whereas the lower part of the Masuporo Formation includes sandstones and conglomerates, which are overlain by a sequence of siliceous rocks that extend continuously into the overlying Wakkanai Formation. The Koetoi Formation is a soft diatomaceous mudstone and the Yuchi Formation is a sandy mudstone containing diatomaceous material. It is currently planned that the experimental drifts of the Horonobe URL will be constructed in the Wakkanai and Koetoi Formations.

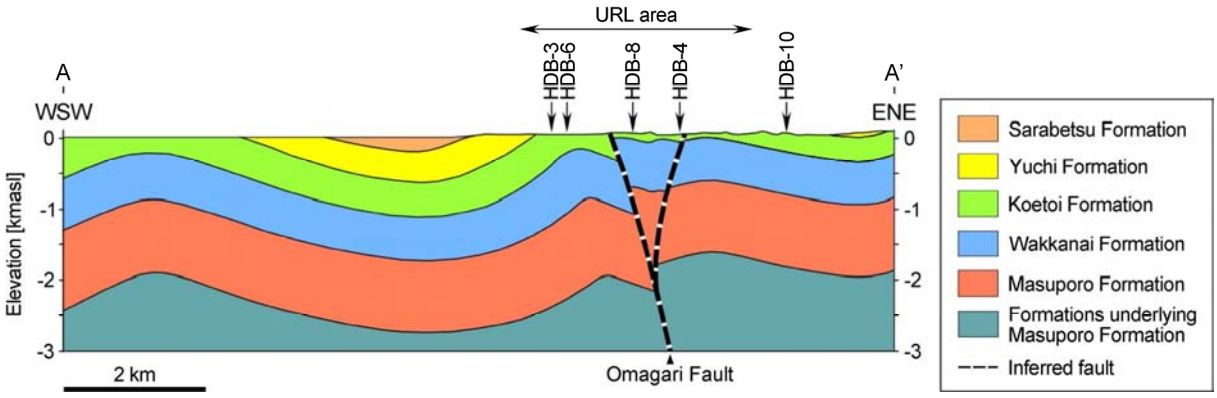

Figure 2.1: Geological cross section oriented along line A-A' in Figure 1.2[1)]

Figure 2.2: Quaternary deposits overlie the Tertiary and Cretaceous sedimentary formations, showing fossil periglacial land form, in the Horonobe area (looking approximately north from the URL)

The hydraulic conductivity of Neogene rocks in the investigation area vary considerably from about 10^{-5} – 10^{-12} ms^{-1} [1)] but it seems to decrease with increasing depth, especially in fracture zones of the Wakkanai Formation[10)]. Fracture zones in the upper part of the Wakkanai Formation have locally higher hydraulic conductivities than the background fractured rock.

2.1 Regional structural geology

Two main fracture forms can be recognised in the sedimentary stack in this area, which cut bedding at a high angle and those that are sub-parallel to bedding planes. The former appear to be important water-conducting features in the URL area[10)] and most are unmineralised or display slickenside, rock polish and fault gouge development[7)]. The most significant structure in the URL vicinity is the NW-SE trending Omagari (reverse) Fault (Figures 1.2 and 2.1). Although now quiescent, it was probably active until Early Quaternary and current activity has been displaced to the west. Subsidence of the land to the west of the URL site began in the Holocene and has resulted in the formation of extensive wetlands.

Several N – S trending en-echelon anticlinal structures are also present in the Horonobe area (Figures 1.2 and 2.1). Small oil and gas fields are present in some of these structures. Reservoir rocks are mainly sandstones in the Masuporo Formation and, to a lesser extent, those in the Miocene Wakkanai and Pliocene Koetoi Formations. Source rocks are believed to be organic-rich shales and mudstones of the deeply-buried Wakkanai and Masuporo Formations[13)]. Oil was produced in the Toyotomi oil Field (about 10 – 15 km north of the URL site) up until 1996. The nearby Toyotomi Hot Springs were discovered as a result of deep drilling during oil/gas exploration and contain strikingly high levels of dissolved organics.

2.2 Regional lithology

The Neogene formations of the Horonobe area are part of the extensive marine diatomaceous deposits of the north Pacific region[14]. Deposition of these highly siliceous sediments is thought to have been contemporaneous with formation of the Japan Sea from about 15 to 5 Ma.

The deposits can be divided generally into five lithological types[15]:

- diatomite;
- opaline porcelanite;
- opaline chert;
- quartzose porcelanite;
- black shale.

Detailed mineralogical investigations to data show that the bulk mineralogy is principally opal-A and/or opal-CT plus minor to trace amounts of quartz, albite, K-feldspar, smectite, kaolinite, undifferentiated mica (muscovite, biotite, illite, illite/smectite, etc.), pyrite, cristobalite, tridymite, chlorite, calcite and gypsum[6), 7), 16)]. The <2 μm size fraction contains substantial amounts of opaline silica phases and quartz along with smectite, illite, kaolinite and trace chlorite.

The same authors have proposed the following diagenetic alteration to the sediment pile in the vicinity of the URL:

- Early diagenetic production of pyrite framboids and spherules.
- Silica diagenesis involving the progressive dissolution of biogenic opal-A and re-precipitation of opal-CT with increasing burial depth and time with the upper part of the Wakkanai Formation representing the transition zone. Minor replacement of opal-CT by fine-grained quartz is also observed in deeper sections. Dissolution of biogenic silica results in an increase in secondary (mouldic) porosity, but re-precipitation of opal-CT and the effects of compaction result in a net porosity loss (the porosity of the Koetoi Formation is about 60 % compared to 30 – 40 % in the underlying Wakkanai Formation). Opal-A in the Yuchi Formation generally has not been altered to opal-CT.
- Early authigenesis of magnesite and siderite as concretions and as crystals disseminated in the rock matrix. These minerals are observed mainly in the Wakkanai Formation, less abundantly in the Koetoi Formation and are absent in the Yuchi Formation.
- Later authigenesis of high-magnesian calcite cement replaces earlier magnesite-siderite cement in concretions and also replaces the silica rock matrix. Cavities formed by silica dissolution are lined by later ferroan dolomite or ankerite. High-magnesian calcite cements are observed only in the Wakkanai and Koetoi Formations.

Although not completely clear, carbonate diagenesis may predate periods of faulting in the area with fragments of carbonate concretions sometimes observed in fault breccia and gouge. Other diagenetic reactions include the presence of authigenic overgrowths on detrital feldspars and trace amounts of a sodium zeolite lining secondary porosity. Late efflorescences of gypsum and barite are almost certainly artefacts of pyrite oxidation during sampling and storage of cores[7].

2.3 Site hydrochemistry

Eleven deep boreholes (HDB-1 – 11) have been drilled for geological, hydrogeological, hydrochemical and rock mechanical investigations at Horonobe (Figure 1.2). Groundwater samples were collected from packed-off intervals of all boreholes and porewater samples were obtained by squeezing drillcore samples. Physico-chemical parameters (temperature, EC, pH and ORP) were measured at the surface during hydraulic testing. Selected groundwater samples were subjected to complete chemical, microbiological and isotopic analyses.

To date, several studies of the site hydrochemistry have been carried out and all come to similar, if slightly different, conclusions based on different samples. Although several of the authors carried out some degree of quality control on the data analysed, none was rigorous or widereaching.

2.3.1 Overview of the interpretation/analysis results to date

(1) Geochemists' Work Bench I

Base on the previous work, the following information was provided via personal communication with R. Metcalfe:

- Assuming that the overall salinity levels reported for borehole D-1 are reliable, fresh water appears to extend to a depth of over 300 m.
- Again, assuming that the D-1 data are reliable, between the base of the fresh water zone and the saline water zone, there could be a transition zone several hundred metres wide.
- Taking the data at face value, fresh and brackish water appear to extend to much greater depth (several hundred metres) in borehole D-1 than in boreholes HDB-1 – 5.
- Saline water may occur at shallower depth in HDB-3 than in HDB-4 and HDB-5.
- In borehole D-1, the first occurrence of saline water appears to coincide with the boundary between the Yuchi Formation and the Koetoi Formation.

The preliminary gas data suggest the origins of the gases dissolved in the groundwaters.

- The preliminary gas data show that the gases are very 'dry'.
- The $\delta^{13}C$ of CH_4 sampled from HDB-3, HDB-4 and HDB-5 is around -45 ‰.
- This isotopic composition is not diagnostic of either biogenic CH_4 ($\delta^{13}C$ < -60 ‰ would clearly indicate biogenic CH_4) or of thermogenic CH_4 ($\delta^{13}C$ > -40 ‰ would clearly indicate thermogenic CH_4).

- The $\delta^{13}C$ of CO_2 sampled from core collected from HDB-3 – 5 are around -15 ‰ to +3 ‰, whereas the $\delta^{13}C$ of CH_4 is -46 ‰ to -72 ‰.
- The ^{13}C fractionation between CO_2 and CH_4 is large ($\delta^{13}C_{CO_2-CH_4}$ = 75 ± 15 ‰) during the production of these gases by microbial fermentation reactions (e.g. $CH_3COOH = CH_4 + CO_2$).

The data favour at least a component of biogenic CH_4 being present and suggest that the CO_2 may have been produced during the same reactions. However, the gas could contain components from several sources, and may include a component of thermogenic CH_4. One possibility is for the low SO_4 concentrations to be explained by sulphate reduction, according to reactions such as:

$$2CH_2O + SO_4^{2-} + H^+ = HS^- + 2H_2O + 2CO_2$$

However, this process is unproven and its relationship to the CH_4 production is not known.

(2) Mineralogy, groundwater and porewater analysis

Looking at preliminary groundwater and porewater data for boreholes HDB-1 and HDB-2 (samples listed in Appendix 1), Kemp et al.[6] concluded:

- A sharply increasing saline transition zone about halfway down each borehole (ca. 430 – 710 mabh in HDB-1 and ca. 410 – 690 mabh in HDB-2) is evident.
- Both boreholes show evidence of the drilling process introducing a sulphate-rich chemical signature into the drilling fluid from either pyrite dissolution or gypsum dissolution or a combination of both.
- Silica-rich components derived from dissolution or suspension of rock material, particularly from the drilling process, are identified in both boreholes.
- Drilling fluid components have been identified in both boreholes and decreases in the relative proportion of drilling fluid down the borehole profile indicate possible regions of increased porosity in the rock where groundwater can flow into the borehole.
- A $CaCO_3$ component was found at the top of both boreholes.

(3) M3 analysis (i)

M3 is an interpretative technique that performs a cluster analysis (using multivariate principal component analysis) to identify waters of different origins[11]. The mixing ratio of these end-members is inferred to reproduce each sample's chemistry and to identify any deviations between the chemical measurements of each sample and the theoretical chemistry from the mixing calculation. Any such deviations are interpreted as resulting from interactions with the solid minerals and the spatial distribution of these reactions can also be assessed by the approach.

Using M3 mixing calculations on a limited Horonobe dataset, the groundwater chemistry could be defined by mixing (and rock-water interaction) between three principle components, namely Rain Water, Seawater and Deep Saline water end-members (Figure 2.3; M. Laaksoharju, personal communication). The rain water contribution is high in samples with less Cl than 8000 mgL^{-1}. The seawater signature is significant for the water samples within the Cl range between 8000 and 12000 mgL^{-1}. Samples with a higher Cl than 12000 mgL^{-1} have a dominating deep water signature. The sea water and deep saline mixing trends are similar, which gives support to the hypothesis that deep saline water may be connate old sea water. Mass-balance calculations with M3 indicated possible reactions associated with ion exchange (Na), dissolution of calcite and pyrite oxidation/sulphate reduction, although all of these observations could also be explained by sampling artefacts for the porewaters (see Chapter 3 for further discussion).

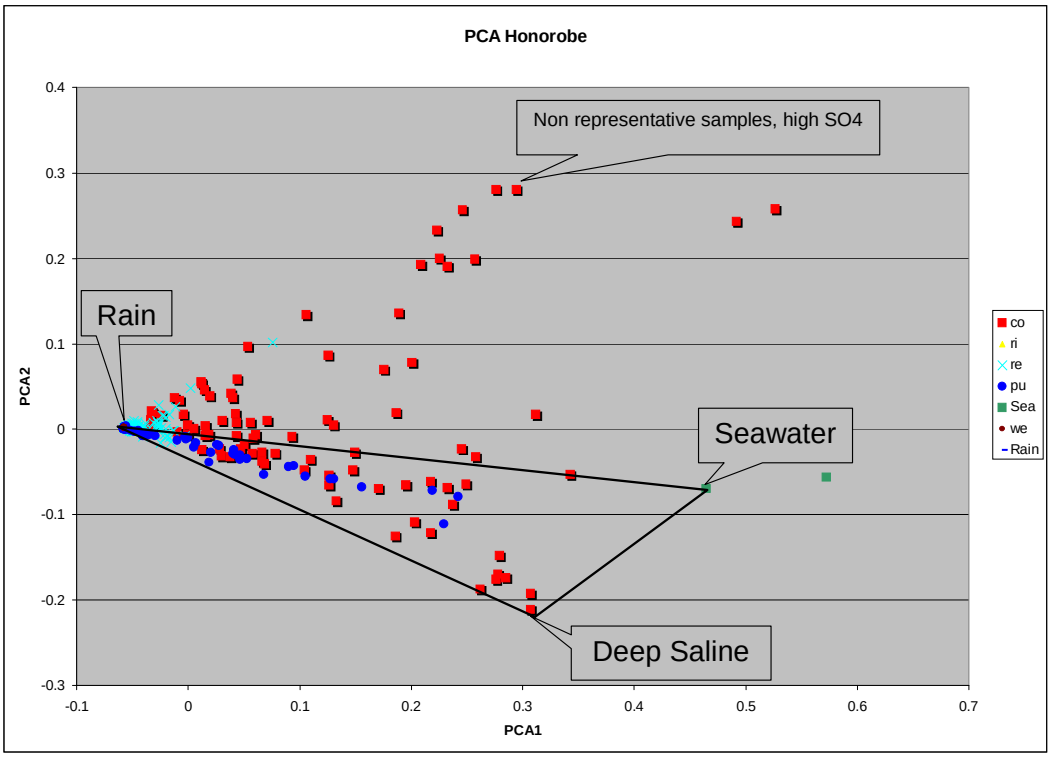

Figure 2.3: The Principal Component Analysis (PCA) plot of the limited Horonobe dataset (M. Laaksoharju, personal communication). The reference waters Rain water, Seawater and Deep Saline water have been selected from the dataset and the non-representative samples with increased SO_4 content were rejected as artefacts. A polygon was drawn between the reference waters in order to define the samples that can be described by the ideal mixing model. The equations for the first (PC1) and second (PC2) principal component describe the loadings from the different elements in the model. The first and second principal components together describe 82 % of the variability or the information of the groundwater samples. Sample key: co – pore water, ri – river water, re – return drilling fluid, pu – groundwater, sea – seawater, we – well water, rain – rain water

(4) Open-system isotope-fractionation model

An open-system isotope-fractionation model was applied to silica-phase transformations, combined with a closed-system dehydration model (after phase transformation), to interpret observed variations in Cl concentration and O and H isotopic ratios in Horonobe groundwaters and porewaters (K. Kai, personal communication). The results suggested that three types of deep end-member groundwaters are present in the Horonobe area:

- relatively shallow and saline groundwaters (maximum burial depth to about 1000 m) associated with the opal-A/opal-CT phase transition;
- intermediate, moderately saline groundwaters (burial depths between 1000 and 1900 m) associated with the opal-CT/quartz transition;
- deep, relatively dilute groundwaters (burial depths between 1900 and 4000 m), where quartz is the only silica polymorph present (lower Masuporo and Onishibetsu Formations).

(5) M3 analysis (ii)

Another examination of a very small dataset (17 groundwater samples pumped from boreholes with a chemical analysis for six major elements; Ca, Mg, Na, K, Cl and SO_4) using the M3 approach was conducted by Yamamoto et al.[9] They noted that, in this case, the major element concentrations could be explained by a simple two-component mixing of river water and deep saline water (see Figure 2.4).

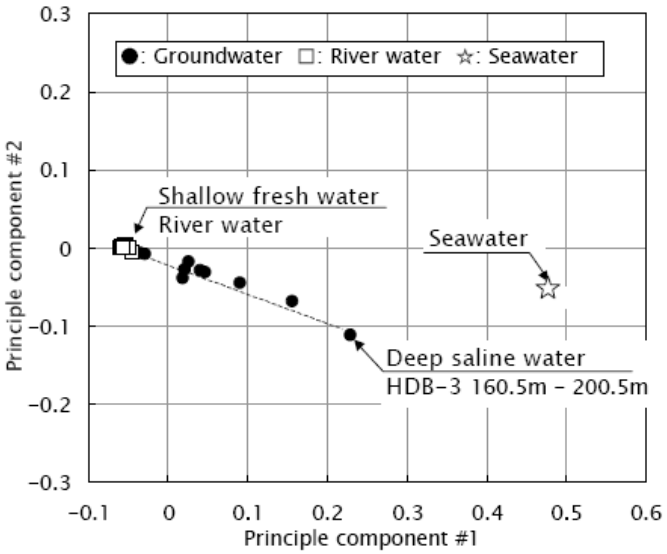

Figure 2.4: The Principal Component Analysis (PCA) plot of the extremely limited Horonobe dataset[9]

This is of interest as it implies that the third end-member is only present in the porewater. However, examination of Figure 2.3 shows that to be only partially the case, with a clear Seawater end-member influence on the groundwater samples plotted here (dark blue circles). While the trend in Figure 2.4 is certainly strong, this may be simply fortuitous due to the

choice of the Deep Saline end-member (cf. with the choice in Figure 2.3). The Deep Saline end-member was a groundwater sample from borehole HDB-7 which had one of the highest Cl concentrations (10613 mgL^{-1}; the highest had 11600 mgL^{-1}) of the dataset available for the work. This was dropped from the analysis of Yamamoto et al.[9] as it was from the shallow Yuchi Formation and it was deemed inappropriate to use this here as all other data in the calculation were from the Koetoi and Wakkanai Formations.

(6) Multivariate geostatistical techniques

Preliminary results of the Phase I hydrochemical studies indicated, in general, that two basic groundwater types were believed present in the Horonobe area (Figure 2.5):

- $NaHCO_3$-type groundwaters at shallow depths;
- NaCl-type groundwaters.

Sasamoto et al.[4] further subdivided these into 5 groundwater categories on the basis of multivariate geostatistical techniques applied to the available groundwater and porewater chemical data for boreholes HDB-1 and HDB-3 – 8 (see Figure 2.6):

- high-salinity, high SO_4-Ca-Mg type;
- moderate salinity, extremely high SO_4 and high Ca-Mg type;
- moderate salinity, low Ca-Mg type;
- high salinity, high K and moderate Ca-Mg type;
- low salinity and low deuterium, low ^{18}O type.

The first two have since been shown to be artefacts of the squeezing technique used to extract porewaters from drillcore samples[5], as this resulted in partial pyrite oxidation and reaction of the resulting acidified porewaters with other minerals in the rock.

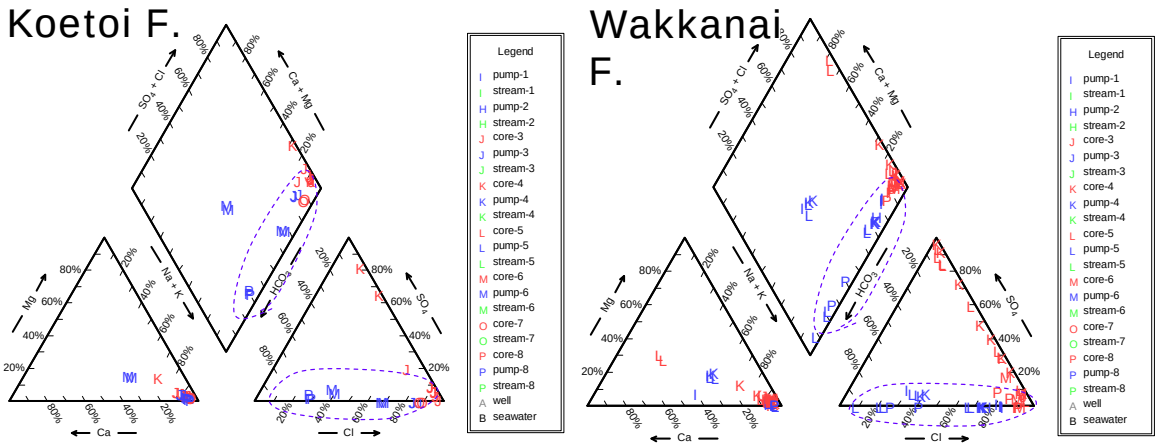

Figure 2.5: Piper plot of selected Horonobe groundwaters (M. Laaksoharju, personal communication)

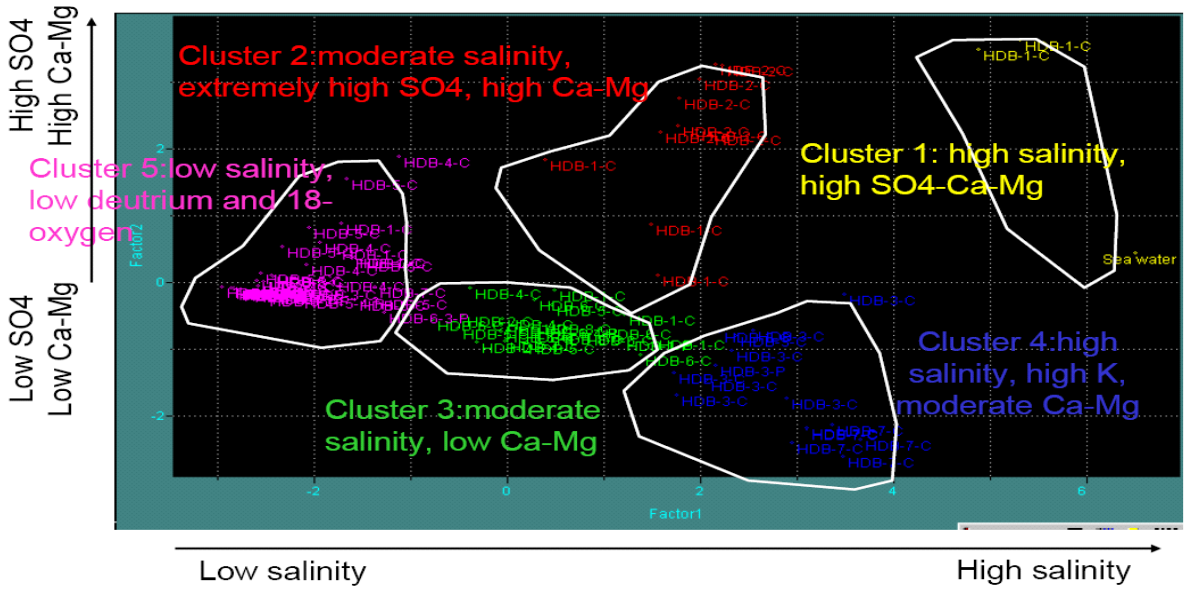

Figure 2.6: Horonobe groundwater categories defined by PCA[5)]

Sasamoto et al.[5)] summarised the interpretations to date as:

- Groundwater evolution was by dilution of seawater accompanied by diagenetic water-rock interactions.
- Multivariate geostatistical analysis indicated the presence of three groundwater types.
- Perturbations during sampling were significant for some sample types (especially porewaters).

(7) Geochemists' Work Bench II

Based on the dataset defined in Appendix 2 (and based only on groundwaters and omitting pH and Eh values from flow through cells), R. Arthur and W. Zhou (personal communication) noted that:

- Degassing will change the groundwater pH a little and the Eh potentially significantly.
- Measured SO_4^{2-}, K^+, Ca^{2+} and Mg^{2+} concentrations may have been altered during sampling.
- Silica concentrations in these groundwaters are compatible with ranges that could be produced by dissolution/re-precipitation processes driven by surface-area effects on solubility accompanying the slow transition from metastable opal-A to stable quartz. These ranges could also be produced, however, by the effects on biogenic silica solubility of adsorption/co-precipitation of Al (and possibly Fe), and formation of authigenic aluminosilicates on the surfaces of biogenic silica particles resulting from the dissolution of detrital phases.
- Silica concentrations are similar in groundwaters from the Koetoi and Wakkanai Formations, which is noteworthy because the boundary between these two formations

is a diagenetic transition zone separating rocks containing predominantly opal-A from rocks containing mostly opal-CT.

- Horonobe groundwaters appear to be at equilibrium, or to closely approach equilibrium, with respect to magnesite, calcite and siderite, which are all present as authigenic phases in the Koetoi and Wakkanai Formations.

(8) HDB-1 – 8 data interpretation

This predominantly represents a re-stating of existing studies, but some novel points are also made. The database used (for boreholes HDB-1 – 8) is shown in Hama et al.[10] The main points are:

- Groundwater salinity generally increases slowly with depth in all boreholes apart from HDB-3 where the salinity is high at relatively shallow depths.
- Groundwater and porewater chemistries at the same borehole depth are similar (also in HDB-3).
- Although not noted in Hama et al.[10], it is of interest that this does not hold completely true for the salinity profiles (see Figure 2.7), but some of the porewater scatter may reflect loss of bound water during squeezing.
- Stable isotope data in both groundwater and porewater suggest only two end-members (one close to the meteoric water line, the other enriched in $\delta^{18}O$ compared to seawater (Figure 2.7).
- It is tentatively suggested that groundwater residence times may be high (up to 1.5 Ma) or that deeper, older, groundwaters are migrating into the area (cf. Figure 2.8).

2.3.2 Comments

Although it is difficult to develop an consistent overview based on these studies – due to the different sample sets examined and different modelling approaches used, some useful points are emerging which will be of use in the preliminary assessment of the HDB-9 – 11 borehole dataset. These include the facts that:

- It seems likely that 3 end-members are involved in producing the current groundwater chemical distribution, but the end-member definition needs to be fully justified (cf. Figures 2.3 and 2.4).
- 'Deep Saline' is probably a misnomer for the disputed end-member.
- The groundwater chemistry cannot be explained simply by end-member mixing as there is strong evidence from several studies that rock-water interactions (from diagenesis through to post-compaction and post-lithification) have played a significant role.
- Sampling artefacts are a significant problem for some datasets and so will be examined with diligence here.

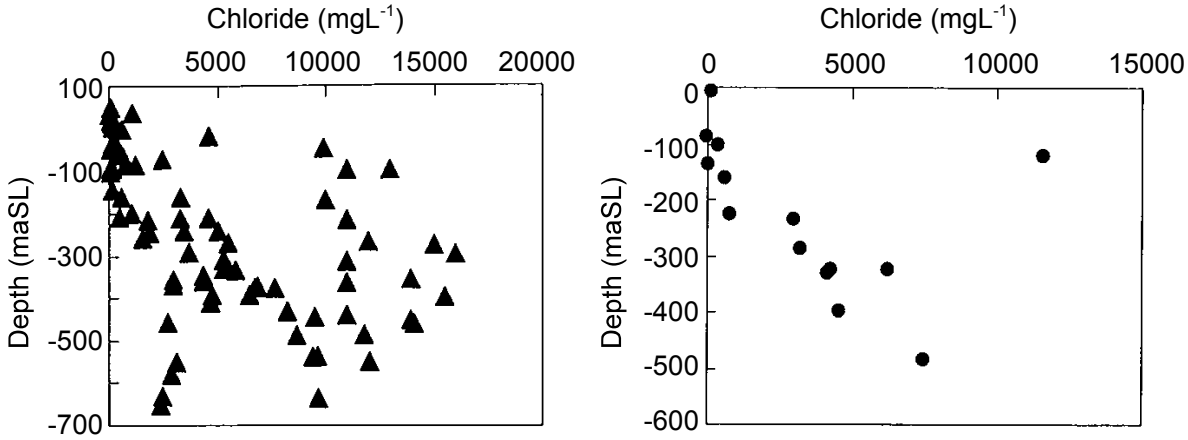

Figure 2.7: Chlorinity vs depth profiles for boreholes HDB-1 – 8. Left: porewater, right: groundwater[10)]

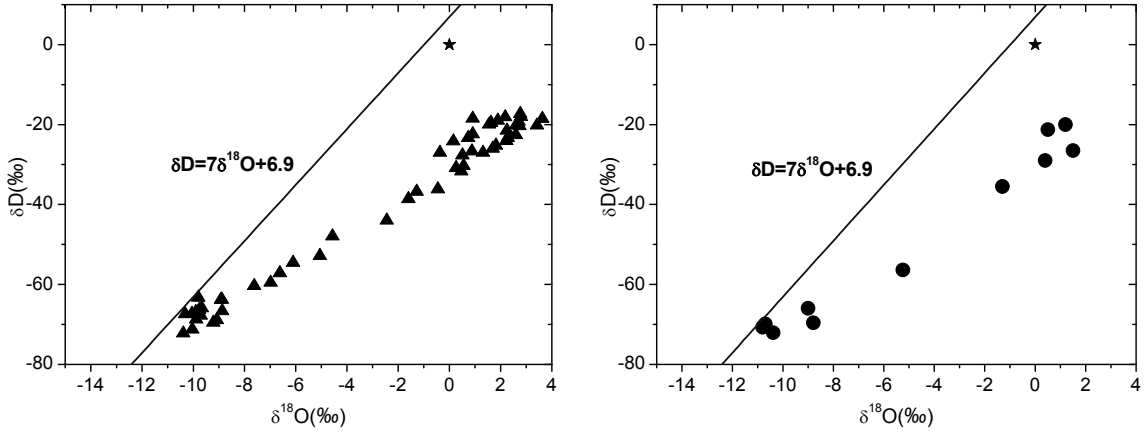

Figure 2.8: δD vs $\delta^{18}O$ for boreholes HDB-1 – 8. Left: porewater, right: groundwater, with the blue line representing the Meteoric Water Line and the star seawater[10)]

3. Sampling and analytical methods

3.1 Description of boreholes

To date, eleven deep boreholes (HDB-1 – 11; see Figure 1.2) have been drilled in the vicinity of the URL site and each borehole fulfilled several primary aims (see Table 3.1).

A multi-phase drilling process was adopted in order to achieve a self-supporting borehole and to ensure successful implementation of the subsequent downhole investigations. The entire drilling process was divided into several steps and the borehole was cased at each step. The layout of the casing was determined on the basis of the:

- geological environment at the actual;
- planned borehole investigations;
- long-term monitoring plan for groundwater chemistry and pressure.

In effect, when drilling in the Phase I, a key assumption was that the boreholes would be used for long-term monitoring of groundwater chemistry and pressure. Thus, the casing programme consisted of four steps and casing was installed along the entire length of the borehole. After completing the drilling and the borehole investigations, the first, second and third stages of the borehole were enlarged using tricone bits with diameters of 17-1/2", 12-1/4" and 8-1/2", respectively. Casing pipes with diameters of 13-3/8", 9-5/8" and 4-1/2" were fixed by gull-hole cementing, based either on single stage cementing or inner string cementing. After installation of the casing pipes, holes penetrating the casing were drilled at given depths using jet perforation for long-term monitoring of groundwater chemistry and pressure. Obviously, this means collecting water that is in contact with the cement and the casing pipe (carbon steel) and this is one of the potential groundwater contamination pathways involved in using this method.

When planning borehole investigations, specifying the overall investigation programme and the details of testing are important. For this purpose, the depths of the lithofacies boundaries, the distribution of groundwater pressure, rock mechanical properties and hydrochemical properties at the investigation location should be estimated before formulating the plans for the investigations. It is also important to plan flexibly so that, if an unexpected event such as fluid loss and seepage of water is observed during drilling, activity can be suspended to conduct tests, providing feedback to the investigation programme.

Table 3.1: Primary aims and approaches to deep boreholes HDB-1 – 11[1)]

Borehole Number	Aims	Drilling Location (World Geodetic System, GRS80)	Drilling Depth	Rationale behind Determination of Drilling Location and Depth	Drilling Diameter	Drilling Fluid
HDB-1	To acquire data on the geological environment to select the URL area	Latitude: 45°02'24.0263" Longitude: 141°51'52.8339" Altitude: 69.102 masl	720.0 m	Sites selected because of good access from main roads; depth determined to obtain geological information below the planned URL depth (500 m)	6-1/4" wireline, triple-tube, core drilling (core Ø 86 mm) from 4.4 to 720.0 mabh	Fresh water from 4.4 to 275.5 mabh; bentonite fluid from 275.5 to 720.0 mabh
HDB-2	To acquire data on the geological environment to select the URL area	Latitude: 44°59'48.3752" Longitude: 141°55'10.3830" Altitude: 42.529 masl	720.0 m		6-1/4" wireline, triple-tube, core drilling (core Ø 86 mm) from 4.4 to 720.0 mabh	Fresh water from 4.4 to 404.9 mbgl; bentonite fluid from 404.9 to 720.0 mabh
HDB-3	To acquire data on the geological environment around the URL area and to select the URL site	Latitude: 45°02'39.5035" Longitude: 141°51'26.6447" Altitude: 58.192 masl	520.0 m	Sites selected on the east and west sides of the Omagari Fault; depth determined based on the planned URL (500 m) and over break (20 m) depths	6-1/4" wireline, triple-tube, core drilling (core Ø 86 mm) from 4.4 to 520.0 mabh	Fresh water from 4.4 to 157.0 mabh; bentonite fluid from 157.0 to 520.0 mabh
HDB-4	To acquire data on the geological environment around the URL area and to select the URL site	Latitude: 45°02'57.7507" Longitude: 141°52'30.2881" Altitude: 63.610 masl	520.0m		6-1/4" wireline, triple-tube, core drilling (core Ø 86 mm) from 4.1 to 520.0 mabh	Fresh water from 4.1 to 162.2 mabh; bentonite fluid from 162.2 to 520.0 mabh
HDB-5	To acquire data on the geological environment around the URL area and to select the URL site	Latitude: 45°02'57.7507" Longitude: 141°51'38.6432" Altitude: 78.768 masl	520.0m		6-1/4" wireline, triple-tube, core drilling (core Ø 86 mm) from 4.1 to 520.0 mabh	Fresh water from 4.1 to 54.0 mabh; bentonite fluid from 54.0 to 520.0 mabh
HDB-6	To acquire data on the geological environment to evaluate techniques for design and construction of URL	Latitude: 45°02'39.0934" Longitude: 141°51'38.6432" Altitude: 60.212 masl	620.0m	Located in the URL site; depth determined to understand groundwater flow around URL and fluid flow deeper than 500 mabh	6-1/4" wireline, triple-tube, core drilling (core Ø 86 mm) from 4.2 to 620.0 mabh	Bentonite fluid from 4.2 to 620.0 mabh
HDB-7	To characterise the geological environment of the Yuchi Formation and upper part of the Koetoi Formation	Latitude: 45°02'51.3035" Longitude: 141°50'39.3235" Altitude: 43.752 masl	520.0 m	Located in the Yuchi Formation distributed area, taking into account social conditions (e.g. land development, ground lease, access to the site etc.); depth determined based on the planed URL (500 m) and over break (20 m) depths	6-1/4" wireline, triple-tube, core drilling (core Ø 86mm) from 11.7 to 620.0 mabh	Bentonite fluid from 11.7 to 620.0 mabh

Table 3.1: Primary aims and approaches to deep boreholes HDB-1 – 11[1)] (continued)

Borehole Number	Aims	Drilling Location (World Geodetic System, GRS80)	Drilling Depth	Rational behind Determination of Drilling Location and Depth	Drilling Diameter	Drilling Fluid
HDB-8	To characterise the geological environment around URL area and understand the Omagari Fault distribution	Latitude: 45°03'00.0458" Longitude: 141°52'09.3122" Altitude: 70.051 masl	470.0 m	Site selected to determine the Omagari Fault distribution; depth determined to confirm geological structure estimated from HDB-1, 3, 4, 5 investigations and the Omagari Fault existence	6-1/4" wireline, triple-tube, core drilling (core Ø 86mm) from 4.2 to 620.0 mabh	Bentonite fluid from 4.2 to 620.0 mabh
HDB-9	To characterise the geological environment on the north side of the URL area	Latitude: 45°03'36.1962" Longitude: 141°51'00.4532" Altitude: 97.188 masl	520.0 m	Located at the north – west boundary of the URL area; depth determined based on the planed URL (500 m) and over break (20 m) depths	6-1/4" wireline, triple-tube, core drilling (core Ø 86mm) from 26.5 to 620.0 mabh	Bentonite fluid from 26.5 to 620.0 mabh
HDB-10	To characterise the geological environment on the north side of the URL area	Latitude: 45°03'31.9231" Longitude: 141°53'38.1125" Altitude: 50.829 masl	550.0 m	Located near the east boundary of the URL area; depth determined to confirm borehole stability and groundwater quality without casing below 500 mabh	6-1/4" wireline, triple-tube, core drilling (core Ø 86mm) from 26.0 to 620.0 mabh; HQ inch wireline, triple-tube, core drilling (core Ø 65 mm) from 500.0 to 550.0 mabh	Bentonite fluid from 26.0 to 620.0 mabh
HDB-11	To characterise the geological environment on the north side of the URL area	Latitude: 45°02'08.7169" Longitude: 141°52'09.1032" Altitude: 66.848 masl	1,020.0 m	Located at the south – east boundary of the URL area; depth determined to confirm the results of groundwater flow analysis	6-1/4" wireline, triple-tube, core drilling (core Ø 86mm) from 23.0 to 1020.0 mabh	Bentonite fluid from 23.0 to 1020.0 mabh

The plan for the investigations in the borehole HDB-11 is shown in Figure 3.1 as an example. The table shows the casing programme, the type of drilling fluid to be used and survey points for geophysical and flow logging planned based on information on the geological environment available before starting the borehole investigations. During the investigations, the plan was modified as more data became available from drilling and other surveys.

It is important to monitor the supply/loss of drilling fluid, rotation speed and torque of the drilling rod and volume of blowout gas during drilling, not only to ensure safety during operations but also for acquiring information on geological structures and hydrogeological and hydrochemical properties in real time. The gas concentration was taken into account in controlling the environment at the drill site and in the safety management of gas blowout. Data on the amount of seepage water and fluid loss were used to determine changes in hydraulic conductivity. For example, when there was a change in the amount of seepage water and fluid loss, drilling was suspended to conduct a hydraulic test and groundwater sampling because such a change can be indicative of the presence of a highly permeable zone. Suspending drilling immediately after discovery of highly permeable zones provides an opportunity to eliminate the effects of drilling mud and less contaminated groundwater samples can be obtained in a short period of time.

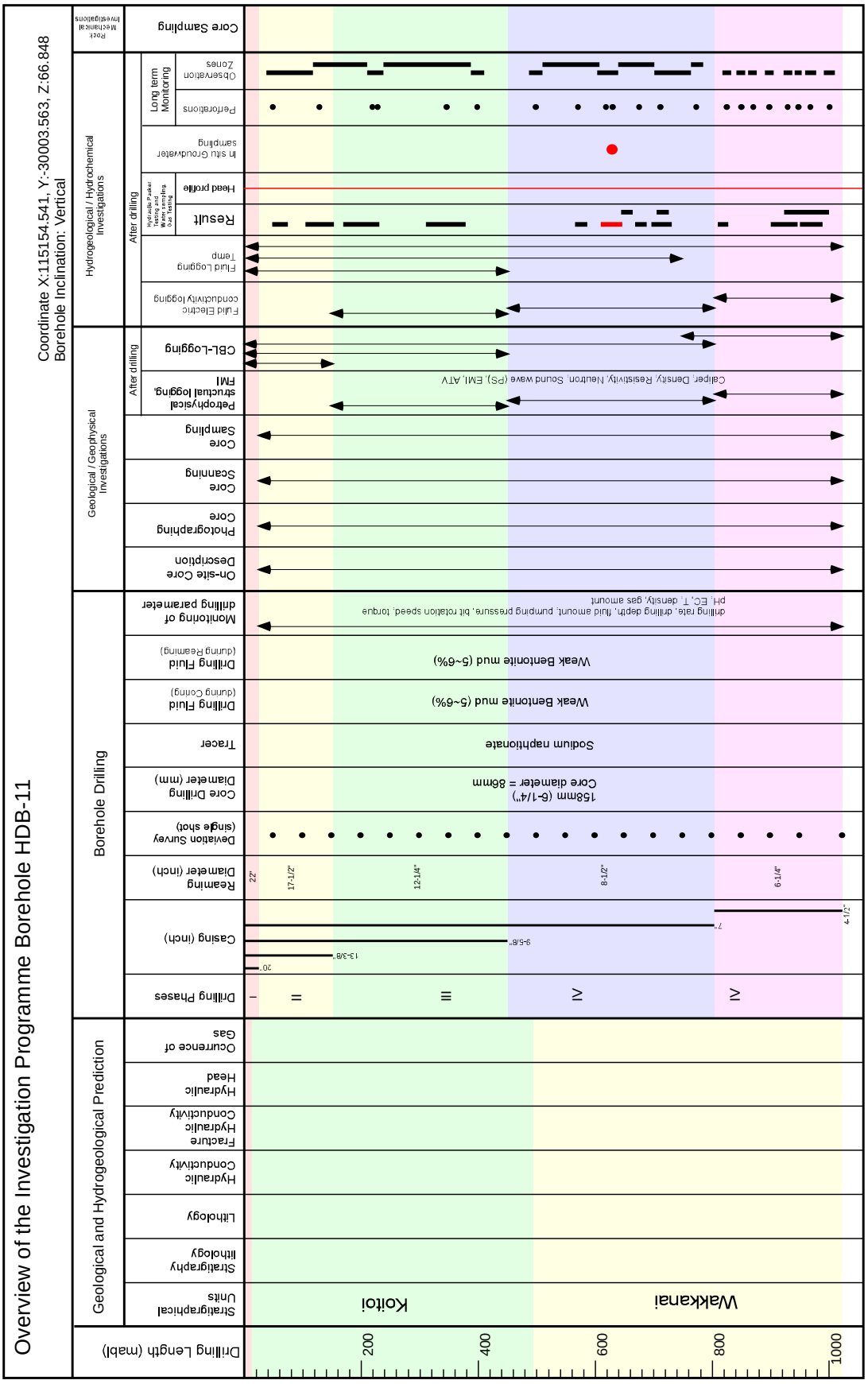

Figure 3.1: Borehole investigation programme for HDB-11[1)]

3.2 Assessment of drilling fluid contamination

Before going on to discuss either the groundwater sampling methodology (Section 3.3) or the detailed QA procedures (Section 4.2), it is worth considering one of the greatest sources of potential sample contamination, namely the drilling fluids. Here, as in most scientific boreholes, drilling fluid behaviour was assessed by adding a fluorescent dye (Na-naphthionate) to the drilling fluid at a known concentration (10 ± 1 mgL^{-1}) and checking the concentration in the drill return water (as part of the assessment of drilling fluid loss to the formation). The dye concentration in the groundwater samples taken for hydrochemical characterisation was measured to define the degree of dilution of the sample (and as a qualitative guide to the sample integrity).

Generally, the method used to measure the dye content (fluorescence spectrophotometry of Na-naphthionate exiting the dye at 320 nm and minor peaks at 237 and 218 nm and fluorescing at 420 nm[17]) has a detection limit of 0.3 μgL^{-1} (or 0.03 % drilling water content here), but groundwater organics can interfere with the measurement. For example, Nilsson[18] examined the impact of TOC on the signal for another fluorescent dye (uranine) in near-surface waters from the Fennoscandian Shield (see Tables 3.2 and 3.3). The data from Table 3.2 are plotted in Figure 3.2 and, although Nilsson[18] could conclude that "...the effect from TOC is relatively small and most often negligible." in the crystalline rocks of Sweden, this is not necessarily the case here and will be further assessed.

Table 3.2: Apparent uranine content of near surface groundwater samples with no added uranine and varying TOC concentrations[18]

Water type	TOC (mgL^{-1})	Uranine concentration (μgL^{-1}) corresponding to the measured blank fluorescence
Near surface groundwater	19.7	0.7
Near surface groundwater	20.0	1.2
Near surface groundwater	20.9	1.0
Near surface groundwater	22.9	1.3
Near surface groundwater	23.3	0.7
Near surface groundwater	24.6	1.0
Near surface groundwater	125	3.5

Table 3.3: Uranine standard solutions (10 μgL^{-1}) prepared from waters with different TOC concentrations[18]

Water type	TOC (mgL^{-1})	Uranine concentration (μgL^{-1}) corresponding to the measured blank fluorescence	Recovery 10 μgL^{-1} uranine
Deionised water	0 – 0.5	0 (adjusted to zero)	9.9
Groundwater	5	0.7	9.7
Groundwater	10	0.6	10.9
Groundwater	13	1.0	10.6
Lake water	20	0.3	9.8

Although not a large dataset, there are clear implications for the Horonobe data (Figure 3.3), even for groundwaters with high TOC (e.g. HDB-11-pu-2-3*, with 39 mgL^{-1}), the natural organics would induce no discernible over-estimation of the drilling water content (based on the data in Table 3.2, between 0.001 and 0.003 %).

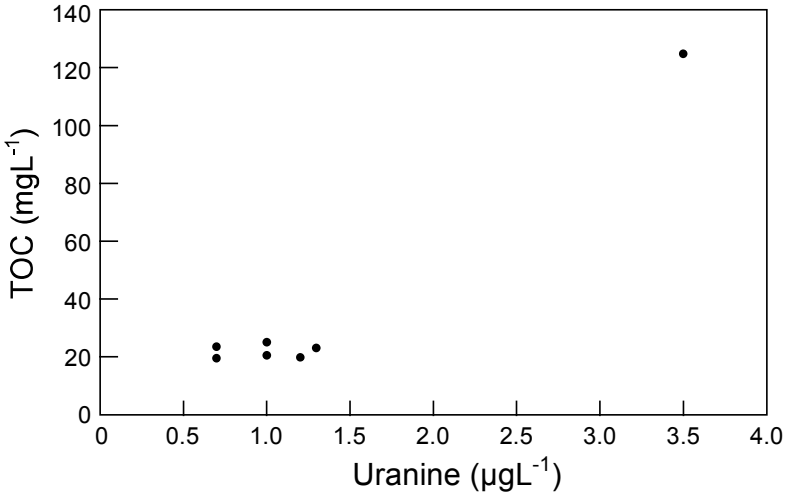

Figure 3.2: Apparent uranine concentration vs TOC for Fennoscandian Shield near-surface waters. Plots refer to data presented in Table 3.2

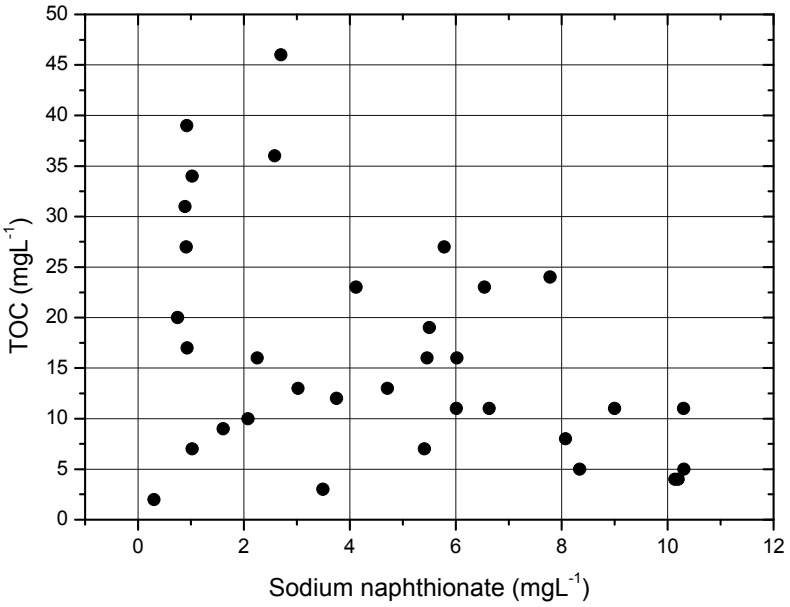

Figure 3.3: Measured Na-naphthionate vs TOC in the pumped samples collected in boreholes HDB-9 – 11 (data for the individual boreholes in Appendix 3)

* Sample numbers are given in the "x-pu-y-z" format, where x: borehole number (excluding the designation HDB-), "pu": "pumped groundwater sample", y: sampling event corresponding to a particular time interval and packer configuration and z: sample number taken in that configuration (increasing with time).

Nevertheless, additional factors which could cause problems in interpreting the drilling water contents[18] include:

- Unstable/inhomogeneous uranine concentration in the drilling water injected into the borehole: Examination of the raw data[19] suggests that this is not a problem here.
- Inadequate mixing prior to sampling of drilling water: this cannot be checked here and would give the impression that the proportion of drilling water in the groundwater sample will seem to vary more than is really the case.
- Too few samples or bias in the sampling (i.e. all samples collected at the same drilling situation – for example, just after core retrieval). This may result in unrepresentative average dye concentrations for the groundwater samples withdrawn from the borehole.

Future sampling of groundwater in the existing boreholes should take all these caveats into account when assessing the QA classification of the samples.

For the porewaters collected at Horonobe, although difficult, it has proven possible to determine the drilling water content on a few samples (Table 3.4). Two points are of note: first, the absolute levels are high (maximum 35 % drilling fluid) and, second, the drilling fluid content drops with depth (to a minimum of 6 %), perhaps indicating that increased compaction is making the matrix less accessible to the drilling fluid (cf. comment in Section 2.2). Although there are no permeability/porosity data on these samples to check this, it is planned to collect relevant data on future boreholes. Certainly the low porosity and permeability samples from the Fennoscandian Shield contained no discernable drilling fluid in the porewaters[20].

Table 3.4: drilling fluid concentrations in some porewater samples from borehole HDB-10

Sample No.	Depth (mabh)		Sample dilution rate before analysis	Drilling fluid concentration (mgL^{-1})
	Upper	Bottom		
H10SQ_01_04	32.76	33.00	200	3.48
H10SQ_02_01	43.70	44.00	100	1.56
H10SQ_03_01	148.65	149.00	100	1.28
H10SQ_04_03	249.68	250.00	200	0.90
H10SQ_06_01	447.00	447.35	50	0.62

3.3 Sampling methodology

3.3.1 Background

For groundwater characterisation in fractured rocks, it is necessary to collect groundwaters in water-conducting features (such as fractures) and from the rock matrix itself (i.e. porewater). Pumping may not be possible (or sufficient time for enough pumping may not be available) if the rock is relatively tight so, as a result, it is always possible that the volume of data acquired will be insufficient for determining the spatial distribution of groundwater chemistry. Paradoxically, in radwaste site characterisation, it is often the tight rock with low

water flux which is precisely the rock volume of greatest interest and this, effectively natural, sample bias must not be forgotten when assessing a site (cf. discussion in SKB[12]).
Note that the 'quality' of the dataset depends on much more than any stated accuracy due to variations in:

- Sample quality: degree of contamination from drilling and lining the hole, contamination from downhole equipment etc.
- Quality of the sampling: This depends on site conditions (e.g. extreme weather conditions affect both equipment and operators), staff experience, mode of sampling (e.g. downhole sampling in a pressurised vessel or downhole sampling with a simple baler or surface sampling of water pumped from depth) and apparatus used (state-of-the-art dedicated equipment or simply whatever container is at hand).
- Appropriateness of the sample: for a representative hydrochemistry sample, it is vital, for example, that no significant hydraulic testing has occurred in the hole beforehand as it may take days to years for the groundwater to recover its original state.
- Amount of sample: for some analyses (e.g. ^{39}Ar and ^{85}Kr), thousands of litres of water are required and this may not be possible in very tight formations.
- Sample storage and transport: must be appropriate for the analysis required. For example, water samples for total metal analysis must be stored in plastic (polythene) vials and be acidified (with ultrapure acid) to pH 2 whereas water samples for gas analysis must be stored in air-tight metal tubes (and analysed as quickly as possible after collection). Samples should be stored in a fridge or even a freezer (e.g. S isotopes will be fractionated by any microbes present in the sample). But, again, care must be taken: freezing samples intended for silicate analysis will change the speciation irreversibly.
- Analytical methods: these vary slightly from laboratory to laboratory and so 'round robin comparisons' must be carried out and laboratory practices formally QAd.
- Analytical operator: in many techniques, an operator bias can be clearly seen and this must also be taken into account.
- Error calculations: it is a disturbing fact that few people really understand error propagation and, to avoid such problems, it is better to devise a common QAd methodology to be used by all analytical laboratories involved.
- Sample QA procedures: these should cover most of the above but also include traceability of the sample, analytical procedures etc.

3.3.2 Methodologies used for boreholes HDB-9 – 11: groundwater

Although a specially formulated silica mud was tested as the drilling fluid[1], it was decided to use local groundwater from the shallower formations, with 10 wt% bentonite added from certain depths or for the entire borehole (see Table 3.1), as this would minimise borehole contamination. Water chemistry (pH, EC, major chemistry) and Na-naphthionate levels were analysed every hour to confirm that no significant change in the water chemistry had occurred during borehole drilling. The concentration of Na-naphthionate added was specified as 10 ± 1 mgL^{-1}.

During pumping tests, the concentration of Na-naphthionate, pH, redox potential and EC was measured every one to two hours in a flow-through cell on the surface, depending on the pumping rate. It would be preferable to pump groundwater until the concentration of the Na-naphthionate dropped below 0.1 mgL^{-1}, but this rarely happened due to limited time. Samples for majors, trace elements, stable isotopes (hydrogen, helium, oxygen, carbon, and chlorine), dissolved gases and specimens for microbial analysis were collected at various times, depending on the borehole status. A downhole probe was developed to measure temperature, pressure, pH, Eh, EC and DO[1)].

Groundwater sampling was carried out with the aim of obtaining samples with residual drilling fluid of 1 % or less. According to the on-site sampling QA handbook, samples were collected (the full sub-sample handling methodology is presented in Kunimaru et al.[19)]):

- Sample preparation for drilling water tracer analysis at field laboratory: Filter a 100 mL volume of the return water sample through a membrane filter (0.45 μm pore size). Use this filtered water as reagent water. Store the remaining unfiltered water in the refrigerator until the next sampling test is conducted (as a back-up in case of problems). Label all bottles appropriately.
- Sample preparation for chemical analysis at field laboratory: Water samples collected from seepage, water-collecting rings, drilling water and tracer-labelled groundwater. Clean and rinse a membrane filter (0.45 μm pore size) with 1000 mL volume of de-ionised water. Filter a 1000 mL volume of the groundwater sample through it and use this filtered water as a sample. Label all bottles appropriately.

3.3.3 Methodologies used for boreholes HDB-9 – 11: porewater

The extraction of porewater from undisturbed rock can be achieved by direct and indirect methods[21)]. The direct method includes in situ sampling of seepage water that accumulates over months to years in isolated intervals in a borehole drilled in a low permeable rock mass[22) – 24)]. Indirect extraction techniques are carried out directly on core material and, in all cases, the obtained water composition is neither a priori representative for the in situ pore water nor is it known if the extracted water comes from the connected porosity in the rock matrix alone (i.e. the porewater) or if it represents a mixture of water/fluids residing in nearby microfractures and/or different types of porosity (e.g. fluid inclusions or bound water). As such, any investigations have to be complemented by detailed investigations of the geology and hydrology of the bedrock mass in order to define precisely the origin of the collected water.

At Horonobe, due to the relatively high matrix porosity and permeability, rock matrix porewater was sampled by a standard squeezing method on samples selected during drilling [6), 25), 26)]. Since the quantity of the squeezed porewater was limited, i.e. a few mL to a few tens of mL, only some major elements and H and O isotopes were analysed). Extensive investigations of the effects of porewater extraction by core squeezing have been conducted

over the last few decades[27), 28)] and the following points should be considered when assessing the obtained data:

- penetration of drilling fluid into the core during drilling;
- oxidation during handling (see Figure 3.4);
- changes in water-rock interaction due to drying of the core during storage;
- changes in porewater chemistry during storage due to oxidation/CO_2 penetration;
- changes in porewater chemistry during squeezing due to oxidation and degassing of porewater and pressure/temperature changes;
- contamination by components of the squeezing tools;
- changes in porewater chemistry during squeezing due to the fractionation of isotopes and elements;
- limitations in analysis due to insufficient porewater volumes.

Some of these perturbations can be minimised by appropriate handling and storage techniques. In the Swedish Äspö HRL, for example, following core recovery, the cores were wiped clean and wrapped successively in two heavy-duty PVC bags and finally in plastic coated aluminium foil; at each stage the bags were repeatedly flushed with N_2, evacuated and then heat-sealed[21)]. Exposure of the samples to the atmosphere was commonly less than 20 minutes and the time period between recovery of the core from the borehole and preparation in the laboratory was normally less than 36 hours. In Nagra's site characterisation campaign at the Wellenberg site, matrix samples were treated in a similar manner to those at Äspö and were then stored in steel drums under a periodically renewed N_2 atmosphere until required[29)]. At Horonobe, samples were tightly wrapped in plastic as soon as possible after core description. Some samples were finally sealed in wax (Figure 3.4). Storage and transit time between sampling and final analysis was in the order of weeks to months.

According to Charlton et al.[26)], all the undisturbed samples were prepared (and squeezed) in an anaerobic glovebox in an atmosphere of less than 100 mgL^{-1} O_2. The samples were cut to the required dimensions (less than 75 mm diameter and less than 100 mm height) with a 75 mm stainless steel cutting ring and a large knife. Potentially contaminated or oxidised material within an approximate 10 mm annulus of the block was discarded. A separate sub-sample was also taken for moisture content determination. A pump pressure of about 5 – 15 MPa was applied initially to remove most of the gas from the cell and allow the sample to 'bed in'. The system was left to stabilise at the ambient temperature of about 16 °C. The syringe tap and labelled syringe of known weight were pushed into the top of the pore-water collection pipe. The system shown in Figure 3.5 was used to squeeze porewater from the core. It is a uniaxial compression injection system with an axial compression of up to 70 MPa. Depending on the core permeability and pore connectivity, this was sufficient to produce 5 – 30 mL of sample.

Figure 3.4: To minimise changes to the porewater during transport and storage, initial sample description (including photographs) were made immediately after core recovery. The cores were then tightly wrapped in plastic and some were sealed in wax until required for squeezing[1)]

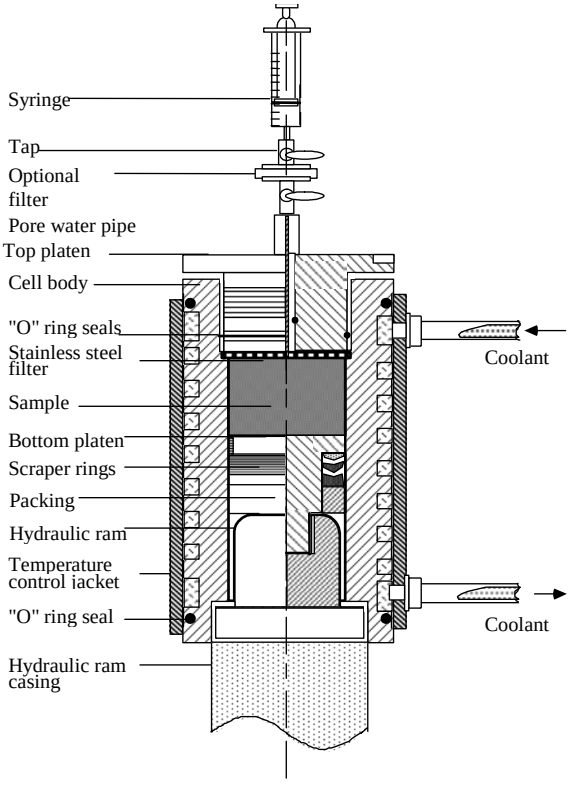

Figure 3.5: Typical core squeezing equipment[26)]

Applied stress was gradually increased throughout the extraction. The stepped increase in stress during testing is dependent on the physical characteristics of the material tested and the volume of water required. A particular stress may be maintained for a few hours or up to several weeks, depending on the rate of pore-water flow, and total squeezing time varied

between 0.5 and 1008 hours under a stress of between 5 and 70 MPa[26]. In order to evaluate the influence on porewater chemistry of the loading pressure, the chemistry of the squeezed porewater was analysed following stepwise increases of the load. As can be seen in Figure 3.6, Na and Cl concentrations gradually decrease with increased load, but H and O isotope ratios remained constant, irrespective of load. The cause of the changes in the porewater salinity noted here is assumed to be the fact that absorbed water and interlayer water in minerals were squeezed out[30] but other mechanisms are also involved – for example, silica speciation is well known to be highly sensitive to load[27].

Comparison of porewater chemistry and nearby groundwater chemistry show little significant difference other than for SO_4 for those cores squeezed under a normal atmosphere (rather than in a low-O_2 glovebox). However, although the SO_4 levels were 2 to 3 orders of magnitude lower than for those cores squeezed in air, they were still generally higher than the adjacent groundwaters, probably due to the fact that the sampling and handling procedure was not stringent enough to avoid oxidation effects. In addition, the so-called 'anaerobic gloveboxes' still contained some 100 mgL^{-1} of O_2, which amounts to a significant flux of O_2 through the squeezing period. This is especially problematic when considering the relatively porous and permeable samples examined here as this would certainly allow relatively rapid access of O_2 to the entire core.

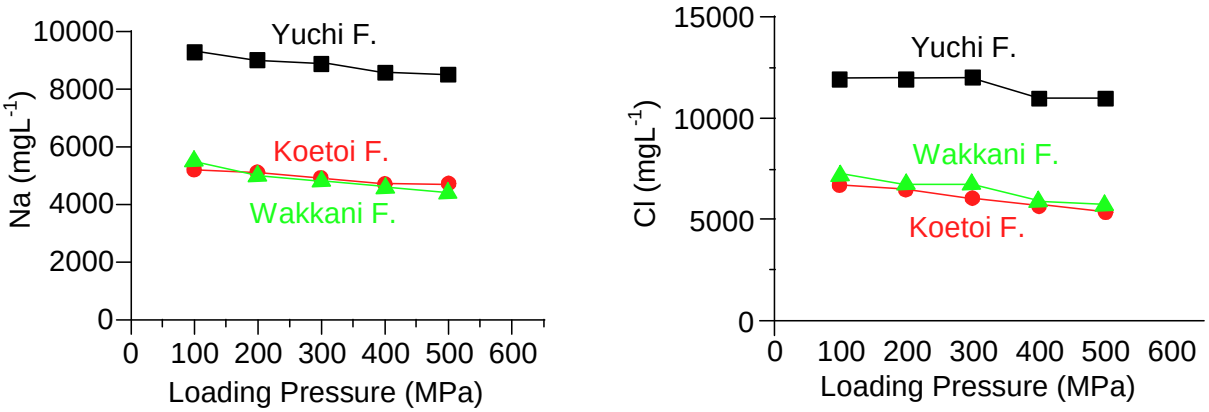

Figure 3.6: Relationship between squeezing pressure and porewater chemistry[1]

3.3.4 Groundwater gas

Significant levels of dissolved gases such as CH_4 and CO_2 are contained in the groundwater in the Wakkanai and Koetoi Formations. When groundwater is pumped from a borehole using a submersible pump, dissolved gases will be released from the groundwater in response to the pressure release[31]. When calculating rock transmissivity and hydraulic conductivity by pumping tests, the amounts of pumped groundwater and the gases separated from the water are required. Generally, pumping test equipment does not have the capability to measure released gas volumes during the pumping test. To solve these problems, the pumping test equipment was improved to collect this information (see Figure 3.7).

Here, although degassing will change the groundwater chemistry, the acquisition of hydrogeological data (such as hydraulic conductivity) and hydrochemical data at the same time and at the same depth is very effective for modelling hydrogeological structures and assessing the validity of the results of groundwater flow analyses. This would also be important in the context of planning effective and efficient borehole investigation programmes, including reduction of investigation times and costs. However, since investigation priorities differ depending on the borehole, groundwater sampling methods have to be selected appropriately according to the specified objective of the investigation, e.g. measurement of in situ pH over a long period of time or determining the depth profile of salinity over a short period of time. In other words, it is simply not possible to achieve perfect results for all parameters in a single borehole (and most certainly not at the same time).

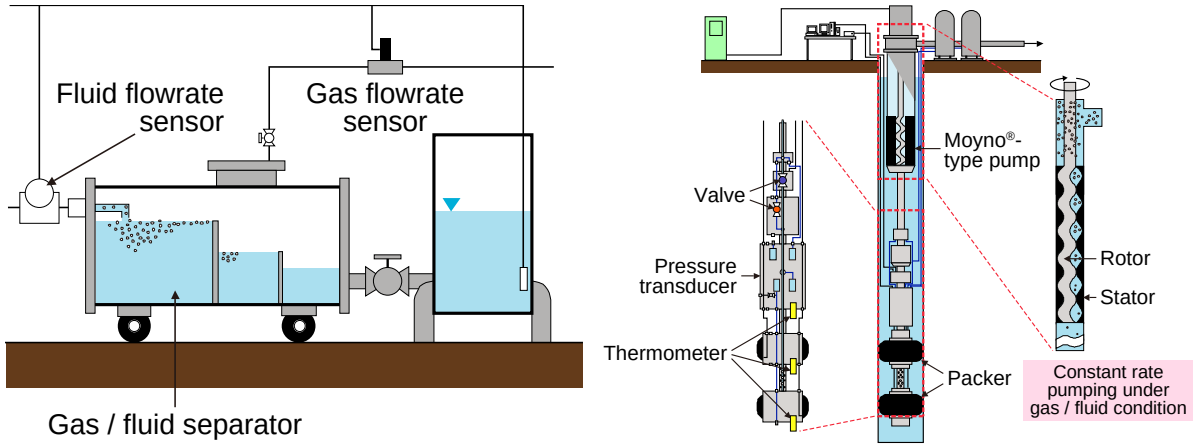

Figure 3.7: The improved hydraulic test equipment (surface on left, downhole on right) showing how gases were collected for metering and analysis[1)]

3.4 Analytical methods

The analytical methods employed are listed briefly in Table 3.5 and presented in detail in Kunimaru et al.[19)]

Table 3.5: The analytical methods employed in the Horonobe hydrochemistry programme[19)]

Sample ID													
	Borehole No.		HDB-1	HDB-2	HDB-3	HDB-4	HDB-5	HDB-6	HDB-7	HDB-8	HDB-9	HDB-10	HDB-11
Monitoring													
	pH		PM	PM	PM	PM	PM	PM	PM	PM	PM	PM	PM
	EC (@25°C)	[mSm^{-1}]	PM	PM	PM	PM	PM	PM	PM	PM	PM	PM	PM
	ORP(Pt)	[mV]	-	-	PM	PM	PM	PM	-	PM	PM	PM	PM
	ORP(Au)	[mV]	-	-	PM	PM	PM	PM	-	PM	PM	PM	PM
	Eh(Pt)	[mV]	PM	PM	PM	PM	PM	PM	-	PM	-	-	-
	Eh(Au)	[mV]	PM	PM	PM	PM	PM	PM	-	PM	-	-	-
	DO	[mgL^{-1}]	PM	PM	PM	PM	PM	PM	-	PM	PM	PM	PM
	Tracer	[mgL^{-1}]	FS	FS	FS	FS	FS	FS	FS	FS	FS	FS	FS
	Temp.	[°C]	PM	PM	PM	PM	PM	PM	PM	PM	PM	PM	PM
Lab.													
	pH		PM	PM	PM	PM	PM	PM	PM	PM	PM	PM	-
	EC (@25°C)	[mSm^{-1}]	PM	PM	PM	PM	PM	-	-	-	PM	PM	-
	Temp.	[°C]	PM	PM	PM	PM	PM	-	-	-	-	PM	-
	Tracer	[mgL^{-1}]	FS	FS	FS	FS	FS	-	-	-	-	FS	-
Major elements													
	Na^+	[mgL^{-1}]	FP	FP	FP	FP	FP	FP	FP	FP	FP	FP	FP
	K^+	[mgL^{-1}]	FP	FP	FP	FP	FP	FP	FP	FP	FP	FP	FP
	NH_4^+	[mgL^{-1}]	A	A	A	A	A	A	A	A	A	A	A
	Li^+	[mgL^{-1}]	ICP	ICP	ICP	ICP	ICP	ICP	ICP	ICP	ICP	ICP	ICP
	Ca^{2+}	[mgL^{-1}]	ICP	ICP	ICP	ICP	ICP	ICP	ICP	ICP	ICP	ICP	ICP
	Mg^{2+}	[mgL^{-1}]	ICP	ICP	ICP	ICP	ICP	ICP	ICP	ICP	ICP	ICP	ICP
	Sr^{2+}	[mgL^{-1}]	ICP	ICP	ICP	ICP	ICP	ICP	ICP	ICP	ICP	ICP	ICP
	Se^{2-}	[mgL^{-1}]	AAS	AAS	AAS	AAS	AAS	AAS	AAS	AAS	AAS	AAS	AAS
	Total-P	[mgL^{-1}]	A	A	A	A	A	A	A	A	A	A	A
	I^-	[mgL^{-1}]	IC	IC	IC	IC	IC	IC	IC	IC	IC	IC	IC
	Mn(II)	[mgL^{-1}]	ICP	ICP	ICP	ICP	ICP	ICP	ICP	ICP	-	-	ICP
	Total Mn	[mgL^{-1}]	-	-	Un	-	-	-	-	-	Un	Un	-
	disolved Si	[mgL^{-1}]	GA	GA	ICP	ICP	ICP	ICP	ICP	ICP	ICP	ICP	ICP
	insoluble SiO_2	[mgL^{-1}]	-	-	Un	Un	Un	-	-	-	-	Un	-
	Ti^{4+}	[mgL^{-1}]	-	-	ICP	ICP	ICP	ICP	ICP	ICP	ICP	ICP	ICP
	Fe(III)	[mgL^{-1}]	-	ICP	ICP	ICP	ICP	ICP	ICP	ICP	ICP	ICP	ICP
	Fe(II)	[mgL^{-1}]	PA	PA	PA	PA	PA	PA	PA	PA	PA	PA	PA
	Total-Fe	[mgL^{-1}]	ICP	ICP	ICP	ICP	ICP	ICP	ICP	ICP	ICP	ICP	ICP
	Al^{3+}	[mgL^{-1}]	ICP	ICP	ICP	ICP	ICP	ICP	ICP	ICP	ICP	ICP	ICP
	F^-	[mgL^{-1}]	IC	IC	IC	IC	IC	IC	IC	IC	IC	IC	IC
	Cl^-	[mgL^{-1}]	IC	IC	IC	IC	IC	IC	IC	IC	IC	IC	IC
	Br^-	[mgL^{-1}]	IC	IC	IC	IC	IC	IC	IC	IC	IC	IC	IC
	NO_3^-	[mgL^{-1}]	IC	IC	IC	IC	IC	IC	IC	IC	IC	IC	IC
	NO_2^-	[mgL^{-1}]	IC	IC	IC	IC	IC	-	-	-	IC	IC	IC
	SO_4^{2-}	[mgL^{-1}]	IC	IC	IC	IC	IC	IC	IC	IC	IC	IC	IC
	S^{2-}	[mgL^{-1}]	-	-	-	-	-	Un	Un	Un	Un	Un	Un
	H_2S	[mgL^{-1}]	MA	MA	MA	MA	<0.0	<0.0	<0.0	<0.0	<0.0	<0.0	<0.0
	Total-B	[mgL^{-1}]	-	Un	-	-	-	-	Un	-	Un	Un	Un
	Total-Be	[mgL^{-1}]	-	-	-	-	-	-	Un	-	Un	Un	Un
	Total-Cr	[mgL^{-1}]	-	-	-	-	-	-	Un	-	Un	Un	Un
	Total-Co	[mgL^{-1}]	-	-	-	-	-	-	Un	-	Un	Un	Un
	Total-Ni	[mgL^{-1}]	-	-	-	-	-	-	Un	-	Un	Un	Un
	HCO_3^-	[mgL^{-1}]	calc	calc	calc	calc	calc	calc	calc	calc	calc	calc	calc
	CO_3^{2-}	[mgL^{-1}]	calc	calc	calc	calc	calc	calc	calc	calc	calc	calc	calc
	M-Alkalinity ($CaCO_3$)	[mgL^{-1}]	NT	NT	NT	NT	NT	NT	NT	-	NT	NT	NT
	P-Alkalinity ($CaCO_3$)	[mgL^{-1}]	NT	NT	NT	NT	NT	NT	NT	-	NT	NT	NT
	TOC	[mgL^{-1}]	CS	CS	CS	CS	CS	CS	CS	CS	CS	CS	CS
	TIC	[mgL^{-1}]	CS	CS	CS	CS	CS	CS	CS	CS	CS	CS	CS

A: Absorptiometry, AAS: Atomic absorption spectrometry, calc: Calculation, CS: Combustion oxidation infrared spectrometry, FP: Flame photometry, IC: Ion chromatography, ICP: Inductively coupled plasma atomic emission spectrometry, NT: Neutralisation titration, PM: Portable meter measurement, Un: Unclear (no detailed record)

Table 3.5: The analytical methods employed in the Horonobe hydrochemistry programme[19] (continued)

Sample ID													
	Borehole No.		HDB-1	HDB-2	HDB-3	HDB-4	HDB-5	HDB-6	HDB-7	HDB-8	HDB-9	HDB-10	HDB-11
Ionic balance													
Cation													
	Na^+	[meq/l]	calc	calc	calc	calc	calc	calc	calc	calc	calc	calc	calc
	K^+	[meq/l]	calc	calc	calc	calc	calc	calc	calc	calc	calc	calc	calc
	NH_4^+	[meq/l]	calc	calc	calc	calc	calc	calc	calc	calc	calc	calc	calc
	Li^+	[meq/l]	calc	calc	calc	calc	calc	calc	calc	calc	calc	calc	calc
	Ca^{2+}	[meq/l]	calc	calc	calc	calc	calc	calc	calc	calc	calc	calc	calc
	Mg^{2+}	[meq/l]	calc	calc	calc	calc	calc	calc	calc	calc	calc	calc	calc
	Sr^{2+}	[meq/l]	calc	calc	calc	calc	calc	calc	calc	calc	calc	calc	calc
Anion													
	F^-	[meq/l]	calc	calc	calc	calc	calc	calc	calc	calc	calc	calc	calc
	Cl^-	[meq/l]	calc	calc	calc	calc	calc	calc	calc	calc	calc	calc	calc
	Br^-	[meq/l]	calc	calc	calc	calc	calc	calc	calc	calc	calc	calc	calc
	NO_3^-	[meq/l]	calc	calc	calc	calc	calc	calc	calc	calc	calc	calc	calc
	NO_2^-	[meq/l]	calc	calc	calc	calc	calc	calc	calc	calc	calc	calc	calc
	SO_4^{2-}	[meq/l]	calc	calc	calc	calc	calc	calc	calc	calc	calc	calc	calc
	M-Alkalinity	[meq/l]	calc	calc	calc	calc	calc	calc	calc	calc	calc	calc	calc
	P-Alkalinity	[meq/l]	calc	calc	calc	calc	calc	calc	calc	calc	calc	-	-
	Σcation	[meq/l]	calc	calc	calc	calc	calc	calc	calc	calc	calc	calc	calc
	Σanion	[meq/l]	calc	calc	calc	calc	calc	calc	calc	calc	calc	calc	calc
	Σcation-Σanion	[meq/l]	calc	calc	calc	calc	calc	calc	calc	calc	calc	calc	calc
Isotopes													
	^3H	[T.U]	MS	MS	MS	MS	MS	MS	MS	MS	MS	MS	MS
	δD	[‰]	MS	MS	MS	MS	MS	MS	MS	MS	MS	MS	MS
	$\delta^{18}O$	[‰]	MS	MS	MS	MS	MS	MS	MS	MS	MS	MS	MS
	$\delta^{13}C$	[‰]	-	-	AMS	-	-	-	AMS	AMS	-	-	-
	$^{14}C/^{12}C$	[pMC]	-	-	AMS	-	-	-	AMS	AMS	-	-	-
	$^{36}Cl/Cl$	[$\times10^{-15}$]	-	-	AMS	AMS	AMS	AMS	AMS	AMS	AMS	AMS	AMS
	$\delta^{34}S$		-	-	-	-	-	-	-	-	AMS	AMS	AMS
	$^{87}Sr/^{86}Sr$		-	-	-	-	-	-	-	-	AMS	AMS	AMS
Organic acid													
	Humin acid	[mg/l]	FS	FS	FS	FS	FS	FS	-	FS	FS	FS	FS
	Fuluvic acid	[mg/l]	FS	FS	FS	FS	FS	FS	-	FS	FS	FS	FS
	Acetic acid	[mg/l]	IC	IC	IC	IC	IC	IC	-	IC	IC	IC	IC
	Formic acid	[mg/l]	IC	IC	IC	IC	IC	IC	-	IC	IC	IC	IC
Microbes													
	Total number of bacteria	[No. /ml]	DCM	DCM	DCM	DCM	DCM	DCM	-	DCM	-	-	-
	Heterotrophic bacteria	[CFU/ml]	PIM	PIM	PIM	PIM	PIM	PIM	-	PIM	-	-	-
	Anaerobic polymers-degrading bacteria	[CFU/ml]	PIM	PIM	PIM	PIM	PIM	PIM	-	PIM	-	-	-
	Anmonia-oxidizing bacteria	[MPN/ml]	-	-	MPN	MPN	MPN	MPN	-	MPN	-	-	-
	Nitrous Acid bacteria	[MPN/ml]	-	-	MPN	MPN	MPN	MPN	-	MPN	-	-	-
	Ion-oxidizing bacteria	[MPN/ml]	-	-	MPN	MPN	MPN	MPN	-	MPN	-	-	-
	Nitrate-reducing bacteria	[MPN/ml]	MPN	MPN	MPN	MPN	MPN	MPN	-	MPN	-	-	-
	Denitrifying bacteria	[MPN/ml]	MPN	MPN	MPN	MPN	MPN	MPN	-	MPN	-	-	-
	Sulfer-reducing bacteria	[MPN/ml]	-	MPN	MPN	MPN	MPN	MPN	-	MPN	-	-	-
	Methane producing bacteria	[MPN/ml]	-	GC	GC	GC	GC	GC	-	GC	-	-	-

AMS: Accelerator mass spectrometry, calc: Calculation, DCM: Direct count method, FS: Fluorescence spectrophotometry, GC: Gas Chromatography, IC: Ion chromatography, MPN: Most probable number method, MS: Mass spectrometry, PIM: Plate method

4. QA procedures

4.1 Background

As noted by Smellie et al.[32], "Assessing groundwater quality and assigning a QA category of suitability requires an evaluation of all the available hydrochemical data with reference to known hydraulic conditions in:

- the borehole;
- the fracture zone sections being sampled;
- the surrounding host bedrock.

The reliability of these data is therefore judged as much as possible on prevailing hydraulic and geologic conditions during drilling and subsequent monitoring and sampling. Without the integration of hydrochemistry, geology, hydrogeology and borehole activities there is a great danger that data can be misrepresented."

The quality of hydrochemical data can be influenced by several processes, including:

- Contamination of the groundwater by drilling fluids or additives and by the material of the drilling equipment (see Section 4.2, below):
  - this will dilute the groundwater solutes;
  - additives, such as bentonite, will change the major element chemistry;
  - metals from the drill bit and lines can change the perceived redox state.
- Damage to the host rock by the physical and chemical process of drilling can produce large colloid populations, for example, when weak rock is badly damaged by the drill bit.
- Alteration of the in situ conditions during sampling:
  - by the introduction of contaminants such as O_2 (trapped in or on sampling equipment) which changes the in situ redox conditions;
  - by degassing groundwater samples as they are brought to the surface, so changing pH and Eh values;
  - by oxidising reduced species (in the porewater and the rock) during rock matrix sample handling and squeezing;
  - by pumping at too great a rate for the local groundwater 'reservoir' in the vicinity of the sampling point. This can induce draw-in of groundwater from further afield and mixing with the in situ groundwater to produce a sample which in non-characteristic of that horizon in the borehole.
- Introduction of surface microbes or additional nutrients will change the *in situ* microbial populations and, as a consequence, the redox state of the groundwater.
- Contamination during sample handling and transport by the introduction of gases or other contaminants from the equipment.

- Contamination during analysis by the introduction of gases or other contaminants from the equipment or analyst (e.g. trace levels of Sr from sweat can be transferred to equipment if gloves are not worn).
- Imprecise or inaccurate analysis:
  - caused by equipment drift during analysis;
  - or by the use of inappropriate standards (e.g. with a significantly different matrix from that of the groundwater);
  - or by operator variability.

Consequently, in several national radwaste programmes, a strict classification of the quality of groundwater samples has been developed[33) – 36)]. Such classifications are generally based on:

- experience of past site investigations[29), 37)];
- comparison with other national site characterisation programmes[11)];
- international programmes of natural analogue studies[38), 39)];
- national and international URL programmes[40) – 42)].

Arguably, the QA methodologies applied in radwaste programmes are much more stringent than in other areas of groundwater research because of the strict requirements of repository site assessments and the expectations of various stakeholders (cf. IAEA[43)]). Although the Horonobe URL will not be used as a radwaste repository, there is no reason that the programme of science conducted here should fall below the standards set elsewhere in the Japanese national programme and other international programmes. This will obviously have clear advantages when developing an integrated conceptual model for the URL site as high quality data are required to model the hydrogeochemical interactions in the groundwater and host rock. In addition, training staff in the application of appropriate QA methods will allow the development of a body of staff fully capable of conducting an actual repository site characterisation.

4.2 QA categorisation

Historically, most site characterisation studies have included some form of assessment of the data quality[44)]. For example, during Nagra's characterisation of the Wellenberg site in central Switzerland, considerable effort went into producing a hydrogeochemically consistent dataset[45)]. Unfortunately, in most national programmes, the detailed work is only included in unpublished internal reports with only very generalised statements openly available such as:

- Changes to the dissolved gases during sampling (due to differences in pressure and temperature) must be corrected.
- Changes to redox due to air contamination of samples must be taken into account.

Recently, this trend has changed with more open reporting of all phases of the work. A very good example of this can be seen in SKB's ongoing site characterisation programme where some very stringent data requirements from the site characterisation group[34) – 36)] has led to the development of a system of ranking the analytical data based on a suite of criteria (Table 4.1).

Table 4.1: Classification criteria for cored boreholes (top) and percussion boreholes (bottom)[32)]

Cored Boreholes	**Category**				
Aspects/Conditions	***1***	***2***	***3***	***4***	***5***
Drilling water (≤1 %)	X	X	X	X	X
Drilling water (≤5 %)		X	X	X	X
Drilling water (≤10 %)			X	X	X
Drilling water (>10 %)				X	X
Time series (adequate)	X	X	X	X	X
Time series (inadequate)			X	X	X
Time series (absent)				X	X
Suitable section length	X	X	X	X	X
Sampling during drilling				X	X
Sampling during hydraulic testing			X	X	X
Tube sampling					X
Charge balance ±5 % (±10 % for <50 mgL^{-1} Cl)	X	X	X	X	X
Major ions (complete)	X	X	X	X	X
Major ions (incomplete)			X	X	X
Environmental isotopes (complete)	X	X	X	X	X
Environmental isotopes (incomplete)		X	X	X	X
Hydraulic effects (short-circuiting)	X	X	X	X	X

Percussion Boreholes	**Category**				
Aspects/Conditions	***1***	***2***	***3***	***4***	***5***
Short restricted section length (e.g. monitoring)	X	X	X	X	X
Flow log available		X	X	X	X
Without flow log (0 – 100m)				X	X
Without flow log (0 – 200m)					X
Time series/monitoring	X	X	X	X	X
Charge balance ±5 % (±10 % for <50 mgL^{-1} Cl)		X	X	X	X
Major ions (complete)	X	X	X	X	X
Major ions (incomplete)		X	X	X	X
Environmental isotopes (complete)	X		X	X	X
Environmental isotopes (incomplete)		X	X	X	X
Monitoring borehole sections	X	X	X	X	X
Hydraulic effects (short-circuiting)	X	X	X	X	X

Categories 1 – 3 primarily meet the requirements of hydrochemical (but also hydrogeological) modelling, while Categories 4 – 5 primarily meet hydrogeological requirements (but may also be of use for more qualitative hydrochemical modelling with caution). Smellie et al.[32] defined a colour code to make sample identification easier when, for example, data are presented in spread-sheet tables or as symbols in scatter plots:

- Category 1 is orange;
- Category 2 is yellow;
- Category 3 is green;
- Category 4 is grey;
- Category 5 is black.

As can be seen from Table 4.1, the final weighting of data for any particular sample is based on providing:

- period of sample collection (e.g. during drilling or hydraulic testing lowers the category);
- a complete set of major ion and isotope analytical data (particularly ^{3}H, ^{2}H, ^{18}O and C isotopes when available);
- an acceptable charge balance;
- a low drilling water content;
- good time-series data coverage;
- reliable redox values;
- a satisfactory coverage of trace element data (including U, Th and rare earth elements (REEs));
- dissolved gas, microbes and organics and colloid data.

Clearly, the higher the sample category, the more confidence can be placed on the dataset and so the more useful are the data for modelling calculations. Nevertheless, as noted by Smellie et al.[32], overall site understanding is still possible using a combination of all categories, "...with the obvious proviso that the lower the category used, the more caution is required in their interpretation." Where possible, confidence can be increased in a given dataset by the inclusion of higher category data, as clearly shown in Figure 4.1 where all five categories are plotted for the conservative element Cl versus borehole depth. The figure shows that the general trends and important outliers indicated by all data are strengthened and constrained by the higher category samples (1 – 3), and even some of the Category 4 samples. As expected, the low quality Category 5 samples show the greatest scatter, but even so many follow the major trends.

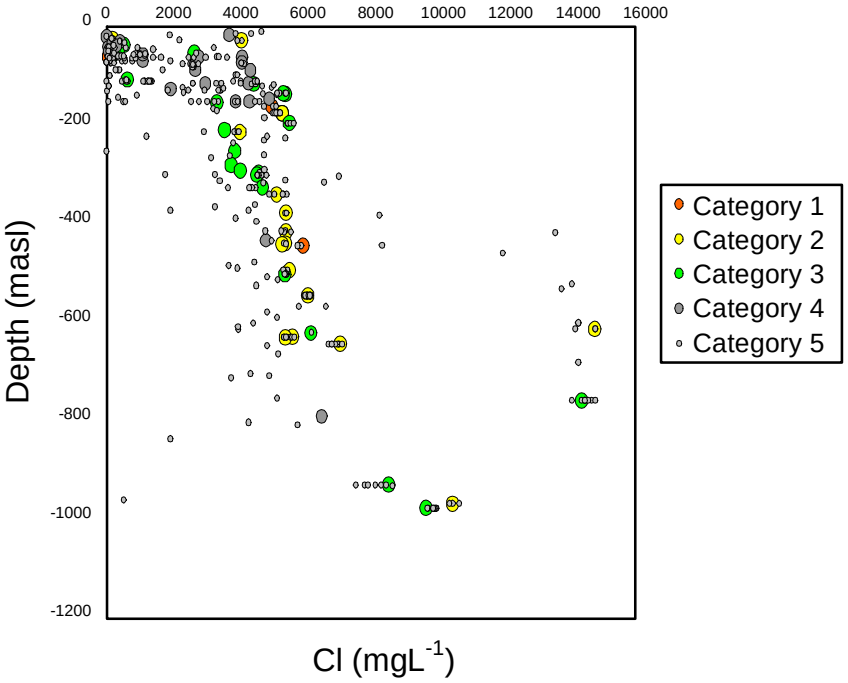

Figure 4.1: Example of a data plot with different categories of data: chloride data vs depth showing all categories[32)]

In addition to the above noted hydrochemical considerations, Smellie et al.[32)] emphasised that additional issues should be considered in parallel. For example:

- An individual sample may be classified Category 1 or 2, but time-series data may indicate chemical instability throughout the sampling period. This poses the question of which composition, if any, is most representative? Here, a Category 1 or 2 classification would be invalid and the sample should be placed in a lower category.
- In other words, when possible, the category assigned should be based on a stable groundwater composition as this gives added confidence in the data quality.
- The sampling interval may be short-circuited (due to the presence of fractures in the rock matrix, for example) and be supplied by mixed groundwaters from higher or lower levels in the bedrock or borehole. Here, the sample, when interpreted in isolation, may be assigned too high a category.

Thus it must be understood that assigning a sample category is based on a combination of hydrogeological input (e.g. differential flow measurements; hydraulic packer tests etc.) and expert judgement based on existing hydrochemical knowledge of the particular borehole (i.e. chemical comparison with higher or lower levels) and the site in general (i.e. what compositional range would be expected at the depth of sampling) and so is not an 'absolute' valuation of the data.

Additionally, it must be emphasised that this stage of QA is already based on an assumption that appropriate QA measures are already in place at the sampling and analysis stages[35)].

For the porewater data, it is clear that the same set of QA conditions cannot be applied – apart from anything else, the vastly reduced sample size simply means that the full range of analyses realistically cannot be carried out. Nevertheless, some QA aspects can be addressed, such as the degree of drilling fluid penetration into the core to be used for porewater extraction[46), 47)], the dataset available and indications of perturbations such as sample oxidation or CO_2 reaction (depending on the rock type, groundwater type etc.).

Although QA systems already exist for core recovery, sampling and description in the mining industry[48)], as far as the authors are aware, nothing comparable exists for rock porewaters. This is probably because of the relative novelty of the work. Nevertheless, a few, preliminary guidelines are proposed here (Table 4.2) which will be 'road tested' over the next few years to assess how they can be improved. Of note is the addition of analytical data quality, including the requirement to properly assess and report analytical uncertainty – and this should be included retrospectively in Tables 4.1.

Table 4.2: Classification criteria for squeezed porewater

Porewaters	Category				
Aspects/conditions	1	2	3	4	5
Drilling water (≤10%)	X	X	X	X	X
Drilling water (≤50%)		X	X	X	X
Drilling water (>50%)				X	X
Oxidation/CO_2 reaction			X	X	X
QAd sampling methodology	X	X	X	X	X
QAd analytical data, including uncertainties	X	X	X	X	X
Chlorinity	X	X	X	X	X
δD	X	X	X	X	X
$\delta^{18}O$	X	X	X	X	X
^{3}H		X	X	X	X
Major elements			X	X	X
pH			X	X	X
Alkalinity			X	X	X
Immediately adjacent groundwater analysis available		X	X	X	X

4.3 Data QA result

Clearly, the full set of criteria noted in Table 4.1 apply only to the groundwater samples, but some of the criteria may be applied to the surface and porewater samples too (with some modification) and this will be addressed here. For all boreholes, it is assumed that the drilling tracer is maintained at a concentration of 10 ± 1 mgL^{-1} [1)] (see also Section 3.2) so, for the drilling fluid contamination calculation, the minimum value of 9 mgL^{-1} is assumed. Here, data for HDB-9 – 11 are presented and boreholes HDB-1 – 8 are in Data Freeze II.

4.3.1 Borehole HDB-9

The surface waters have a full set of analyses (apart from environmental isotopes) and a reasonable time series (some 16 months) and so could be assigned to Category 2 (pending a charge balance check). One point of concern is whether the range of pH values (4.44 – 6.53) is consistent – in future, this should be checked in the laboratory – and what effect this might have on the groundwater analyses if this water is used for drilling fluid. It is of note that sample B9RID_01 has an almost complete set of environmental isotope data (none of the others of this series have any), the problems with carbon isotopes being noted above.

(1) Deep groundwaters

Series B9RW1_01

As can be seen in Kunimaru et al.[19], the return water tracer concentration varies between 9.05 and 10.7 mgL^{-1}, i.e. within the stated uncertainty. It is also clear that all HDB-9 samples (apart from B9GW1_01, depth 26.5 – 82.6 mabh) lie in Category 4, based on drilling water content (see below for further refinement of category). Sample B9GW1_01, with a drilling water content of around 3 % is in Category 2. However, the fact that the sample comes from an inadequate time series (i.e. not quite 4 days, 19:13 on 21.10.04 to 06:30 on 24.10.04) relegates it to Category 3. It is worth noting that this sample also has an almost complete set of environmental isotope data (none of the others of this series have any), the problems with C isotopes being noted above.

All other samples from this time series (i.e. B9RW1_01 to _06) are effectively Category 4 (Category 5 only refers to tube sampled waters).

Series B9RW2_01

The samples in the time series B9RW2_01 to _05 plus B9GW2_01 are also all ranked as Category 4 on the basis of drilling water content, as this ranges from an initial 115 % down to 18 % for 9GW2_01 (N.B. cf. the groundwater EC variation across this period). Although not remarkable in sample series B9RW1_01 (due to the low salinity of the near-surface water), the dilution of the groundwater is very clear here with low Cl value in the first sample (B9RW2_01) mirroring the high drilling fluid content.

The time series is also inadequate (only 2 days, or 49 hours in total). It is worth noting that sample B9GW2_01 has an almost complete set of environmental isotope data (none of the others of this series have any), the problems with C isotopes being noted above.

(2) Porewater

The fact that the porewaters have not been assessed for drilling fluid interaction should relegate them to Category 4 immediately (and the obvious oxidation effects to Category 3). However, more crucial here is the fact that chlorinity and stable isotope data are available and, while the data are of immense value, they are degraded by the fact that there is no possibility of assessing drilling fluid effects (e.g. dilution of the chlorinity) on these conservative tracers. Thus, the porewater data would all plot as Category 4.

Incidentally, the value of the porewater data is also decreased by the fact that no adjacent groundwater data are available. In the case of the groundwater sample series 9RW1 and 9RW2, the intervals are simply too large to make any meaningful comparison with the porewater data as it is not possible to define precisely the source of the groundwater.

4.3.2 Borehole HDB-10

(1) Surface/shallow waters

The surface waters have a full set of analyses (apart from environmental isotopes) and so could be assigned to Category 2 (pending a charge balance check). However, the relatively short time series (some 3 months), might consign the series to Category 3, depending on the use of the data. Here, the river water pH shows much less variation than in the HDB-9 dataset, with no sign of the apparent winter acidification seen in that dataset. Finally, it is of note that sample B10RIU_07 has an almost complete set of environmental isotope data (none of the others of this series have any), the problems with C isotopes being noted above.

(2) Deep groundwaters

Series B10RW1_01

As can be seen in Kunimaru et al.[19], the return water tracer concentration varies between 9.11 and 9.64 mgL^{-1}, i.e. within the stated uncertainty. It is also clear that all Series B10RW1_01 samples lie in Category 4, based on drilling water content. The samples also come from an inadequate time series (i.e. not quite 12 hours, 20:37 on 13.10.04 to 08:08 on 14.10.04), which would relegate them to Category 3 were they not already Category 4. It is worth noting that sample B10GW1_01 has an almost complete set of environmental isotope data (none of the others of this series have any), the problems with C isotopes being noted above.

Series B10RW2_01

The samples in the time series B10RW2_01 to _05 are also all ranked as Category 4 on the basis of drilling water content, as this ranges from an initial 113 % down to 25 % for 9GW2_01 (N.B. note the recovery in the groundwater EC across this period). The time series is also inadequate (from only 18:00 on 19.12.04 to 22:00 on 22.12.04, or 28 hours in total). Of note is the fact that the last two samples of this series (B10RW2_06 and B10GW2_01) are ranked as Category 3 due to their much lower tracer content (of 10 % and 8 % respectively). The latter sample also has an almost complete set of environmental isotope data (none of the others of this series have any), the problems with C isotopes being noted above.

(3) Porewater

The fact that the porewaters have not been assessed for drilling fluid interaction should relegate them to Category 4 – 5 immediately and the obvious oxidation effects to Category 3. However, more crucial here is the fact that chlorinity and stable isotope data are available and, while the data are of immense value, they are degraded by the fact that there is no possibility of assessing drilling fluid effects on these conservative tracers. Thus, the porewater data would all plot as Category 4 – 5.

Incidentally, the value of the porewater data is also decreased by the fact that no adjacent groundwater data are available. In the case of the groundwater sample series B10RW1 and B10RW2, the intervals are simply too large to make any meaningful comparison with the porewater data. At least in the case of porewater samples H10SQ02_01 (43.7 – 44.0 mabh) and H10SQ09_01 (59.1 – 59.3 mabh), they are bracketed by groundwater sample B10RW1 (41.3 – 59.9 mabh).

Note that the three samples squeezed in the 'low O_2' glovebox, although showing indications of less oxidation, the SO_4 levels are still significantly higher than groundwaters from a similar depth (cf. H10SQ_13_02 and B10GW2_01 – although this is the last in the time series). As noted above, 'low O_2' is far from O_2-free and the flux of O_2 remains high enough to perturb the cores (also lowering their classification).

4.3.3 Borehole HDB-11

(1) Surface/shallow waters

The surface waters have a full set of analyses (apart from environmental isotopes) and so could be assigned to Category 2 (pending a charge balance check). However, the relatively short time series (some 10 months), might consign the series to Category 3, depending on the use of the data. Here, the river water pH shows much less variation than in the HDB-9 dataset, but with some sign of acidification seen in that dataset. Finally, it is of note that samples B11RIU_01 and BRIU_12 have an almost complete set of environmental isotope data (none of the others of this series have any), the problems with C isotopes being noted above.

(2) Deep groundwaters

Series B11RW1_01

As can be seen in Kunimaru et al.[19], the return water tracer concentration varies between 9.13 and 10.94 mgL^{-1}, i.e. just within the stated uncertainty, showing somewhat more variation than normal. It is also clear that all Series B11RW1_01 samples lie in Category 4, based on drilling water content. The samples also come from an inadequate time series (i.e. just 5 days, 02:00 on 07.12.04 to 09:00 on 12.12.04), which would relegate them to Category 3 were they not already Category 4. It is worth noting that sample B11GW1_01 has an almost complete set of environmental isotope data (none of the others of this series have any), but the 61 % drilling fluid content must not be overlooked.

Series B11LRW1_01

The samples in the time series B11LRW1_01 to _05 are also all ranked as Category 4. B11LRW1_01 on the basis of drilling water content of 11 % and B11LRW1_012 to _05 and B11LGW1 due to the inadequate time series (from only 09:50 on 13.03.05 to 14:48 on 30.03.05, or 17 days in total). Of note is the fact that, apart from this, all of this series would have been ranked as Category 3 due to their much lower tracer content (of around 10 %). The last sample, B11LGW1, also has an almost complete set of environmental isotope data but, unlike B11GW1_01, a much lower drilling fluid content.

(3) Porewater

The fact that the porewaters have not been assessed for drilling fluid interaction should relegate them to Category 4 – 5 immediately and the obvious oxidation effects to Category 3. However, more crucial here is the fact that chlorinity and stable isotope data are available and, while the data are of immense value, they are degraded by the fact that there is no possibility of assessing drilling fluid effects on these conservative tracers. Thus, the porewater data would all plot as Category 4 – 5.

Incidentally, the value of the porewater data is also decreased by the fact that almost no adjacent groundwater data are available. Porewater sample H11SQ_05_03 (171.6 – 171.8 mabh) is bracketed by groundwater sample B11LRW1 (171.00 – 237.05 mabh) and porewater sample H11SQ_14_03 (644.8 – 645.0 mabh) is close to groundwater sample B11LGW1 (606.0 – 644.1 mabh), but the groundwater sampling intervals are generally too large to make any meaningful comparison with the porewater data.

Note that the six samples squeezed in the 'low O_2' glovebox all (apart from H11SQ_21_01) show SO_4 levels which are similar to the groundwaters from the site. Unfortunately, none of these samples can easily be correlated to a specific groundwater sample. Nevertheless, this may be a sign that the sampling and analytical groups responsible for the work may now have gained enough experience in the methods employed to make an appreciable difference and so these samples will be the focus of future geochemical modelling studies.

5. Hydrochemistry: data and discussion

Although the data categorisation in Chapter 4 shows all current data to be in the lower categories (cf. Tables 4.1 and 4.2), it is nevertheless worthwhile carry out a preliminary assessment as at least major trends should still be discernable in the data (cf. Figure 4.1). In addition, it is hoped that an assessment of potential drilling fluid contamination of the porewater samples can be conducted in the near future, allowing any necessary corrections to be made at a later date.

Here, all the porewater data for boreholes HDB-9 – 11 will be examined whereas, for the groundwater samples, only data from the last sample of a time series have been taken, viz:

- samples 9-pu-1L and 9-pu-2L from HDB- 9;
- samples 10-pu-1L and 10-pu-2L from HDB-10;
- samples 11-pu-1L and 11-pu-2L from HDB-11.

Although the last of sample of a time series, the drilling fluid content still varied between 3 and 61 % (see Appendix 4). In addition to these 6 samples, an additional 2 from HDB-11 were included:

- 11-pu-2-1 as it contained only 11 % drilling fluid and was therefore relatively pristine. It will also allow comparison of changes during the time series.
- 11-pu-1-1 with 113 % (i.e. pure drilling fluid, within measurement error) is considered to assess if it immediately stands out from the other data (as it should do).

With so few data and only 2 depth intervals per borehole, it makes little sense to look at each borehole in isolation. As such, the data will be clumped together to look for general trends and only in specific cases will individual boreholes be discussed (mainly in association with the porewater data in Section 5.2). Note that the depths quoted are the mid-depth of the borehole sampling sections (groundwaters) and core lengths (porewaters). No uncertainties are quoted for the chemical parameters as fully QAd information are not yet available.

5.1 Groundwaters

5.1.1 Overview

All the parameters measured in the groundwater samples are presented in Appendix 4 and the stable isotope data are included here but, from these, several have not been interpreted for the following reasons:

- Se^{2-}: all data below detection limit;
- Mn(IV): only 2 data points and these are in HDB-11 (whereas all the ΣMn are in HDB-9 and HDB-10);
- Ti^{4+}: all are noted as < and this is assumed to be the detection limit;
- Al: all <0.01 mgL^{-1}, so also assumed to be the detection limit;

- S^{2-}: all <0.1 mgL^{-1}, so also assumed to be the detection limit;
- H_2S: all <0.1 mgL^{-1}, so also assumed to be the detection limit;
- ΣBe: all <0.002 mgL^{-1}, so also assumed to be the detection limit;
- Cr, Co and Ni are all present at very low concentrations but are, in any case, assumed to be drilling related contaminants at this stage of the borehole evolution.

5.1.2 Major element chemistry

The concentration versus depth profiles for Cl, Ca, K, Mg, Na and Si are plotted in Figure 5.1a – f and all display a remarkably similar form. The concentration of all majors increases slowly with depth, reaching a maximum in the deepest samples at 625 mabh. In most cases, the lowest levels are observed at 54.5 mabh (drilling fluid content of 3 %) with higher levels at the slightly shallower 50m level. As the latter samples contain 29 % drilling fluid, this increase is presumed to reflect contamination by and reaction with the drilling fluid.

Likewise with the 2 samples at 204 mabh, all of the lower values, apart from ΣP, are associated with the sample which is effectively pure drilling fluid. As such, the higher concentration at this depth, despite containing 61 % drilling fluid, is more representative of the 'true' value. At 625 mabh, where the first and last of a time series have been plotted, the differences are not so strong, partly reflecting that the first sample had only 10 % drilling fluid and the last 10 %.

Removing the 50 mabh and the first 204 mabh samples from the profiles would certainly produce a 'cleaner' profile of slowly increasing solute concentration with depth for all 3 boreholes. The Cl profile is not dissimilar to that of Hama et al.[10] for uncorrected Cl data in HDB-1 – 8 (see Figure 2.7, bottom), although the Cl levels immediately below 200 mabh are slightly higher in this dataset.

The Ca, Na and Mg curves generally follow that of Cl and, despite the coastal nature of the site, all are considerably diluted when compared to standard mean ocean water (SMOW) values (at between 50 and 60 %), in agreement with Sasamoto[5] proposal that the groundwater includes at least a marine end-member. In fact, Mg and Cl and Na and Cl show a close correlation (Figure 5.2), although no correlation exists for Ca versus Cl. A similar Mg/Cl correlation has been reported before for the groundwaters of the Forsmark site in Sweden[12] and it appears to be related to the presence of relict marine groundwater from the Littorina sea of immediate post-glacial times. Although there has clearly been reaction of Mg with the crystalline rocks at Forsmark, there nevertheless remains enough of a signal from the marine waters to stand out from the background noise. The possibility that the Mg/Cl and Na/Cl correlations seen here in these borehole groundwaters will be investigated further to assess if this is also evidence of the presence of marine waters in the Horonobe system. At Forsmark, only Mg stands out with such a clear signal and this is presumably due to rock water interaction 'diluting' the other signals. Interestingly, here, Na has also retained a clear signal (whereas Ca has presumably been lost due to interaction).

K and Si display slightly more complex profiles with a kick around 200 mabh. However, examination of Appendix 4 shows that the sample at 204 mabh contains 61 % drilling fluid while that at 237 mabh 'only' 18 % and so the apparent anomaly may simply be due to contamination by and reaction with a greater amount of drilling fluid in the 204 mabh sample. Certainly, this should be an area of focus for any future work in these boreholes.

The Si concentrations are comparable with those for the other boreholes (see Figure 5.3) and there is no sign of the much higher levels observed at depth in HDB-1 and HDB-2. In agreement with data offered from R. Arthur and W. Zhou (personal communication), the silica concentrations in the Koetoi and Wakkanai groundwaters cannot be distinguished simply on the basis of differences in solubility, which might have been expected given the different opal phases present in each formation (see Chapter 2). This possibly indicates thorough mixing between the formations.

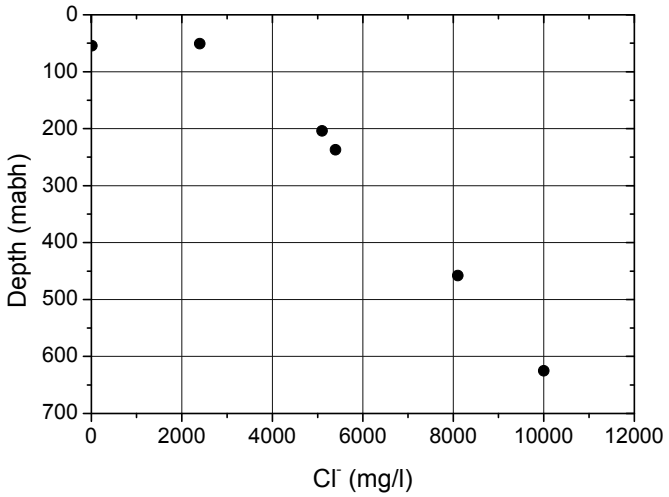

Figure 5.1a: Groundwater Cl^- vs depth, boreholes HDB-9 – 11

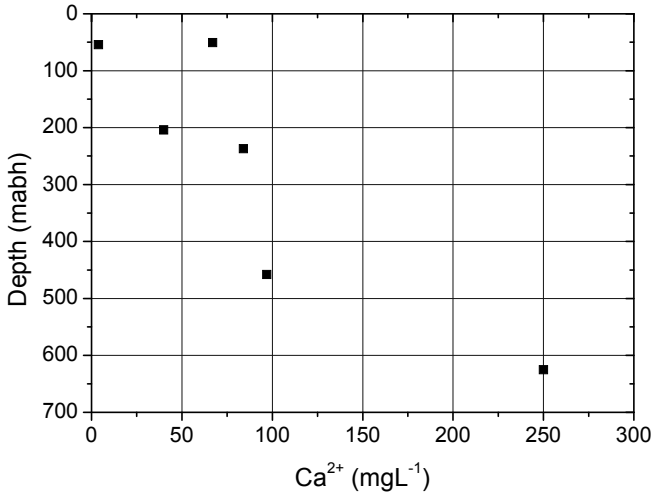

Figure 5.1b: Groundwater Ca^{2+} vs depth, boreholes HDB-9 – 11

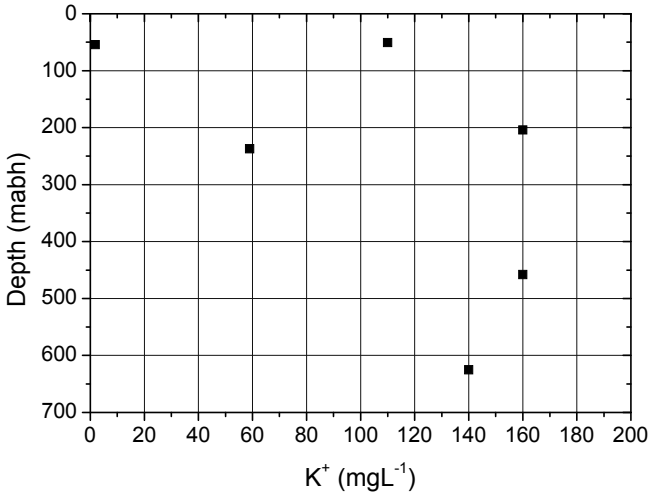

Figure 5.1c: Groundwater K^+ vs depth, boreholes HDB-9 – 11

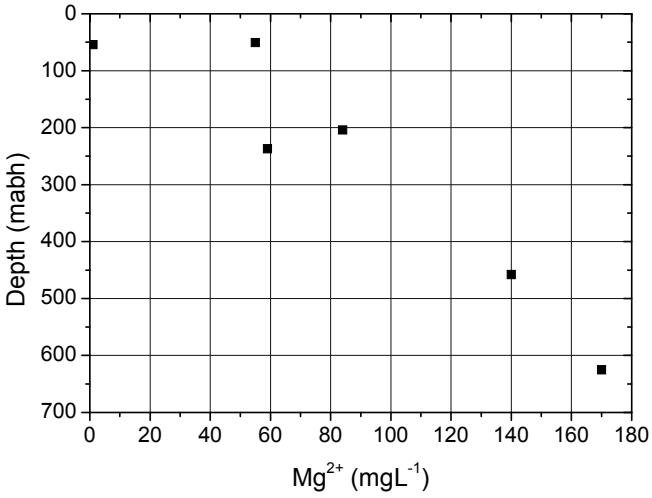

Figure 5.1d: Groundwater Mg^{2+} vs depth, boreholes HDB-9 – 11

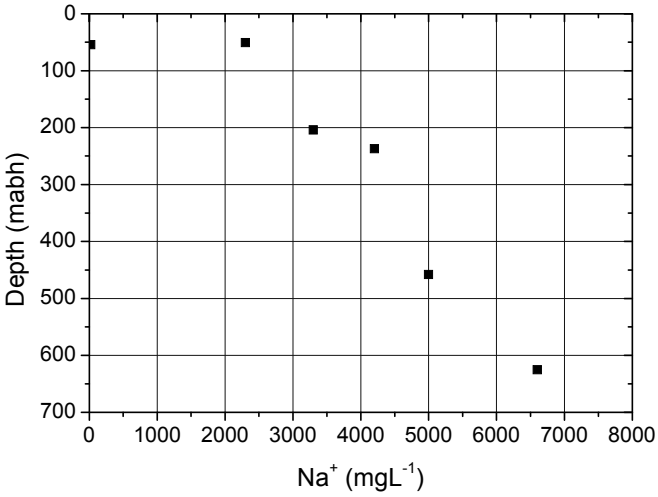

Figure 5.1e: Groundwater Na^+ vs depth, boreholes HDB-9 – 11

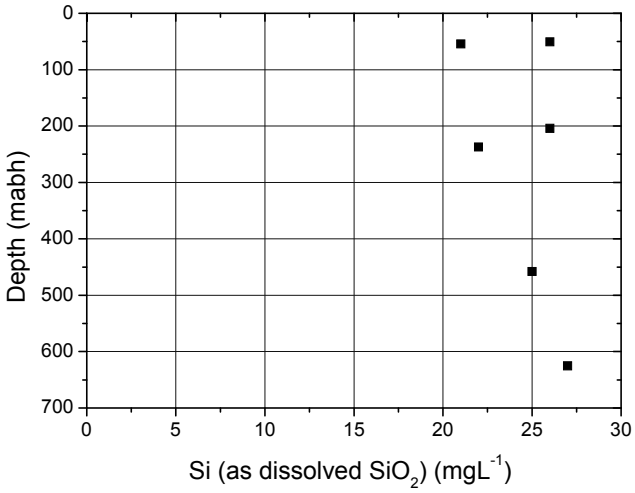

Figure 5.1f: Groundwater Si (as dissolved SiO_2) vs depth, boreholes HDB-9 – 11

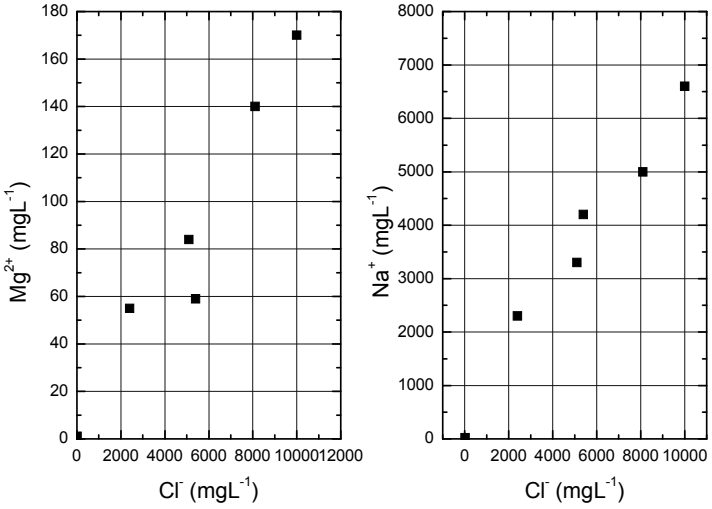

Figure 5.2: Groundwater Mg^{2+} (left) and Na^{+} (right) vs Cl^{-}, borehole HDB-9 – 11

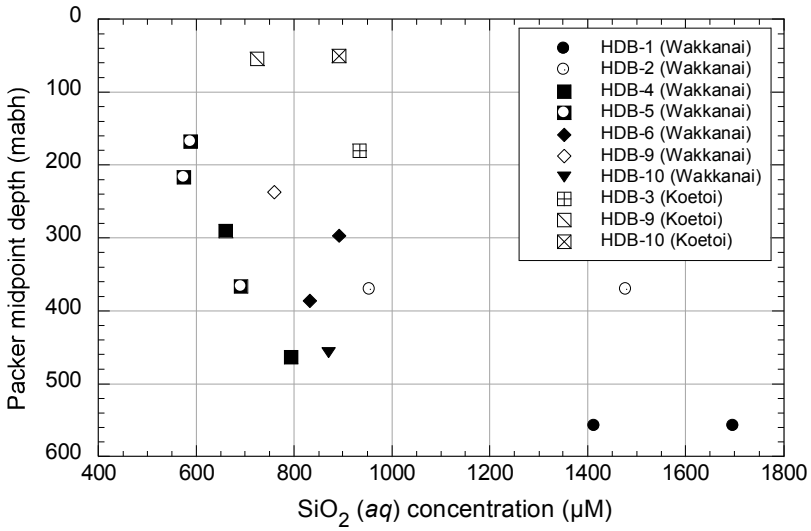

Figure 5.3: Si (as dissolved SiO_2) vs depth, boreholes HDB-1 – 10

5.1.3 Trace elements, including redox

The Li versus depth plot (Figure 5.4) shows a great deal of scatter with no obvious trends whereas the ΣP versus depth plot (Figure 5.5) is generally invariant with depth (note that the high value at 50 mabh is from a sample with 29 % drilling water and so may be an artefact). The Sr concentration increases slowly with depth (Figure 5.6a) to a maximum of 4.5 mgL^{-1} and shows a weak correlation with the Ca concentration (Figure 5.6b) suggesting a common source (as might be expected). The $^{87}Sr/^{86}Sr$ isotopic ratios for these samples[19] show a wide variation, from 0.708504 to 0.705568 (cf. seawater ratio of 0.709198 ± 0.000093), indicating that a wide range of sources are involved (probably including the drilling fluid).

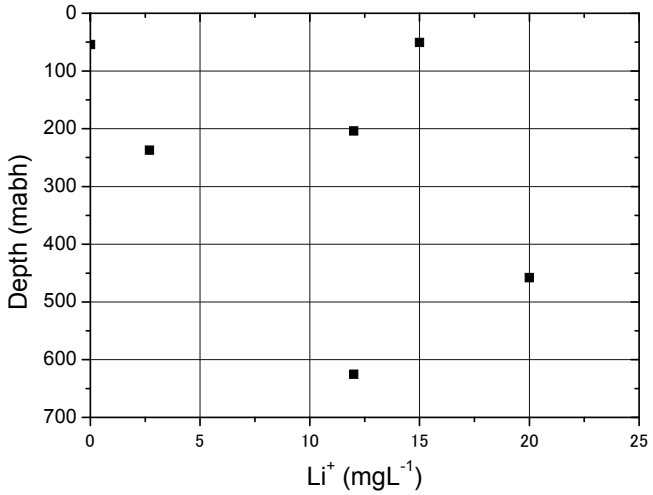

Figure 5.4: Groundwater Li^+ vs depth, boreholes HDB-9 – 11

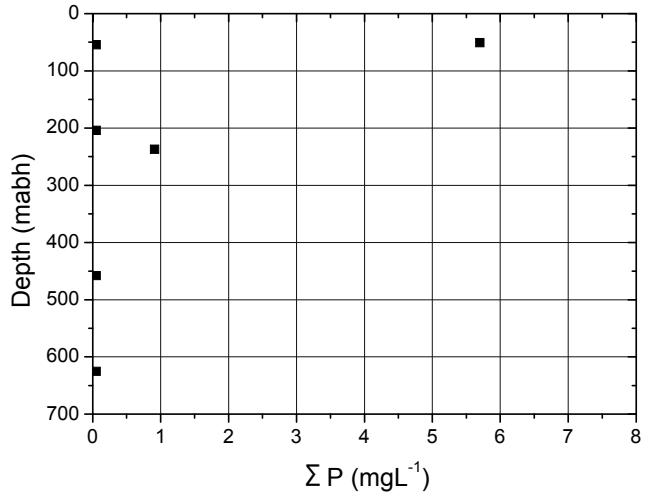

Figure 5.5: Groundwater total-P vs depth, boreholes HDB-9 – 11

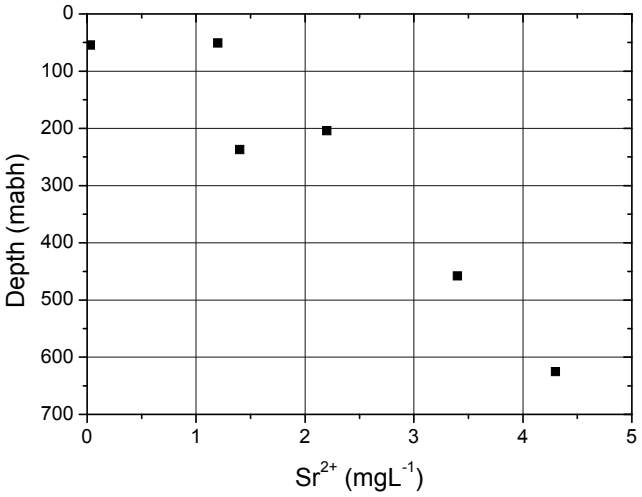

Figure 5.6a: Groundwater Sr^{2+} vs depth, boreholes HDB-9 – 11

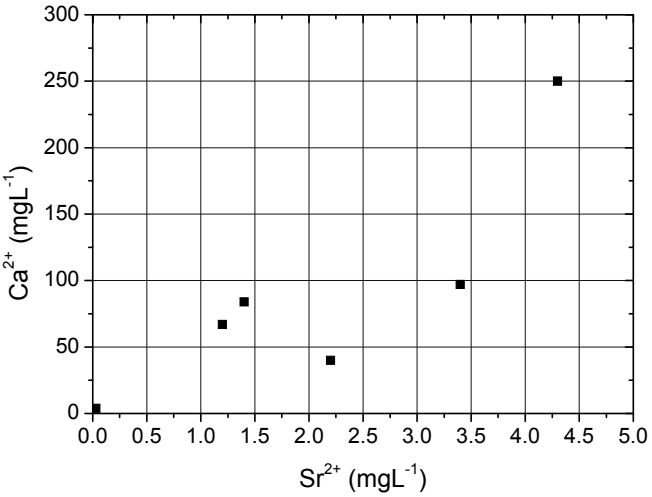

Figure 5.6b: Groundwater Sr^{2+} vs Ca^{2+}, boreholes HDB-9 – 11

For the halogens, the I and Br versus depth plots show very similar trends (Figure 5.7a, b) and a strong correlation, as would be expected if they had a common source, such as in marine organics[28]. This is an interesting point worth further consideration when higher category samples are available as it may prove to be a valuable marker for potential groundwater mixing end-members. The third halogen, F, shows no obvious correlation with depth and this may simply represent the fact that the data are at or near the analytical limit (of 0.1 mgL^{-1}).

The plot of ΣB versus depth (Figure 5.8a) shows a similar trend of slowly increasing concentration with depth to that seen in the majors. Plotting B against Cl indicates a close correlation, but at a B : Cl ratio (around 2×10^{-2}) which is much higher than observed in seawater (around 2×10^{-4}), indicating an additional source of B to the groundwater. Similarly with both the I/Cl and Br/Cl ratios, although it should be noted that all three of these trace

elements would be present in marine organics contained in the sediments and could be released from this source during burial.

For the bicarbonate system, the HCO_3 versus depth plot (Figure 5.9a) shows significant scatter whereas pH is less extreme, generally showing a slow drop with depth (Figure 5.9b).

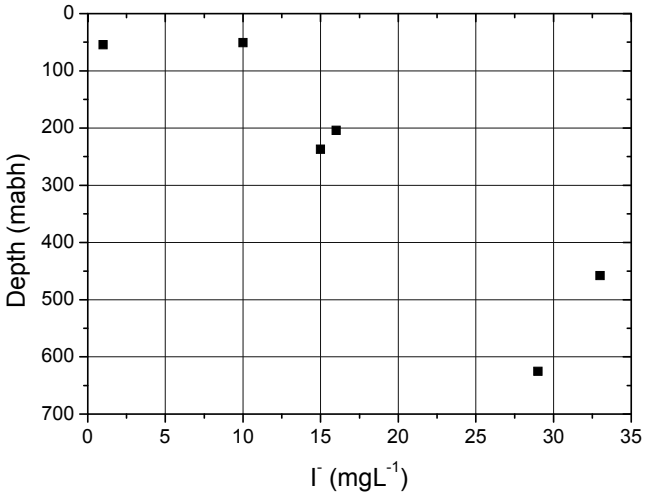

Figure 5.7a: Groundwater I^- vs depth, boreholes HDB-9 – 11

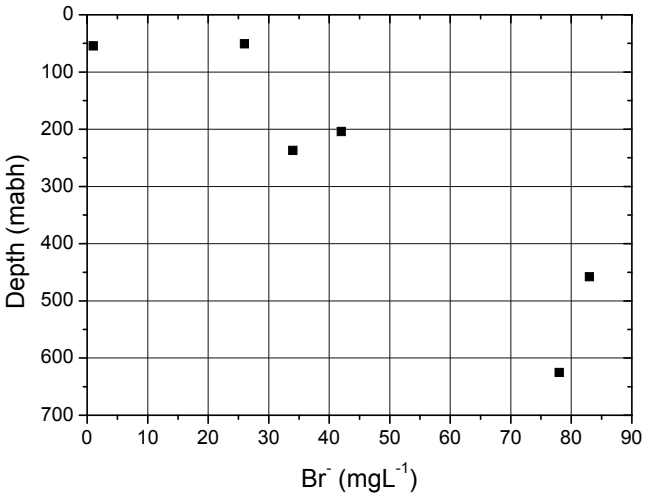

Figure 5.7b: Groundwater Br^- vs depth, boreholes HDB-9 – 11

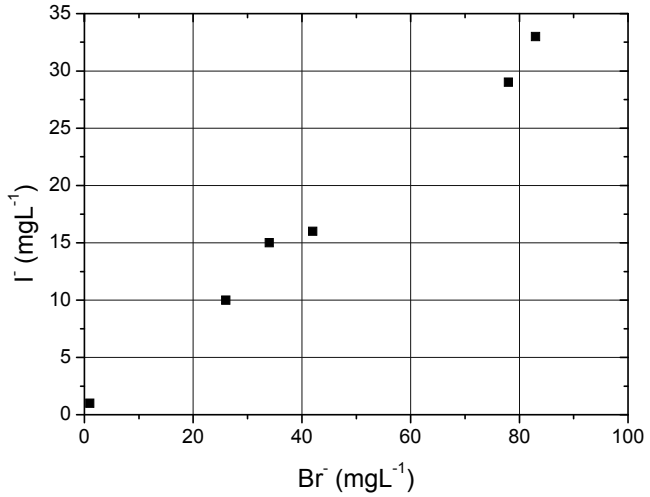

Figure 5.7c: Groundwater Br^- vs I^-, boreholes HDB-9 – 11

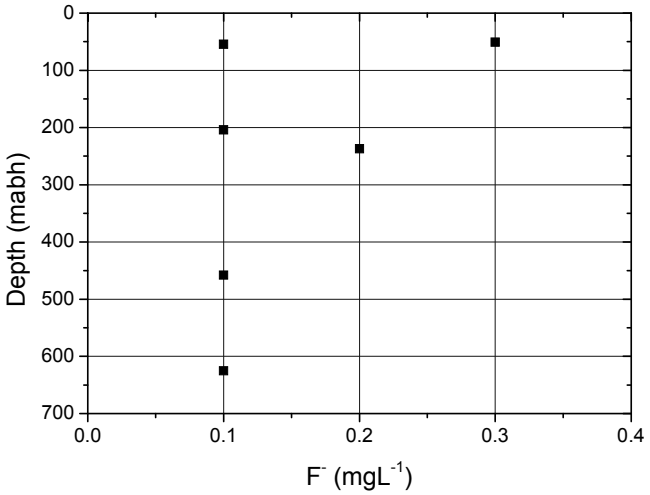

Figure 5.7d: Groundwater F^- vs depth, boreholes HDB-9 – 11

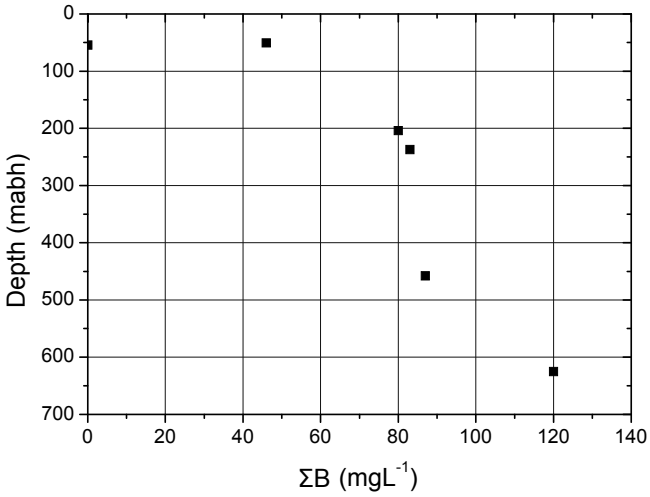

Figure 5.8a: Groundwater total-B vs depth, boreholes HDB-9 – 11

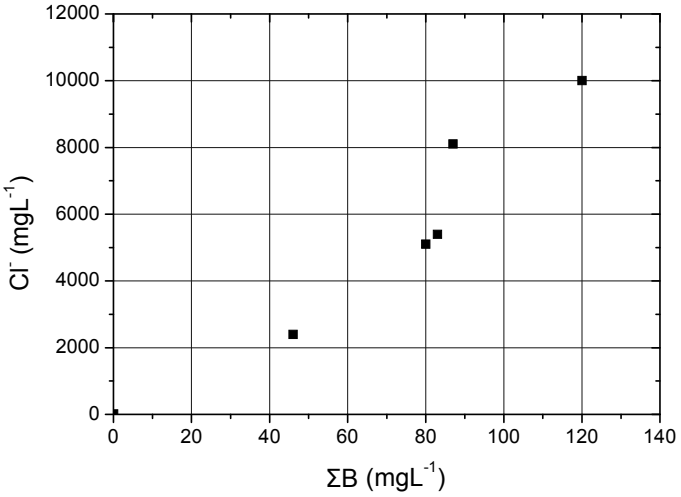

Figure 5.8b: Groundwater total-B vs Cl^-, boreholes HDB-9 – 11

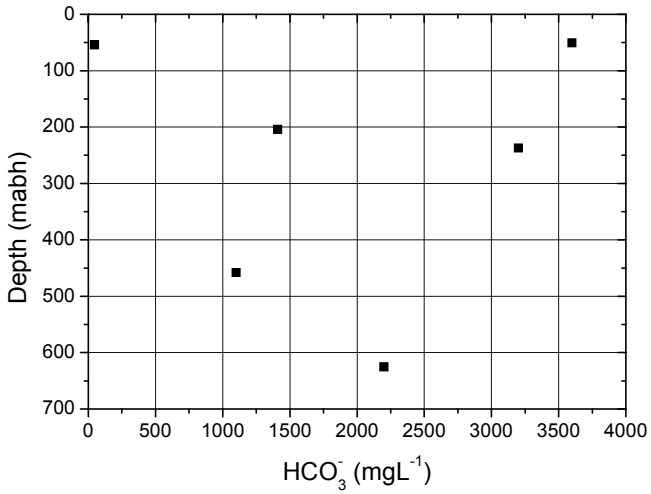

Figure 5.9a: Groundwater HCO_3^- vs depth, boreholes HDB-9 – 11

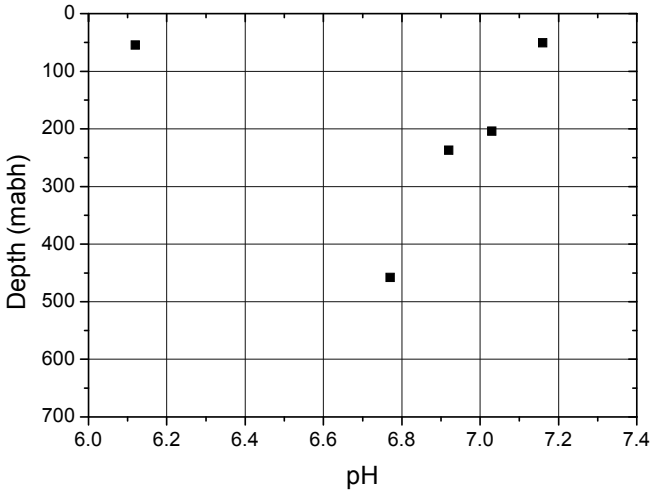

Figure 5.9b: Groundwater pH vs depth, boreholes HDB-9 – 11

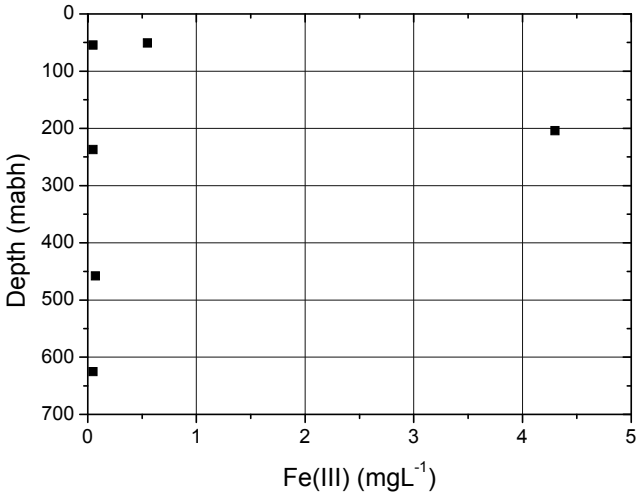

Figure 5.10a: Groundwater Fe(III) vs depth, boreholes HDB-9 – 11

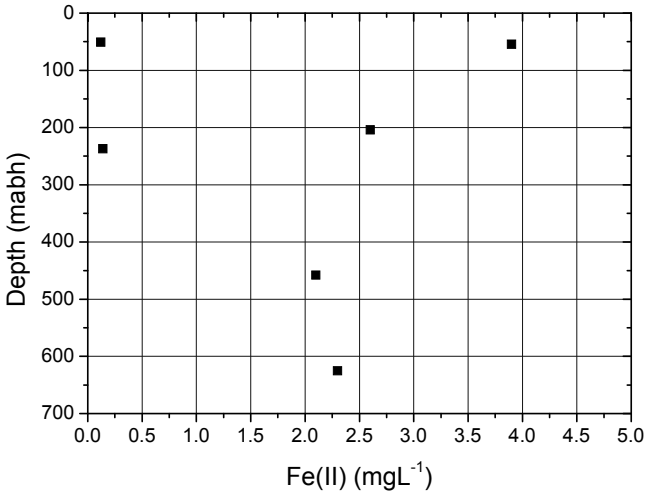

Figure 5.10b: Groundwater Fe(II) vs depth, boreholes HDB-9 – 11

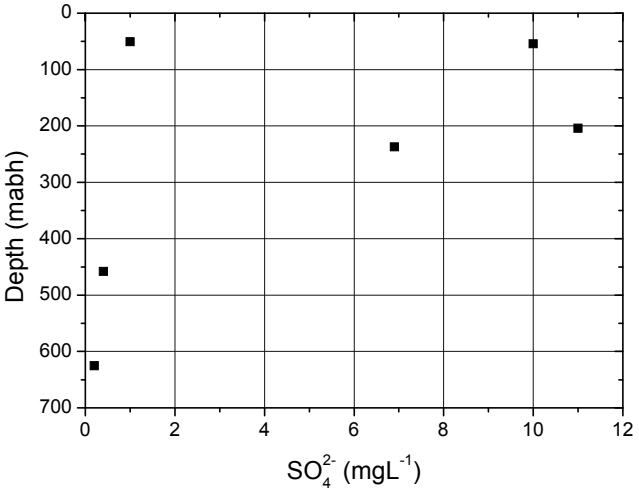

Figure 5.11: Groundwater SO_4^{2-} vs depth, boreholes HDB-9 – 11

The redox sensitive elements indicate the generally reducing nature of the system*, but there is also a clear impact of drilling fluid and other drilling disturbances on the system. In the case of Fe (Figure 5.10), Fe(III) is generally low (<0.1 mgL^{-1}), but with a couple of higher values. Fe(II), in comparison, shows an almost random pattern with no correlation with either the Fe(III) concentrations or those of SO_4 (Figure 5.11). The general pattern of low Fe(III) coupled with relatively high Fe(II) and moderate levels of SO_4 may be taken to indicate pyrite oxidation, presumably in connection with the drilling operations. Unfortunately, there are no data for any other S species with which to further compare the SO_4 data as both H_2S and S^{2-} are below detection limit. Considering the generally disturbed nature of these samples, no particular meaning should be read into those figures. The $\delta^{34}S$ data vary between +5.8 and -9 (cf. modern ocean sulphate of +20 ‰ and modern evaporites of +22 – +23 ‰) and the negative values would tend to suggest the oxidation of ^{34}S – depleted organic S or sedimentary sulphide[49]. However, as noted in Kemp et al.[6] for the HDB-1 and HDB-2 boreholes, "Both boreholes show evidence of the drilling process introducing a sulphate-rich chemical signature into the drilling fluid from either pyrite dissolution or gypsum dissolution or a combination of both mechanisms. Petrographical and core observations clearly show that significant pyrite is present in the host rocks, and that this is susceptible to oxidation. However, the sulphate may also have been derived from the oxidation of trace amounts of pyrite (if present at all) in the bentonite drilling mud."

As such, there is little point in trying to analyse the $\delta^{34}S$ values of these samples further here.

The N system also appears to be at disequilibrium, with generally low values of both NO_2 and NO_3, with NO_2 effectively below detection[19] and NO_3 also present at low concentrations (Figure 5.12a). NH_4 is present at appreciably higher concentrations (Figure 5.12b) and shows a general increase with depth.

Both TOC and TIC depth profiles (Figures 5.13a, b) display a large degree of scatter, but removal of sample 10-pu-1L (depth 50m) which contains 29 % drilling fluid suggests a slowly increasing concentration of organics with depth. Similarly, removal of the same sample from Figure 5.13c leaves a strong correlation between TOC and TIC. Interestingly, comparison with the other boreholes shows large variation in both the TOC and TIC concentrations between boreholes. Once again, these data should not be over-interpreted until they can be put in the context of future higher category data.

* Despite the imperfect nature of the data provided by Eh electrodes, the results are still of use as qualitative indicators of the groundwater conditions at depth. Unfortunately, no in situ data are currently available for these three boreholes.

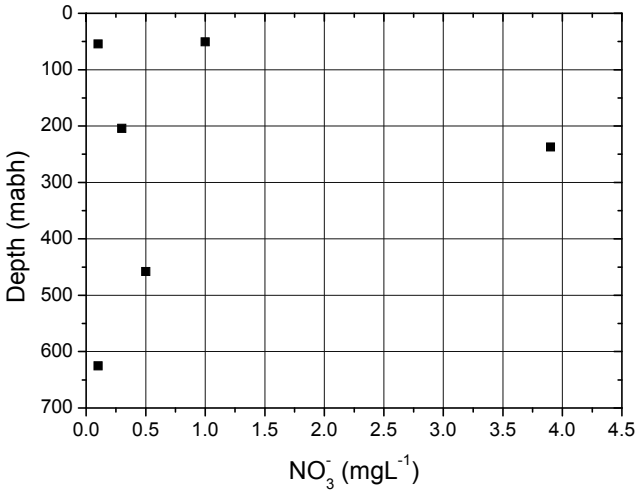

Figure 5.12a: Groundwater NO_3^- vs depth, boreholes HDB-9 – 11

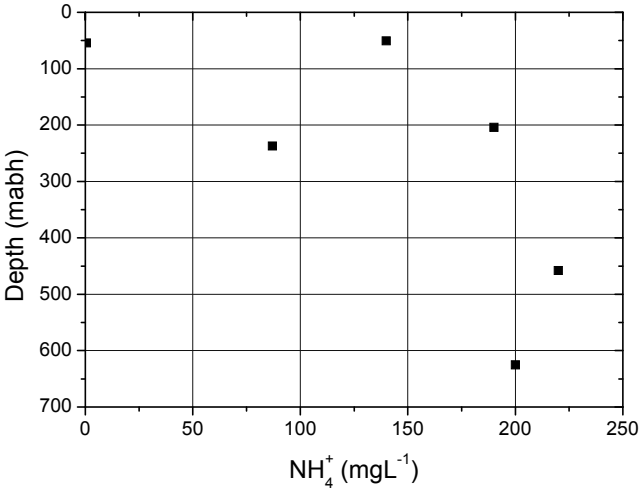

Figure 5.12b: Groundwater NH_4^+ vs depth, boreholes HDB-9 – 11

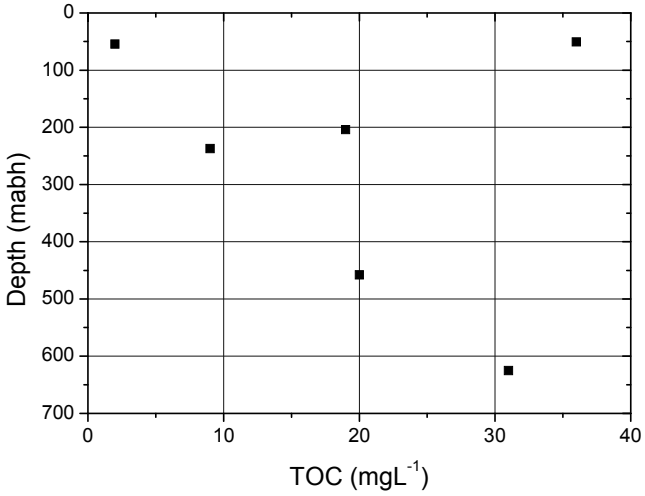

Figure 5.13a: Groundwater TOC vs depth, boreholes HDB-9 – 11

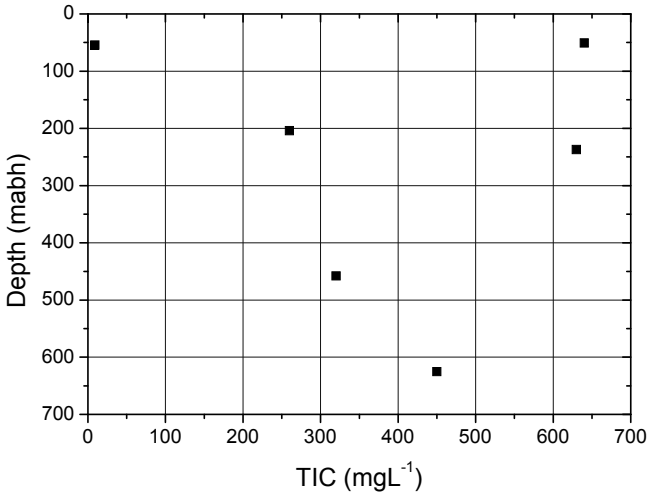

Figure 5.13b: Groundwater TIC vs depth, boreholes HDB-9 – 11

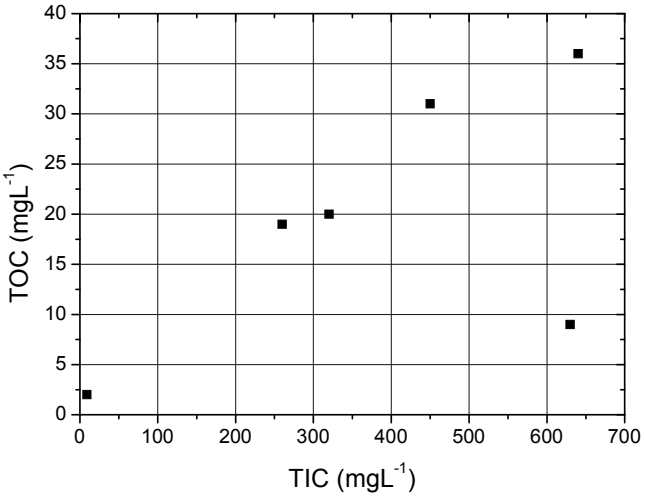

Figure 5.13c: Groundwater TIC vs TOC, boreholes HDB-9 – 11

5.1.4 Stable isotopes

Here, the groundwater stable isotope data will be presented here and discussed briefly. In Figure 2.9, the stable isotope data for boreholes HDB-1 – 8 are plotted and both groundwaters and porewaters suggest only two end-members (one close to the meteoric water line, the other enriched in $\delta^{18}O$ compared to seawater) and, although representing only 6 data points, this trend is very much replicated here (Figure 5.14).

Interestingly, plots of δD and $\delta^{18}O$ versus depth (Figure 5.15a, b) show a slow but continuous enrichment with increasing depth. Not surprisingly, both isotopes show similar trends when plotted against Cl (Figure 5.16a, b).

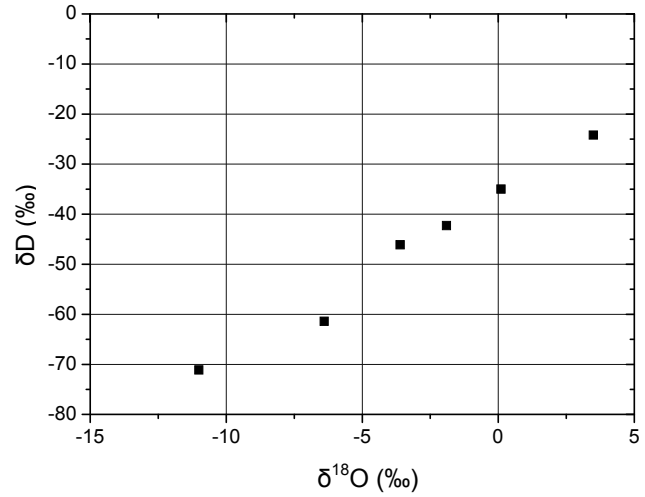

Figure 5.14: Groundwater $\delta^{18}O$ vs δD, boreholes HDB-9 – 11

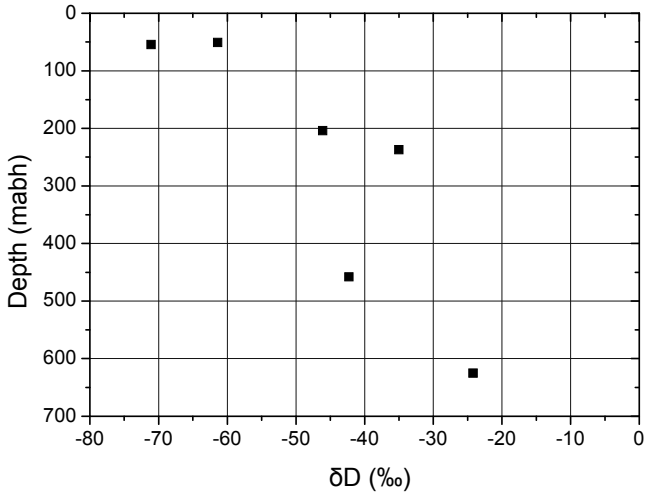

Figure 5.15a: Groundwater δD vs depth, boreholes HDB-9 – 11

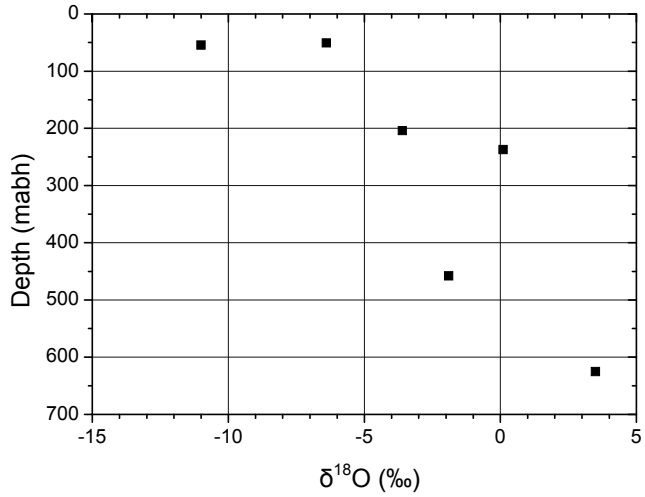

Figure 5.15b: Groundwater $\delta^{18}O$ vs depth, boreholes HDB-9 – 11

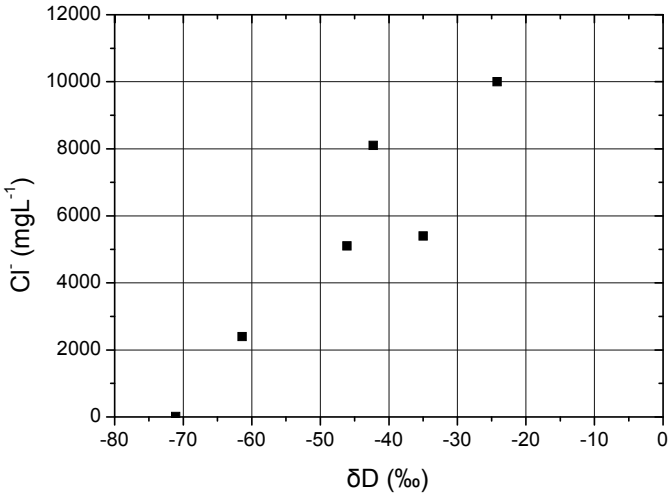

Figure 5.16a: Groundwater δD vs Cl^-, boreholes HDB-9 – 11

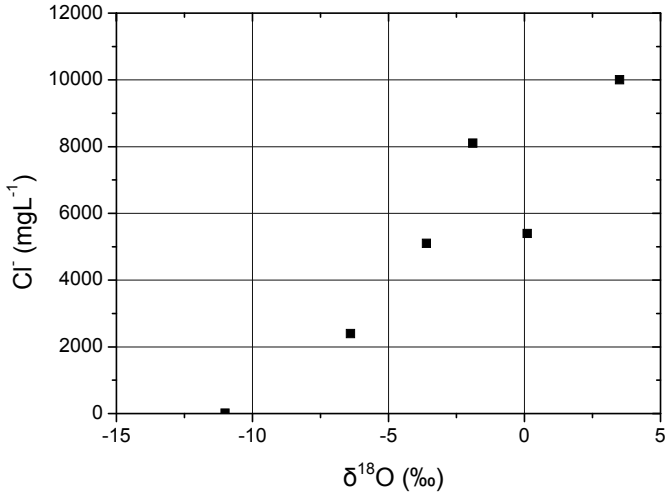

Figure 5.16b: Groundwater $\delta^{18}O$ vs Cl^-, boreholes HDB-9 – 11

5.1.5 Conclusions

The groundwater data presented above are all classified as low category as they were collected during the drilling and hydraulic testing phase of the respective boreholes. As the brief discussions above have shown, the generally large percentages of drilling fluids present make any more detailed analysis of the samples senseless. Nevertheless, it should be noted that the data presented here show pretty much the same trends as has been observed for the HDB-1 – 8 data and, as such, support the preliminary site conceptual model. In addition, although these data will be supplemented by new data from samples taken in the post-drilling and testing phase, they will not be superseded as they will still be of use in qualitative support of the higher category data.

As noted above, most elements show similar trends, with slow but sure increases in concentration with depth, masked slightly in those more reactive elements. Despite the

coastal nature of the site, all are considerably diluted when compared to SMOW values (at between 50 and 60 %), and Sasamoto[5] proposal that the groundwater includes at least a marine end-member.

Interestingly, the B/Cl, I/Cl and Br/Cl ratios of the groundwaters are significantly higher than that for seawater, indicating an additional source of all three trace elements. Plotting B against Cl indicates a close correlation, but at a B : Cl ratio (around 2×10^{-2}) which is much higher than observed in seawater (around 2×10^{-4}), indicating an additional source of B to the groundwater. As all three of these trace elements would be present in marine organics contained in the sediments, they could be released from this source during burial. Intriguingly, both TOC and TIC also increase in concentration with depth, perhaps backing up the marine-derived organic source. This could be checked in future by a more detailed analysis of the form of the organics, looking for evidence of marine signatures.

Perhaps of greatest interest is the clear signature from the stable isotopes of a two end-member system, with one representative of current surface waters while the other represents a significantly enriched source. This will be discussed further in Section 5.3.4 where significantly more porewater samples are available.

Finally, there would appear to be evidence for a mixing zone in the top 0 – 200 m of the sediment column, presumably indicating the presence of a more active hydrogeological system than at depth. This needs to be examined further in collaboration with the site hydrogeological conceptual model, but there certainly appears to be indications of signals more representative of deeper groundwaters in this zone.

5.2 Porewaters

5.2.1 Overview

This is a unique dataset insofar that never before have so many samples been collected for porewater analysis in a site characterisation. Certainly it is part of an increasing trend since the first dedicated samples were collected as an integral part of Nagra's site characterisation of the Opalinus Clay at Benken in northern Switzerland[50]. This has now been successfully repeated in other relatively tight rocks in the ongoing Swedish site characterisation programme[12), 34) – 36)] and at the Mont Terri, Büre, Äspö and Grimsel URLs.

In Horonobe, the higher porosity and permeability of the host rock means that much more data are available on the porewater than in any of the previous studies – in fact, there are currently more porewater data on the site than there are groundwater data (cf. Figure 2.6). Unfortunately, the current lack of information on potential drilling fluid contamination (and dilution) of the porewater means that the true QA category of these samples is unclear. Although JAEA cleaned up the core samples on site (see Section 3.3) and they were then further treated in the laboratory[26] as would also be done with tight rock samples, it does not immediately follow that these porous and permeable samples are now free of drilling fluid.

Waber and Smellie[21] tried to check this for their tight rock samples from the Fennoscandian Shield, but a lack of porewater precluded any definitive answer.

5.2.2 Major elements

(1) Cl

Cl versus depth in all 3 boreholes shows a general slow increase with depth, but the details vary from borehole to borehole. In HDB-9, there is a clear, near-surface, low Cl zone down to at least 80 mabh and this is followed by a gap to 150 mabh by which point the Cl concentration has increased by more than an order of magnitude (Figure 5.17a). Interestingly, this is also observed in the groundwater from the same core (although the presumed mixing zone is also not sampled here). Porewater Cl then increases slowly to 8600 mgL^{-1} at 347 mabh after which it slowly falls again. Similar effects have been observed at depth in HDB-2 (at around 650 mabh) and in HDB-1 (around 550 mabh).

In HDB-10, the increase is more uniform with depth and at a greater gradient than in HDB-9. The near-surface very low Cl zone is missing here, also reflected in the groundwater Cl data[19]. There is also some scatter at depth, between 400 and 550 mabh, which may be due to the presence of fractures. For example, in sample 10SQ_06_01 (447.0 – 447.35 mabh) with a Cl concentration of 7400 mgL^{-1} (which is higher than the sample above and below; Figure 5.17b), the groundwater Cl concentration for the appropriate sampling interval (445.89 – 469.89 mabh) increases through the time series (10-pu-2-1 to 10-pu-2L) to a maximum of 8100 mgL^{-1} (with 8 % drilling fluid). Unfortunately, this core section is missing from the photographic record and so cannot be checked for the existence of fractures. Likewise for sample H10SQ_12_02 (397.4 – 397.7 mabh) where it appears that the sub-sample has been removed before the photographic record could be made. All other samples are available, unfortunately only the two which lie at the point of the main increase with depth trend are not available.

In HDB-11, there is a very sharp increase in porewater Cl over the first 300 m (from 1400 to over 10000 mgL^{-1}; Figure 5.17c). From here to the borehole bottom at ~853 mabh, there is considerable scatter in the Cl concentration, but with a definite low around 449 mabh with sample H11SQ_10_02 (448.7 – 449 mabh) containing only 6930 mgL^{-1} Cl. Here the core record is intact (Figure 5.18) and there is clear evidence of a fracture in the core at 448.7 mabh. Unfortunately, there are no groundwater data for anywhere near this horizon for comparison with this lower Cl zone.

The next zone where groundwater data do exist is sample 11-pu-2L (606.00 – 644.15 mabh) which has a Cl content of 10000 mgL^{-1} (10 % drilling fluid). Here, the 2 porewater samples which straddle this zone (H11SQ_14_03, just below the zone at 644.81 – 645.00 mabh and, just above the zone, H11SQ_13, 599.05 – 599.50 mabh) contain 9200 and 9400 mgL^{-1} Cl respectively. Both these samples are defined by fractures, one at the top of H11SC_14_03 and one at the top and the base of H11SQ_13.

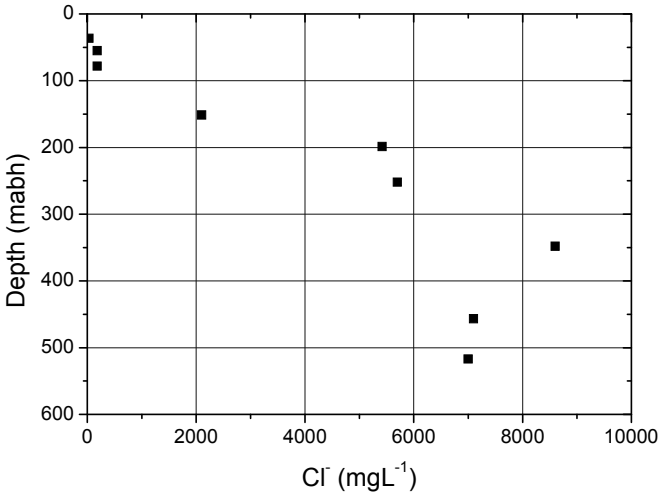

Figure 5.17a: Porewater Cl^- vs depth, borehole HDB-9

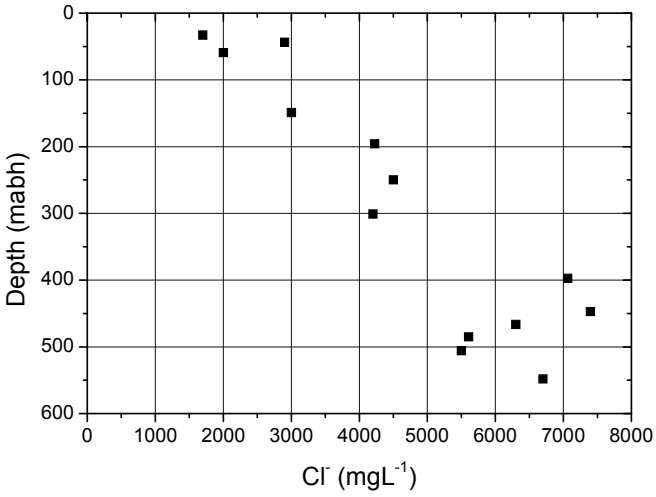

Figure 5.17b: Porewater Cl^- vs depth, borehole HDB-10

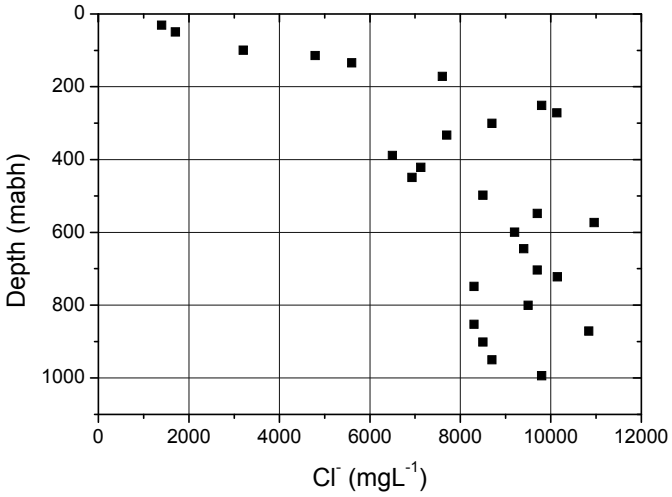

Figure 5.17c: Porewater Cl^- vs depth, borehole HDB-11

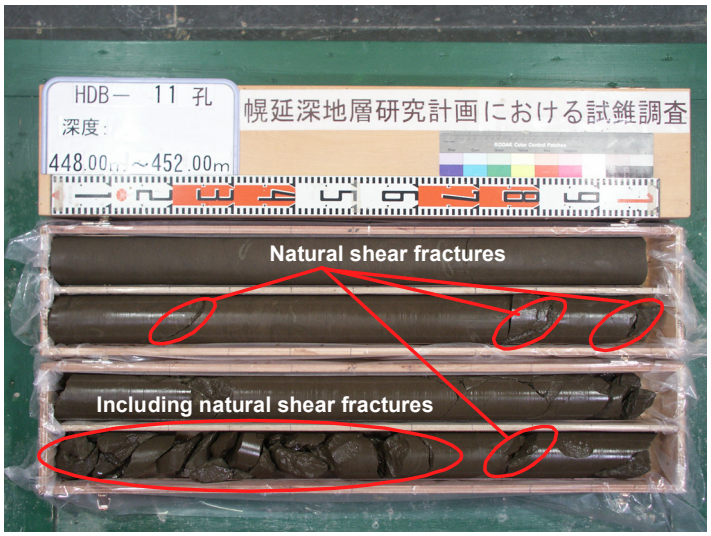

Figure 5.18: Photographic record of core section HDB-11 448 – 452 mabh. The base of the sampled section (448.7 – 449 mabh) shows clear evidence of a fracture

(2) Ca

The porewater Ca concentrations versus depth are shown in Figure 5.19a – c. There is a significant amount of scatter in all 3 boreholes, especially in HDB-11, but there is a general increase in Ca concentration with depth in HDB-9 and HDB-10, reflecting the very general trend in the groundwater Ca concentrations. There is also a significant increase in the maximum Ca concentrations from around 70 mgL^{-1} in HDB-9 to 200 mgL^{-1} in HDB-10 to over 250 mgL^{-1} in HDB-11. Interestingly, there appears to be no particular correlation between Ca concentrations for those samples squeezed in gloveboxes ranging, in HDB-11, for example, between 72 and 259 mgL^{-1} Ca. The large scatter is presumably a reflection of oxidation effects (e.g. pyrite oxidation releasing sulphate which combines with Ca in solution to form gypsum) and CO_2 uptake forming carbonate etc.) due to the relatively high O_2 content in the system[26].

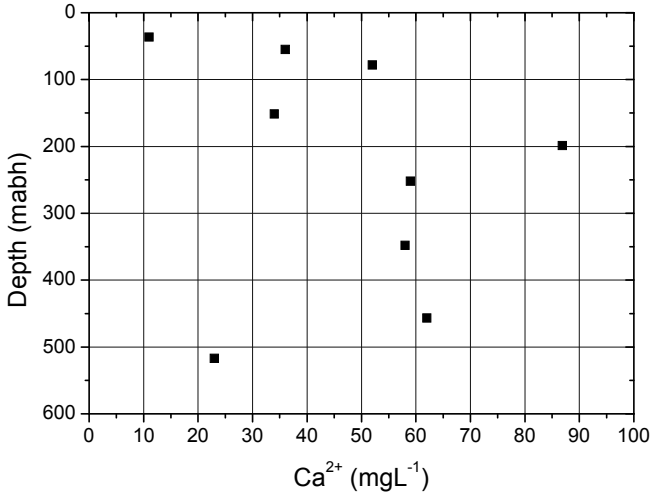

Figure 5.19a: Porewater Ca^{2+} vs depth, borehole HDB-9

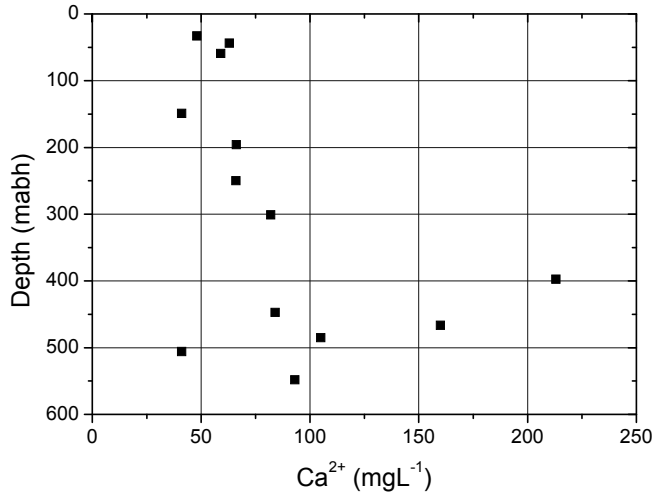

Figure 5.19b: Porewater Ca^{2+} vs depth, borehole HDB-10

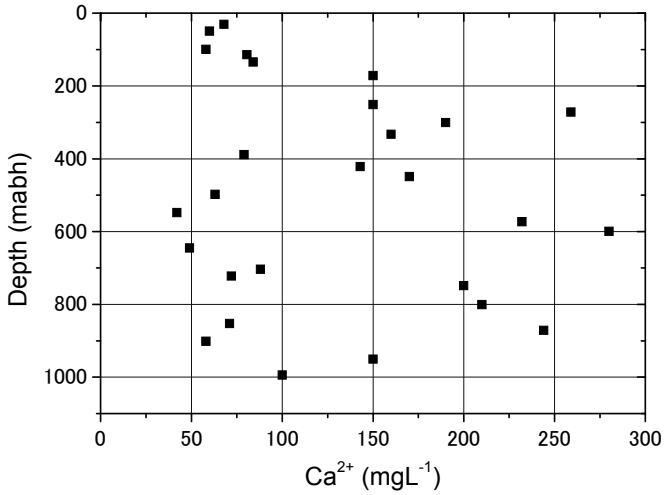

Figure 5.19c: Porewater Ca^{2+} vs depth, borehole HDB-11

(3) K

The porewater K concentrations versus depth are plotted in Figure 5.20 and the trends are similar to Ca in that the highest porewater K concentration increases from HDB-9 – 11. Once again, the glovebox squeezed samples are scattered throughout the concentration range (e.g. 87 – 279 mgL^{-1} in HDB-11) and show no particular pattern compared to the non-glovebox samples. Interestingly, the form of the K versus depth profile for all 3 boreholes is quite similar, showing a fast increase at shallow depths which tails of slightly (in HDB-9 and HDB-10) to a maximum around 200 m (slightly deeper in HDB-11) followed by a general drop back to near-surface levels at core bottom (N.B. remember the absolute concentration differences between the three cores and the fact that HDB-11 is over 200 mabh deeper than the other two). This general form is similar to that seen in the groundwaters (cf. Figure 5.1c).

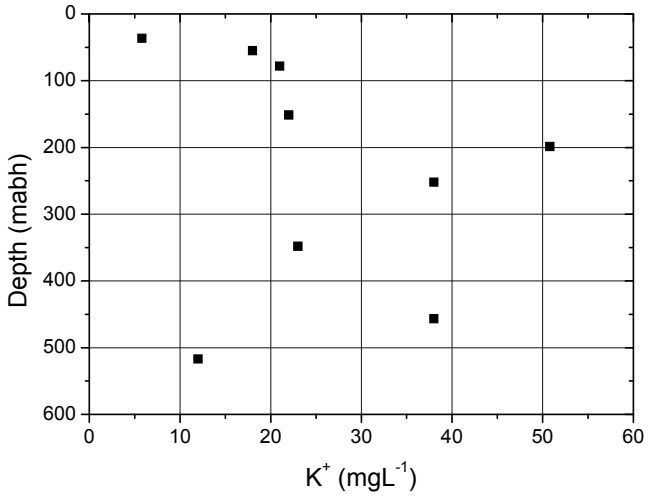

Figure 5.20a: Porewater K^+ vs depth, borehole HDB-9

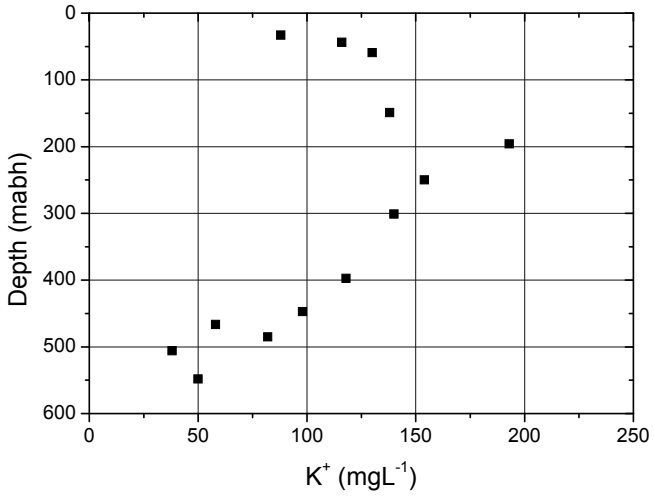

Figure 5.20b: Porewater K^+ vs depth, borehole HDB-10

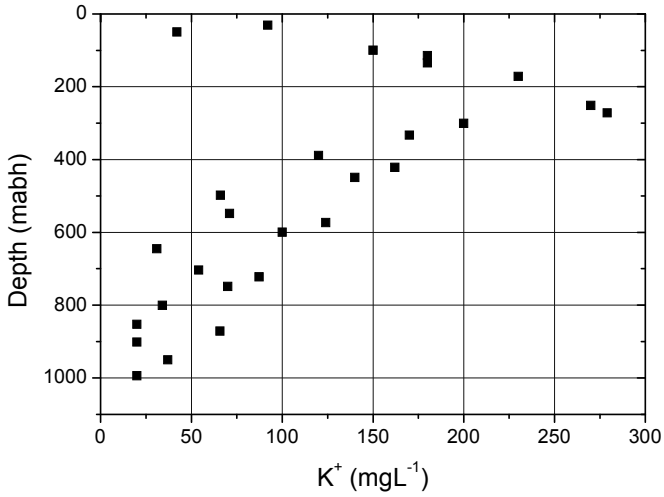

Figure 5.20c: Porewater K^+ vs depth, borehole HDB-11

(4) Mg

The porewater Mg concentrations versus depth are plotted in Figure 5.21a – c and the trends are similar to Ca (and K) in that the highest porewater Mg concentration increases from HDB-9 – 11. Once again, the glovebox squeezed samples are scattered throughout the concentration range and show no particular pattern compared to the non-glovebox samples. The HDB-9 profile is similar to the HDB-9 – 11 groundwater profile, showing a slow, but steady, concentration increase with depth. The Mg versus depth profile for HDB-10 is quite different, showing a very slow increase in concentration until around 400 mabh followed by a very rapid increase to a maximum of 140 mgL^{-1}.

The Mg versus depth profile for HDB-11 is different again, showing a mid-depth peak not dissimilar to K. However, unlike with K, the concentration decrease stops at 400 mabh and is followed by another increase with depth (Figure 5.21c). This is similar to the Cl versus depth profile for HDB-11 (Figure 5.17c), and the correlation between both elements can be clearly seen in Figure 5.21f. Although less strong, Mg and Cl also show correlation in boreholes HDB-9 and HDB-10 (Figures 5.21d and 5.21e, respectively). This would appear to be additional evidence for the possible presence of a relict marine signal in the Horonobe groundwater system (cf. Figure 5.2).

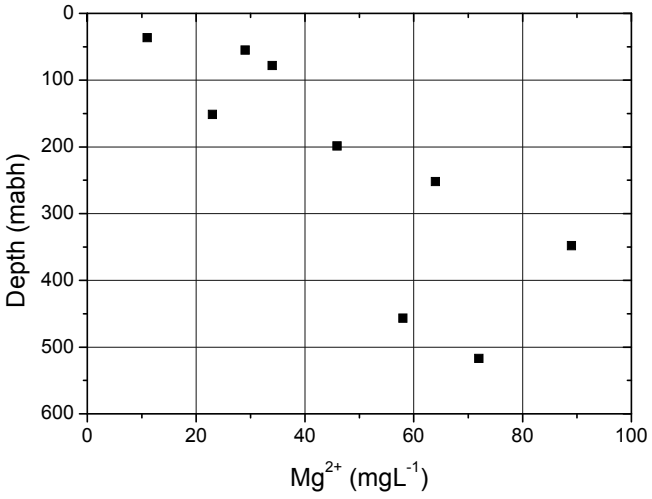

Figure 5.21a: Porewater Mg^{2+} vs depth, borehole HDB-9

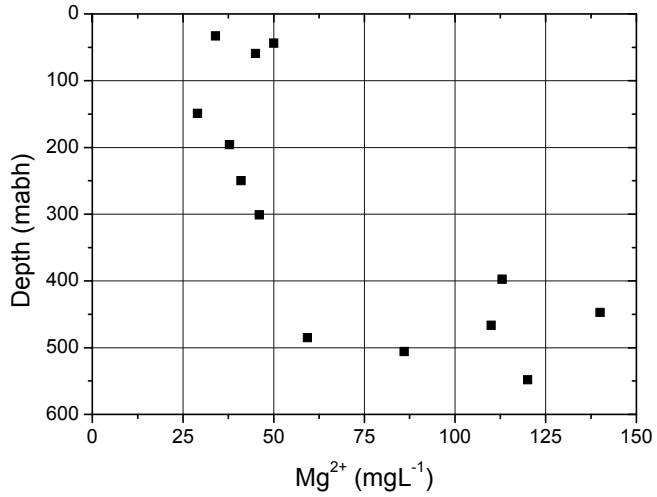

Figure 5.21b: Porewater Mg^{2+} vs depth, borehole HDB-10

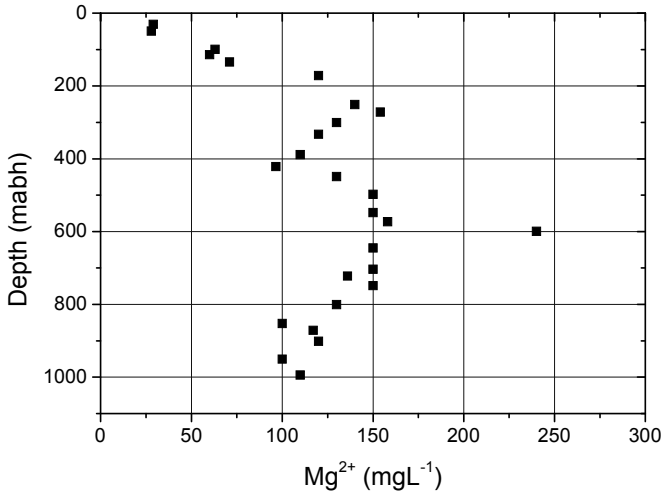

Figure 5.21c: Porewater Mg^{2+} vs depth, borehole HDB-11

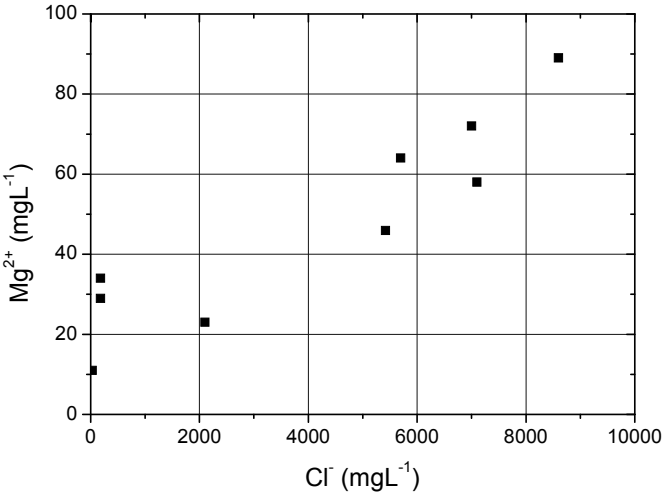

Figure 5.21d: Porewater Mg^{2+} vs Cl^-, borehole HDB-9

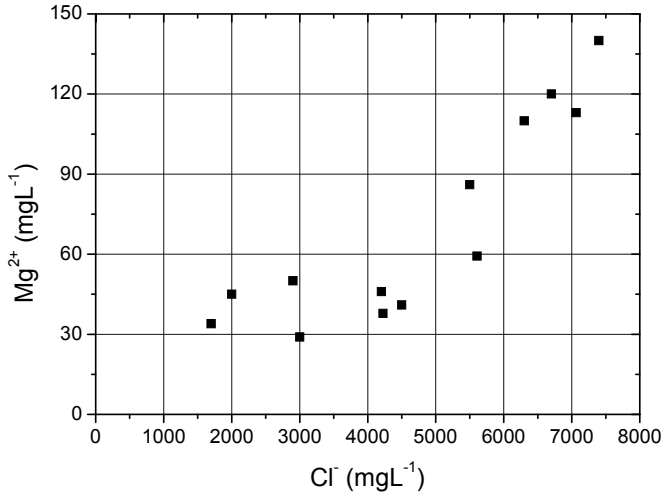

Figure 5.21e: Porewater Mg^{2+} vs Cl^-, borehole HDB-10

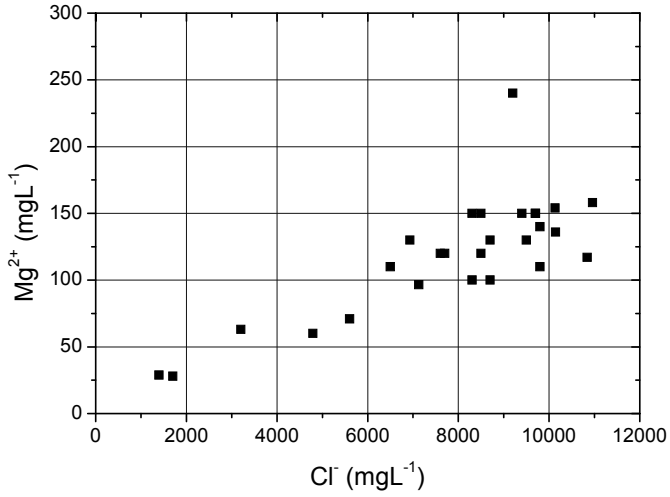

Figure 5.21f: Porewater Mg^{2+} vs Cl^-, borehole HDB-11

(5) Na

The similar behaviour of Mg and Na has been noted for the HDB-9 – 11 groundwaters and this appears to be reflected in the porewaters too with the HDB-9 and HDB-11 Na versus depth profiles looking strikingly similar to that of Mg (Figure 5.22). The Na versus depth profile for HDB-10 is less similar to that of Mg but, for all 3 boreholes, there is a strikingly strong Na versus Cl correlation, once again in agreement with that seen for the groundwaters (cf. Figure 5.2).

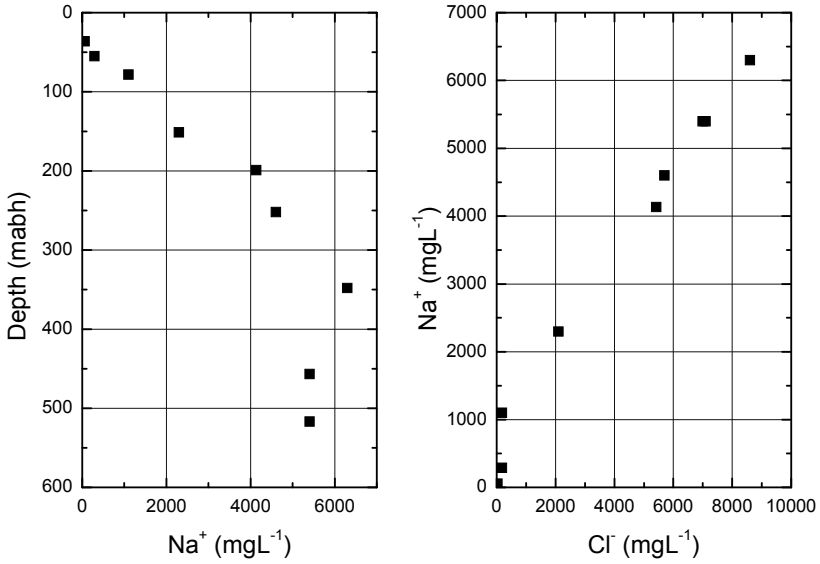

Figure 5.22a: Na^+ vs depth in the HDB-9 porewaters (left) and Na^+ vs Cl^- in the HDB-9 porewaters (right)

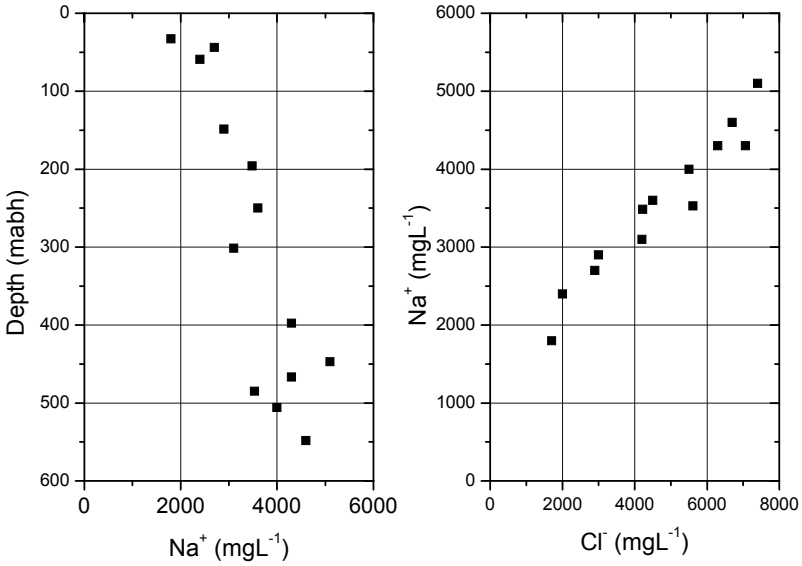

Figure 5.22b: Na^+ vs depth in the HDB-10 porewaters (left) and Na^+ vs Cl^- in the HDB-10 porewaters (right)

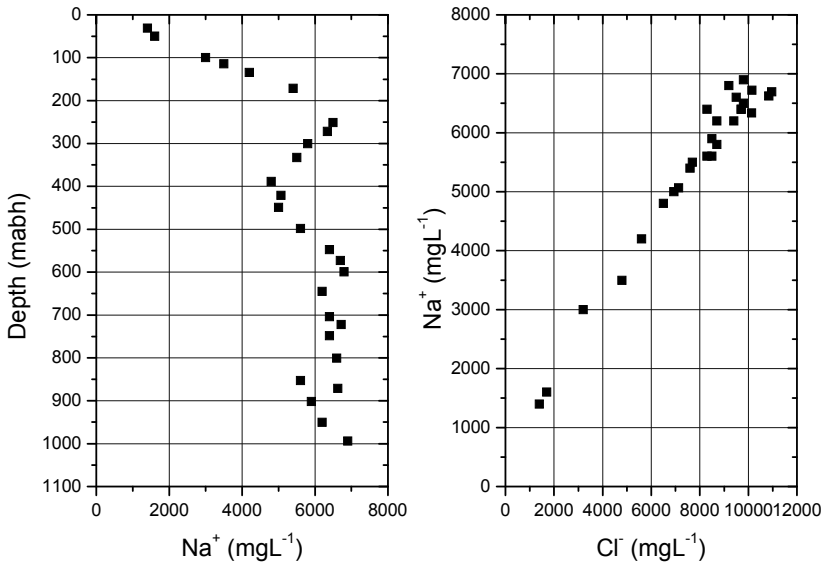

Figure 5.22c: Na^+ vs depth in the HDB-11 porewaters (left) and Na^+ vs Cl^- in the HDB-11 porewaters (right)

(6) Li

Once again, the pattern of maximum concentrations increasing from HDB-9 – 11 can be seen here. Li concentration versus depth profiles in boreholes HDB-9 and 11 (Figure 5.23a – c) are similar to those of K in the same boreholes (Figure 5.20a – c) and there is clearly a correlation between them in the porewater (stronger in HDB-11), presumably reflecting a similar source, such as reaction with clays or feldspars (the other obvious source, biotite, appears to be absent from these sediments). The relationship is clearly non-existent in HDB-10, suggesting that a different Li reaction is ongoing here. Unfortunately, groundwater Li data are limited to only 5 analyses above the detection limit, so making any interpretation of this dataset more difficult, but there may be mineralogical differences between the boreholes which could shed light on the differing controls on Li concentrations in the 3 boreholes.

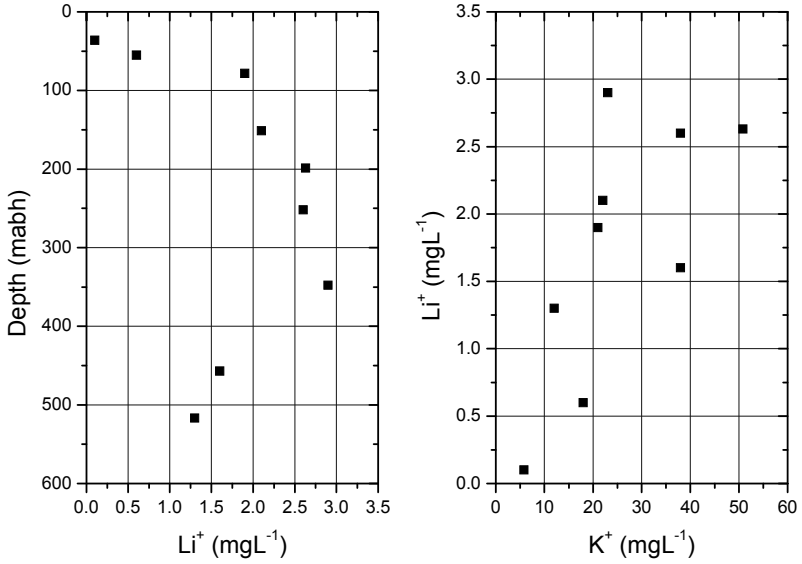

Figure 5.23a: Li^+ vs depth in the HDB-9 porewaters (left) and Li^+ vs K^+ in the HDB-9 porewaters (right)

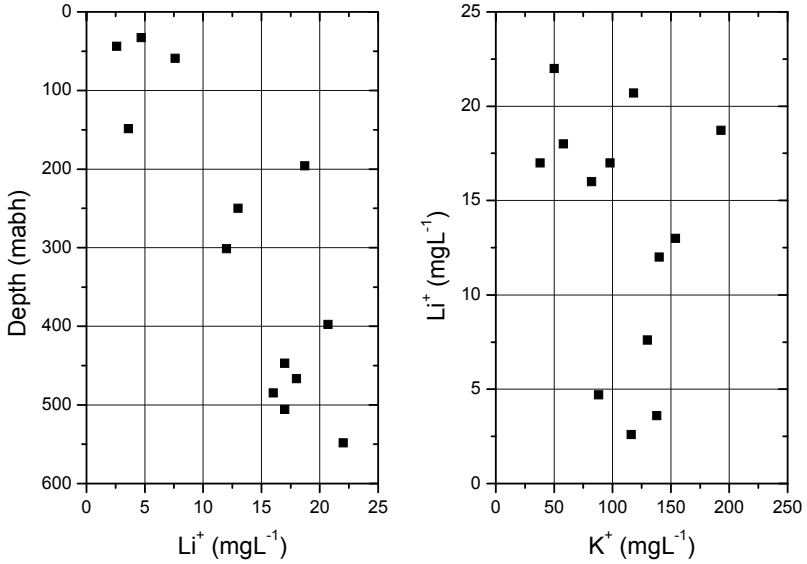

Figure 5.23b: Li^+ vs depth in the HDB-10 porewaters (left) and Li^+ vs K^+ in the HDB-10 porewaters (right)

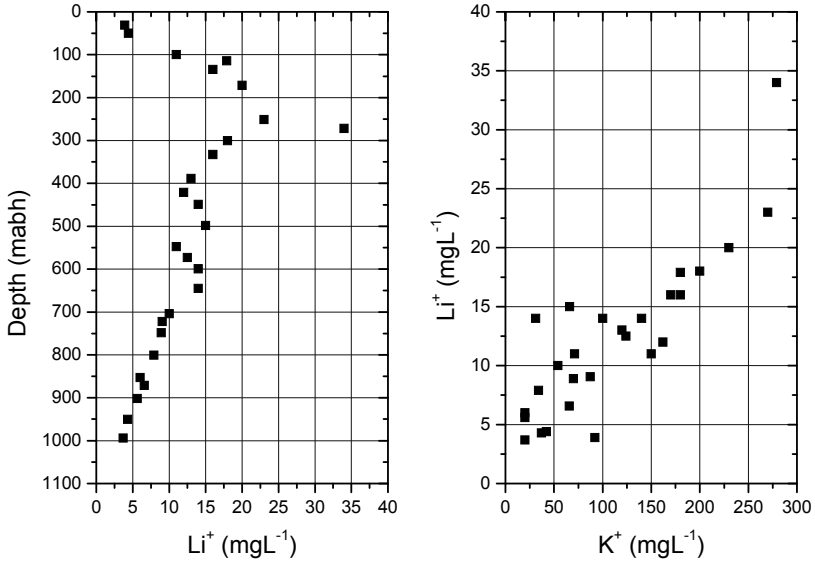

Figure 5.23c: Li^+ vs depth in the HDB-11 porewaters (left) and Li^+ vs K^+ in the HDB-11 porewaters (right)

(7) pH, CO_3 and HCO_3

pH, CO_3 and HCO_3 all appear to be showing signs of handling-induced perturbations, with all showing scatter in the data (Figures 5.24 – 5.26). Once again, the glovebox squeezed samples appear to have fared no better than those squeezed in air. For example, for HDB-11, the pH of the glovebox samples range from almost the lowest (7.93) to the highest (8.7; see Figure 5.24 and Kunimaru et al.[19]) and a similar picture emerges for CO_3 and HCO_3. The scatter in the pH data is probably no greater than that seen in the groundwaters (cf. Figure 5.9), but has been shifted around a pH unit higher in the porewaters, presumably due to consumption of CO_2.

Nevertheless, some trends are clear; for CO_3, outside the handling-induced scatter, the concentration is generally <20 mgL^{-1} in all 3 boreholes (Figure 5.25) and, for HCO_3 (Figure 5.26), there is a decrease in concentration with depth (from around 2500 to 3000 mgL^{-1} near-surface to <500 mgL^{-1} at depth), suggesting consumption of HCO_3 at depth. Although there is also a lot of scatter in the groundwater HCO_3 data, a similar trend with similar concentrations is observed (unfortunately, no groundwater CO_3 data exist for comparison).

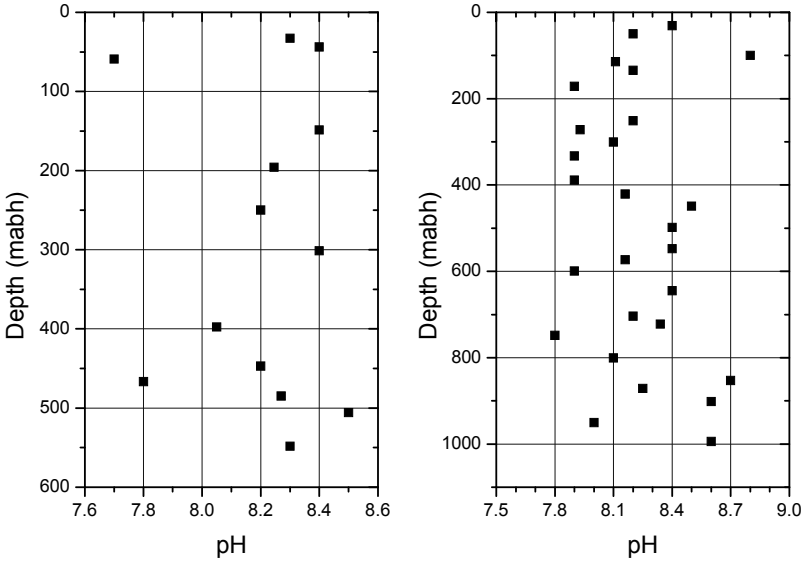

Figure 5.24: pH vs depth in the HDB-10 (left) and HDB-11 (right) porewaters

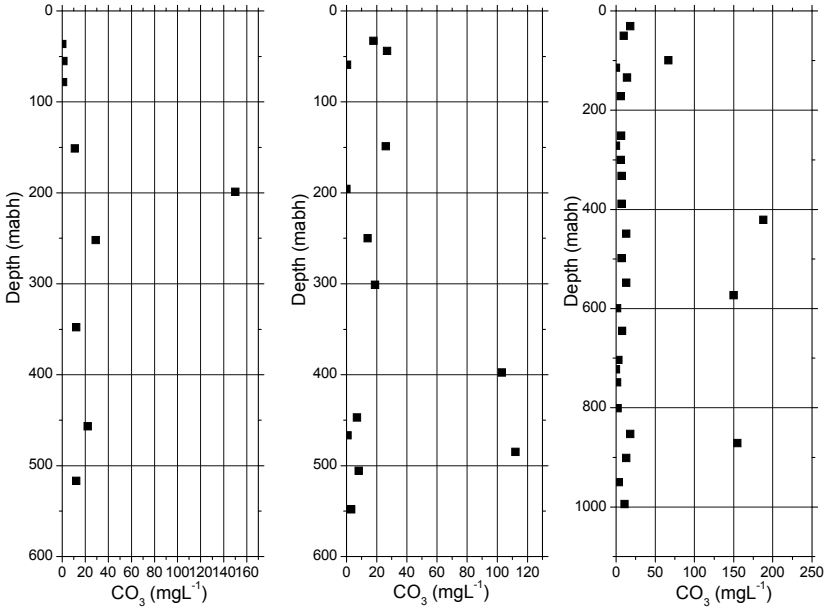

Figure 5.25: CO_3^{2-} vs depth in the HDB-9 (left), HDB-10 (centre) and HDB-11 (right) porewaters

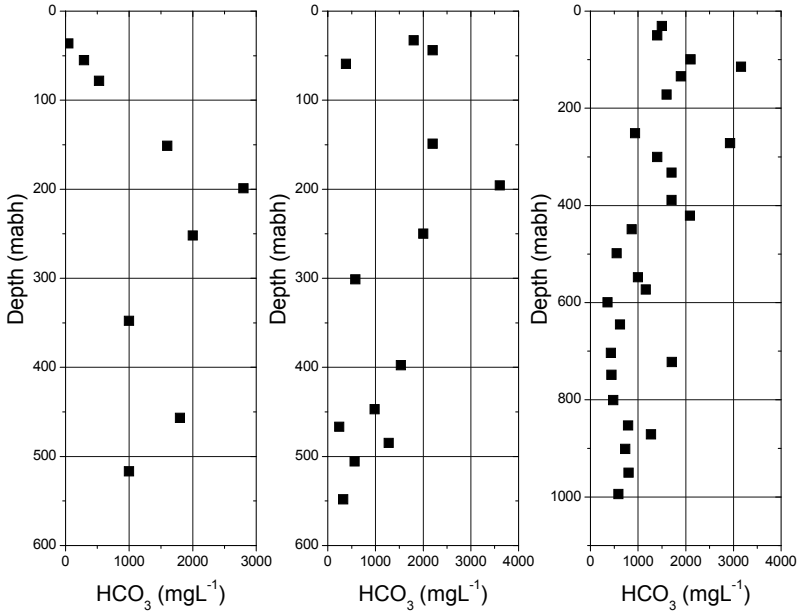

Figure 5.26: HCO_3^- vs depth in the HDB-9 (left), HDB-10 (centre) and HDB-11 (right) porewaters

(8) ΣFe

Some ΣFe data are available for all 3 boreholes and the concentrations (e.g. HDB-11 in Figure 5.27) do not compare well with the Fe(II)and Fe(III) groundwater concentrations (cf. Figure 5.10), suggesting sample disturbance. Pyrite, siderite and magnesite have all been reported in these sediments[6] so it will be necessary to examine directly the core mineralogy to assess which phase is controlling the Fe concentrations.

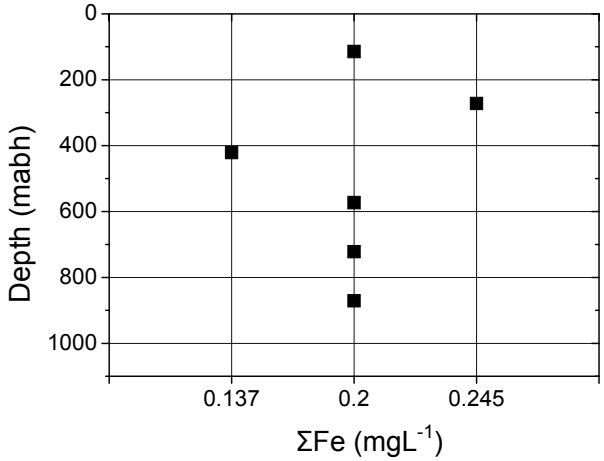

Figure 5.27: Porewater total-Fe vs depth, borehole HDB-11

(9) SO_4

Plots of SO_4 versus depth for all 3 boreholes are presented in Figure 5.28. As with the carbonate system, the S system also looks to have been affected by sample handling, with the pyrite reacting with O_2 to release pyrite and possibly dissolution of gypsum[6]. That the pH has remained high (Figure 5.24) favours the latter mechanism. The fact that the levels observed in the porewater are significantly higher than the groundwater SO_4 concentrations (maximum of 11 mgL^{-1}, some 2 orders of magnitude lower than the porewaters) gives additional weight to the sample disturbance thesis as otherwise a significant SO_4 signal would be evident in the groundwaters.

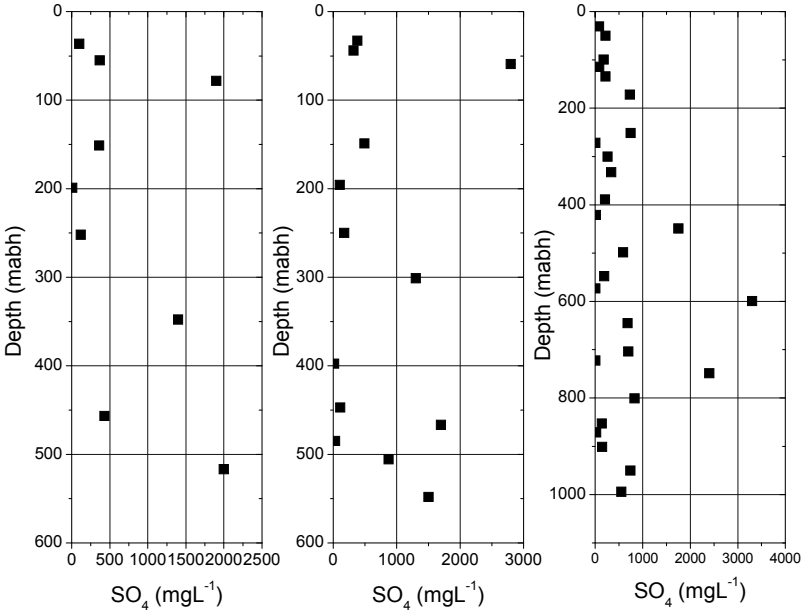

Figure 5.28: SO_4^{2-} vs depth in the HDB-9 (left), HDB-10 (centre) and HDB-11 (right) porewaters

(10) TIC and TOC

As in the HDB-9 – 11 groundwaters, the TIC in HDB-9 – 11 porewaters is about an order of magnitude higher than are the TOC levels (Figure 5.29a – d). In HDB-9, both TOC and TIC show a peak at around 200 mabh and then concentrations decrease with depth. A not dissimilar picture can be seen in borehole HDB-10, with similar absolute concentrations to those seen in HDB-9. In HDB-11, the peak in TIC occurs at shallower depth as it may also do in the TOC plot, but the greater degree of scatter here makes this less convincing. No such peak can be discerned in the groundwater samples (cf. Figure 5.13a, b) and the porewater TIC/TOC correlation is much weaker than in the groundwaters (cf. Figure 5.29d and 5.13c).

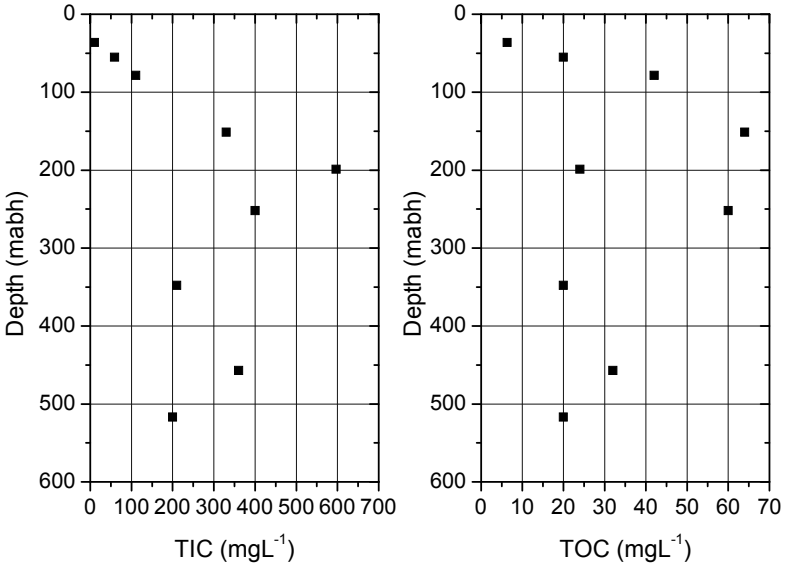

Figure 5.29a: Porewater TIC (left) and TOC (right) vs depth, borehole HDB-9

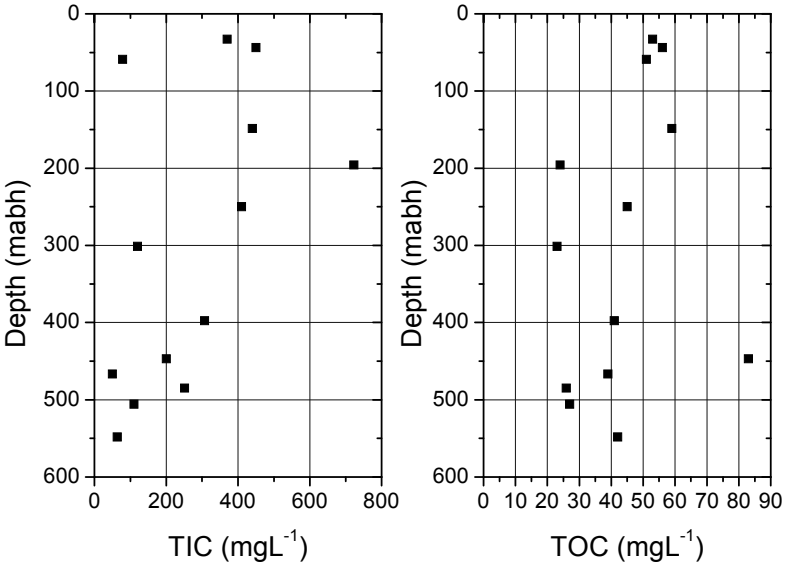

Figure 5.29b: Porewater TIC (left) and TOC (right) vs depth, borehole HDB-10

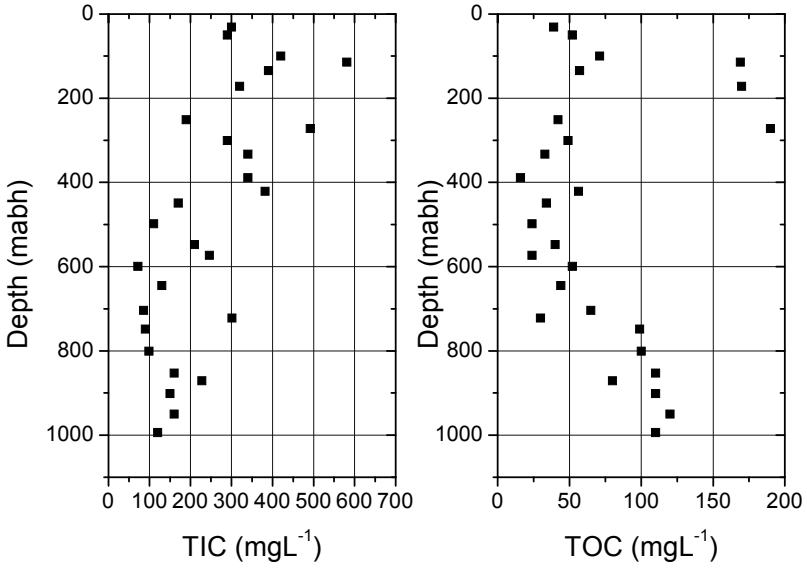

Figure 5.29c: Porewaters TIC (left) and TOC (right) vs depth, borehole HDB-11

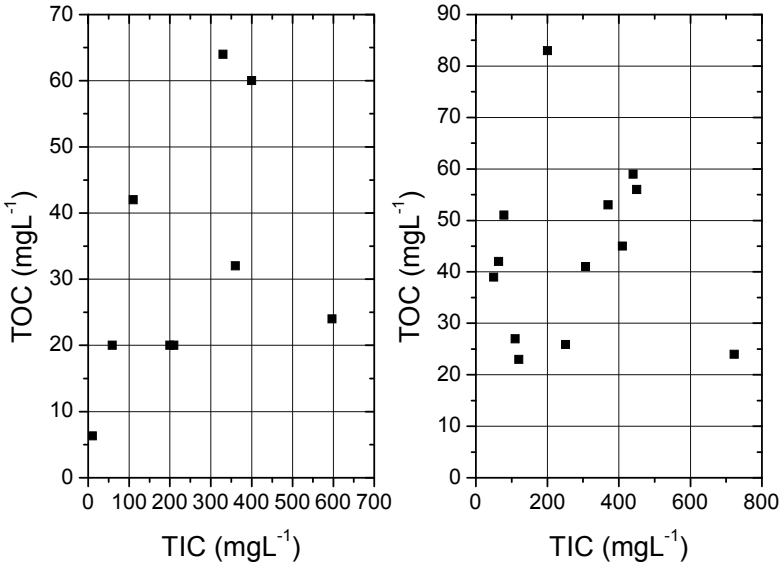

Figure 5.29d: TIC vs TOC in the HDB-9 porewaters (left) and TIC vs TOC in the HDB-10 porewaters (right)

(11) Stable isotopes

The stable isotope data for all 3 boreholes are presented in Figures 5.30a, b and 5.31a, b, but here it is of note that there is an increase in enrichment with depth to around 200 – 300 mabh followed by a generally invariant signal below this depth, similar to that reported for HDB-1 – 8[51]. Due to the few groundwater samples, it is difficult to make a meaningful comparison of the data, but the general trends and degree of enrichment are very similar. Not surprisingly, the plots of the stable isotopes against Cl (Figure 5.31a, b), show a strong correlation in both cases.

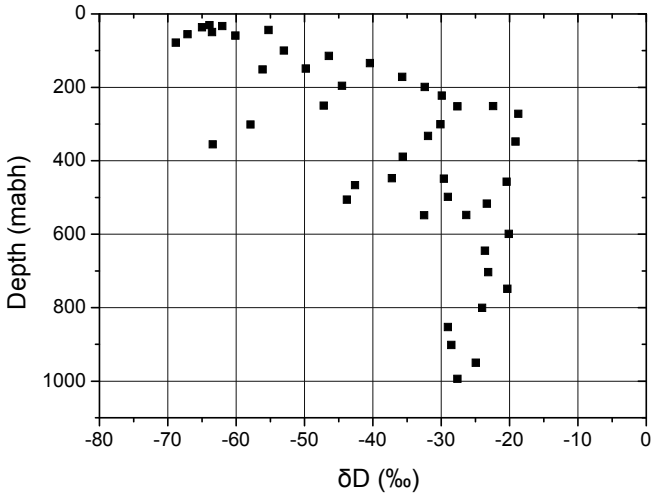

Figure 5.30a: Porewater δD vs depth, boreholes HDB-9 – 11

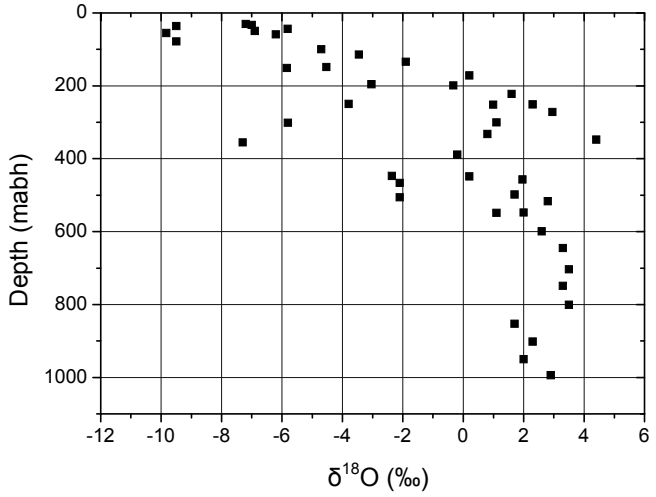

Figure 5.30b: Porewater $\delta^{18}O$ vs depth, boreholes HDB-9 – 11

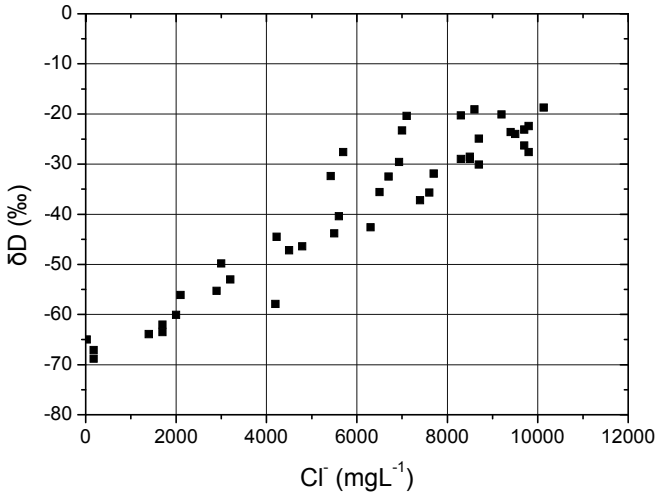

Figure 5.31a: Porewater δD vs Cl^-, boreholes HDB-9 – 11

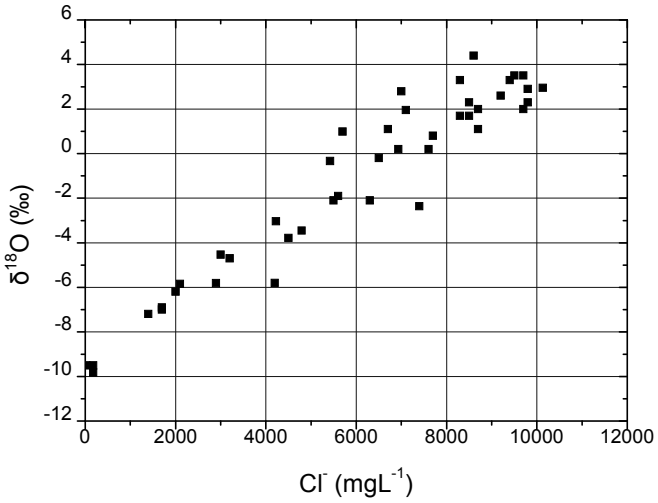

Figure 5.31b: Porewater $\delta^{18}O$ vs Cl^-, boreholes HDB-9 – 11

(12) Conclusions

The porewater concentrations are very similar to those of the groundwaters for most elements other than those which are strongly disturbed by handling and squeezing. Similarly with the concentration versus depth trends (cf. K in Figures 5.1c and 5.20), although a lack of groundwater data means that the fine details observed in the porewater profiles are often lost in the groundwaters (cf. Mg in Figures 5.1d and 5.21). In addition, the fact that few porewater samples coincide with the groundwater sampling intervals makes direct comparison problematic. Unfortunately, flow-logging[1)] has shown it to be impossible to unambiguously define specific inflow points in boreholes, even when specific fractures have been identified, so this is unlikely to change in future.

What is clear is that the data here stand in significant contrast to those from the Fennoscandian Shield[20), 21)] where clear contrasts may be seen between the porewater and groundwater. There, this is due to a slow equilibration between both reservoirs because of the generally tight nature of the crystalline rock matrix. Although no matrix permeability or porosity data are yet available, it would appear that the Horonobe site is either hydrologically very quiescent, so allowing long-term equilibration between the two reservoirs or the matrix is relatively open, so allowing relatively fast equilibration. Clearly, this can be checked by examining existing core samples and this should be a major priority for any future work at the site.

The more numerous porewater data also indicate the presence of a shallow zone of rapid change in the groundwater chemistry, followed by more stable conditions below 200 – 300 mabh (e.g. Figure 5.30) or a slow decrease in concentration with depth (e.g. Figure 5.22). Although this is often less evident in HDB-10, in most cases, there is a strong correlation with the porewater chlorinity

The stable isotopic data shed some light on the above questions:

- Although the Horonobe area was not directly glaciated, permanent ice did exist nearby (e.g. just offshore, on the upper slopes of Rishiri Island[52), 53)]) and the surrounding seas were significantly cooler than today[54), 55)]. The fact that no striking cold climate/glacial depletion signature is seen in the groundwater today suggests that either the Horonobe groundwater system is flushing relatively quickly – certainly quickly enough to remove any evidence of cold waters from the last glaciation – or that permafrost was present for a significant period, so 'sealing' the groundwater against the cold climate signature (permafrost effectively acts like a aquaclude: cf. Dingman[56)]; Person et al.[57)]). While permafrost existed in northern Hokkaido during the local equivalent of the Older Dryas (the Kenbuchi Stadial of approximately 11.8 to 12.4 ka BP[53), 58) – 60)]), the evidence suggests that it was not continuous[61)], so allowing groundwater recharge. This suggests relatively rapid flushing has effectively diluted the cold climate signal, as the recent results[62)] would appear to confirm.
- The deeper waters are more saline than those near the surface, but are still more dilute than seawater. This is coupled with $\delta^{18}O > 1$ ‰, ruling out the possibility that the isotopic signature of these more saline waters is caused by mixing with seawater. Instead a relatively dilute, ^{18}O-enriched water is required and one possibility is that the saline groundwater contains a component of water liberated during diagenesis. Although, such ^{18}O-enriched, relatively low salinity waters have been reported from accretionary prism complexes[63) – 66)], nothing similar has been reported for geological terrains which are more relevant to the conditions at Horonobe.

Barnes and Milodowski[16)] noted kicks in the temperature log near the faults at the base of the transition zone between the Koetoi and Wakkanai formations in HDB-6 and near the top of the transition zone in HDB-8 and suggested that these structures may be conducting warmer water from depth. In addition, the Toyotomi thermal springs just to the north of the URL contain elevated levels of hydrocarbons that may be migrating from the deep-seated oil reservoirs in the region. It would be worth examining any fracture coatings or veins in these features to establish if there is any relationship with the currently circulating fluids.

An isotopic enrichment similar to that observed in the Horonobe groundwaters can also be produced by evaporation[67), 68)], but it is difficult to reconcile this mechanism with the known palaeohydrogeological evolution of the area.

5.2.3 Redox

It is clear from the discussions above that the samples are generally disturbed, as would be expected for groundwaters collected during drilling and hydraulic testing. Interpretation of the system is not helped by a complete absence of Eh electrode values which could have provided a qualitative insight into downhole conditions. In previous holes, Eh measurements were routinely made in surface flow-through cells, but this was discontinued due to

atmospheric contamination and effects of degassing as the groundwaters are pumped to the surface.

Personal communication from Sasamoto constructed Eh-pH diagrams comparing Eh and pH measurements made using the flow-through cells with mineral stability relations in the system FeO-CO_2-SO_4-H_2O at 25°C and found that the measured Eh values generally lie considerably above the predicted stability field of pyrite, which conflicts with the observation that framboidal pyrite is ubiquitous in the Koetoi and Wakkanai Formations.

To estimate in situ redox conditions at Horonobe, siderite and pyrite were assumed to be the controlling phases and, together with groundwater data for HDB-11, to predict Eh-pH values for HDB-11. The results (pH = 6.72 and Eh = -144 mV) do not compare too badly for the observed groundwater pH values (6.96 – 7.11), although it should be noted that these samples contain high drilling fluid levels (>60 %) and so are not representative of in situ conditions. The porewater values are, however, much higher, lying in the range pH 7.8 – 8.7, with the least disturbed samples (i.e. those sampled in gloveboxes; see comments in Section 3.3.3 and Chapter 4) lying in the pH range of 7.93 – 8.34. Additionally, calculated groundwater ΣFe concentrations are only within an order of magnitude of the measured values (Figure 5.32), suggesting that additional phases may be involved in controlling redox in the Horonobe groundwater system.

Clearly, a more detailed investigation of redox-controlling reactions should be based on reliable measurements of in-situ redox conditions, using both downhole Eh probes for qualitative values and new groundwater data from less disturbed samples (coupled with existing information on matrix and fracture-filling mineralogy) for quantitative calculations.

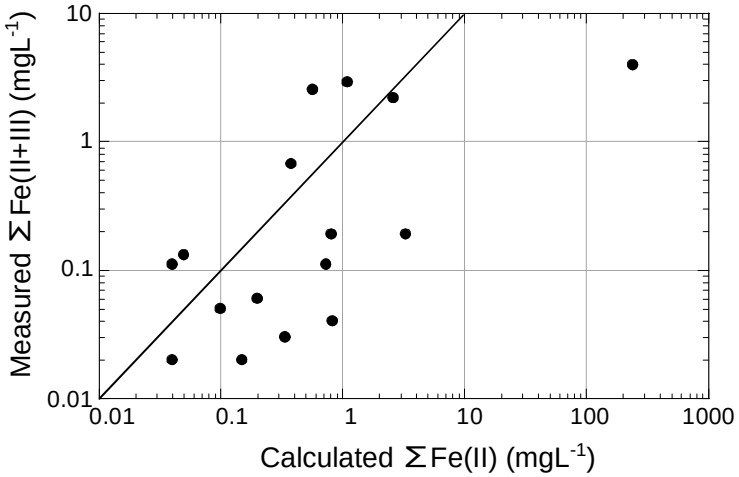

Figure 5.32: Plot of measured total-Fe concentrations vs calculated total-Fe assuming equilibrium with respect to pyrite and siderite at 25 °C. The line represents agreement between calculated and measured values

6. Conclusions and recommendations

At this point in a site characterisation, it is normal to have only low category data such as those discussed here, but these nevertheless provide the basis for building the preliminary site conceptual model. These data will be supplemented shortly by higher category data as samples are obtained from the finished boreholes which have had enough time* since drilling and hydraulic testing to return to their near-pristine state. However, the existing data will not be superseded by the new, higher category, data, they will remain as supporting information which can add weight to proposed trends in the groundwater chemistry, for example. Currently, the only area where these lower category data are of little help is in assessing the in-situ redox state of the groundwaters and porewaters. Eh measurements made in flow-through cells at the surface were not available for HDB-9 – 11, because they were shown to be highly susceptible to the effects of degassing and possible contamination by contact with air in the earlier boreholes and so their use was discontinued. Future studies aimed at characterising in-situ redox conditions at Horonobe, preferably using downhole chemical probes developed by JAEA, are strongly recommended.

Producing a quality-based dataset is, by necessity, a dynamic process with the implementation of changes with each new data freeze as new (or modified) data become available. Thus, this current dataset (Data Freeze I) represents no more than the first steps in producing the definitive site hydrochemistry database. On occasion in the future, data previously judged to be representative may have to be downgraded and/or data considered inadequate (e.g. lacking isotopes or incomplete sampling) may be upgraded if nothing else is available.

Other major points to consider include:

- *Borehole activities:* these activities include everything from the actual drilling all the way to groundwater sampling. All downhole activities may result in contamination of the samples, as can short-circuiting of the flow system (i.e. where groundwaters from higher or lower than the sampling point can be drawn into the sampling interval along zones of damage, such as the borehole skin). The quality of each sample can be assessed by examining the local geology, borehole condition, other borehole test data (e.g. EC logs) and, perhaps as importantly, what would be expected at that depth. The reliability or otherwise of each sample can be semi-quantitatively assessed and the degree of uncertainty either increased or reduced accordingly – *this has not been carried out on any of the HDB data yet and should be addressed in the future.*

- *Drilling fluid content:* an important indication of sample quality is reflected in drilling fluid contents in excess of 1 %. This cut-off contamination limit is historically based on earlier JAEA site investigation programmes (and is reflected in other

* Just how long is 'enough time' depends on the rock type, rock matrix and fracture permeability, groundwater flux etc.

national programmes). An integral part of the groundwater quality classification is therefore based on the amount of drilling water present, and different percentage ranges have been used to categorise each sample. Here, most samples are low category due to relatively high drilling fluid contents, but also due to a lack of time series measurements which would allow the observation of long-term changes to the boreholes. *Re-sampling of some of the HDB boreholes is now planned and this should enable the collection of high category samples in the future.*

- *Drilling fluid impact study:* using drilling fluid tracers balance to estimate the degree of pumping required to get rid of drilling water before high quality sampling can go ahead, should be considered for any new boreholes. This has been applied to the drilling programme of AECL in the past and it was possible to determine how much water should be pumped out from the sections before high quality sampling could begin. This type of water balance could help guide the sampling at Horonobe and so shepherd resources – *but the highly permeable nature of the site host rock may invalidate the method. Back calculations on current boreholes would be a valuable test before investing too much effort in any new boreholes*.

- *Porewater samples:* additional samples, sample handling and data from any future samples would be useful because quantitative interpretation of the porewater/groundwater interaction as a function of time is complex and depends on many factors such as the transport properties in the rock matrix, the distance to the next water-conducting fracture, the time period of fracture water circulation with constant chemical and isotopic conditions, etc. To facilitate better understanding of the matrix/groundwater interaction, the areas to focus on are:
  - Improve sample collection and handling procedures. There is no doubt that all porewater samples show signatures of atmospheric contamination. This can probably be traced back to the standard on-site core description methods and has to be adapted to ensure rapid and immediate protection of these highly permeable samples.
  - Collect hydraulic conductivity and porosity data on the matrix in any new samples as this will help with assessing the likely ages of porewater signatures which differ from those of the groundwater. If possible, this could be carried out on existing sections, especially on surviving samples in and around H11SQ_13 and H11SQ_14_03, as these data will help to clarify whether the system is quiescent, so allowing long-term equilibration, or relatively open, so encouraging relatively short term equilibration between the two hydrochemical reservoirs.
  - Compare the porewater data directly with groundwater collected within the same sampling interval. This will allow better fine-tuning of the hydrogeological conceptual model of the site.
  - Compare the porewater data directly with the mineralogy of the same sample. This could begin with any existing core material from squeezed samples, but is a must for any new samples.

- Try and collect a statistically relevant amount of matrix samples (i.e. assess beforehand).
- Include, within the limitations of borehole observations with respect to the 3D distribution of water-conducting fractures and rock matrix transport properties, an assessment of the likely impact of nearby fractures on the matrix porewaters.
- Squeeze some of the deeper samples in HDB-11. Deepest at the moment is 850 mabh, but have core sections down to 1020 mabh. Even just the last one would be good to better assess the source of deeper signatures in the groundwater.

- *Groundwater samples:* this analysis indicates that several additional points are worthy of consideration in Data Freeze II and future boreholes, including:
  - Mixing zone samples: there is indication that a mixing zone (or a zone of relatively rapid change in concentration) exists at depths of 100 – 300 mabh (depending on the borehole) and this should be a zone of focus in any new boreholes. This can clearly be seen in the Cl profiles in HDB-9 – between ~100 and 150 mabh. Focus here would also allow a check on the apparent 'kick' in Mg, K and Si concentrations at 200 mabh.
  - Is it real or just a drilling fluid induced artefact? The fact that the porewater K concentration is generally similar to that in the groundwaters suggests this is real.
  - Further investigate the Mg/Cl correlation in Horonobe data (check HDB-1 – 8) and look for other potential hydrochemical signals (e.g. the I/Br ratio and B/Cl, I/Cl and Br/Cl ratios).
  - Utilise downhole redox measurement systems.
  - Further investigate the nature of the organics in the system – do they have clearly identifiable signatures of source?
  - Look at attached microbes on recovered borehole samples (fracture faces, matrix etc.) versus free-swimming microbes (and viruses).
  - Organic versus inorganic colloids.
  - Examine fracture coating minerals to better define the site palaeohydrogeology and to look for signatures of a possible deep groundwater source.

- *On-site procedures:* the biggest problem influencing on QA is contamination of water samples during sampling, sample handling and treatment by the following likely processes; introduction of contaminants such as O_2 and other oxidants (trapped in or on sampling equipment) which changes the in situ redox conditions, degassing of groundwater samples as they are brought to the surface – so changing pH and Eh values, oxidation of reduced species (in the porewater and rock) during rock matrix sample handling and squeezing, pumping at too great a rate for the local groundwater 'reservoir' in the vicinity of the sampling point, which can induce draw-in of groundwater from further afield and mixing with in situ groundwater to produce a sample which is non-representative of that horizon in the borehole. To minimise such problems, on-site procedures (cf. Appendix 5 and 6) should be reviewed and corrected in an appropriate manner and finally formalised. It is emphasised that an

appropriate QA system for site characterisation will save on effort by reducing errors and the requirement to re-sample and analysis – but this can be guaranteed by continuously assessing if the QA system truly fit-for-purpose and amending it where necessary.

Finally, much weight has been laid here on QA – both in defining the processes and applying them in a novel manner (e.g. with respect to the porewater data). But, as this is the basis of any full site characterisation programme, this is to be expected – and to be repeated in future Data Freezes at Horonobe. This report, Data Freeze I, is thus only the first step in the production of a fully QAd hydrochemistry dataset for the Horonobe URL project.

By practicing now, at Horonobe, what will be required later in the national programme, JAEA is building the necessary experience to guide the implementing and regulatory organisations in the future. Only by having a fully functional QA system in place *before* the detailed characterisation of a potential repository site begins, can stakeholders' needs for confidence in the outcome of the process be met.

Acknowledgements

The authors would like to thank all of our colleagues in the Horonobe URL programme whose long-term input is greatly appreciated. Special thanks to J.A.T. Smellie (Conterra, Stockholm, Sweden) and E.-L. Tullborg (Terralogica, Gråbo, Sweden) for constructive discussions with WRA on their work on groundwater QA within SKB's site characterisation programme and R. Metcalfe (Quintessa Limited, Oxfordshire, UK), M. Laaksoharju (GeoPoint AB, Sollentuna, Sweden), R. Arthur and W. Zhou (Monitor Scientific, Denver, Colorado, USA) and H. Sasamoto (JAEA Tokai, Japan) for providing relevant data and information.

References

1) Ota, K., Abe, H. et al. (2007): Horonobe Underground Research Laboratory Project, Synthesis of Phase I Investigations 2001–2005, Volume "Geoscientific Research". JAEA-Research 2007-044, JAEA, Tokai, Japan. (in Japanese with English abstract; English version, in press)
2) JNC (2004): International Workshop on Horonobe Underground Research Laboratory Project: Abstracts. JNC TN5400 2004-004, JNC, Tokai, Japan.
3) Sasamoto, H., Yui, M. and Arthur, R.C. (2001): Modelling Studies of Saline Type Groundwater Evolution. JNC TN8400 2001-016, JNC, Tokai, Japan.
4) Sasamoto, H., Yui, M. and Arthur, R.C. (2007): Estimation of in situ ground-water chemistry using geochemical modeling: A test case for saline-type ground water in argillaceous rocks. Physics and Chemistry of the Earth, 32, pp.196-208.
5) Sasamoto, H., Yui, M. and Hama, K. (2007): A preliminary interpretation of groundwater chemistry in the Horonobe area, Japan. In: Bullen, T.D. and Wang, Y. (Eds.) Water–Rock Interaction. Proceedings of 12th International Symposium, July/August 2007, Kunming, China. Taylor and Francis, London, UK, pp.385-389.
6) Kemp, S.J., Cave, M.R., Hodgkinson, E., Milodowski, A.E. and Kunimaru, T. (2002): Mineralogical Observations and Interpretation of Porewater Chemistry from the Horonobe Deep Boreholes HDB-1 and HDB-2, Hokkaido, Japan. BGS Report CR/02/303, BGS, Keyworth, UK.
7) Milodowski, A.E., Barnes, R.P., Kemp, S.J., Bouch, J. and Wagner, D. (2004): Characterisation of Fractured Rock and Fracture Mineralisation in Horonobe Boreholes HDB-6, HDB-7 and HDB-8: Final report. BGS Report CR/04/251, BGS, Keyworth, UK.
8) Takahashi, K. (2005): Data Book of Various Measurements and Analyses on Geological and Drilling Surveys for Horonobe URL Project. JNC TN5400 2005-010, JNC, Tokai, Japan. (in Japanese with English abstract)
9) Yamamoto, H., Kunimaru, T., Kurikami, H., Shimo, M. and Xu, T. (2006): Long-term simulation of ambient groundwater chemistry at Horonobe Underground Research Laboratory, Japan – Application of coupled hydrogeochemical model. Proceedings of the GeoProc 2006, 2nd International Conference on Coupled Thermo-Hydro-Mechanical-Chemical Processes in Geosystems and Engineering, May 2006, Nanjing, China, pp.382-387.
10) Hama, K., Kunimaru, T., Metcalfe, R. and Martin, A.J. (2007): The hydrogeochemistry of argillaceous rock formations at the Horonobe URL site, Japan. Physics and Chemistry of the Earth, 32, pp.170-180.
11) Laaksoharju, M., Smellie, J., Ruotsalainen, P. and Snellman, M. (1993): An Approach to Quality Classification of Deep Groundwaters in Sweden and Finland. SKB Report TR-93-27, SKB, Stockholm, Sweden.
12) SKB (2009): Hydrogeochemical Evaluation. Preliminary site description Forsmark area – version 2.2/2.3. SKB Report, SKB, Stockholm, Sweden (in press).

13) Wasada, A., Kajiwara, Y., Nishita, H. and Iwano, H. (1996): Oil-source rock correlation in the Tempoku basin of northern Hokkaido, Japan. Organic Geochemistry, B24, pp.351-362.
14) Iijima, A. and Tada, R. (1981): Silica diagenesis of Neogene diatomaceous and volcaniclastic sediments in northern Japan. Sedimentology, 28, pp.185-200.
15) Minoura, K, Susaki, T and Horiuchi, K. (1996): Lithification of biogenic siliceous sediments: Evidence from Neogene diatomaceous sequences of northeast Japan. Sedimentary Geology, 107, pp.45-59.
16) Barnes, R.P. and Milodowski, A.E. (2004): Characterisation of Fractures in Horonobe Boreholes HDB-6, HDB-7 and HDB-8: Results of core examination, February 2004. BGS Report CR/04/043, BGS, Keyworth, UK.
17) Werner K. (1998): Tracing Techniques in Geohydrology. A.A.Balkema, Amsterdam, The Netherlands.
18) Nilsson, A-C. (2008): Analytical uncertainties. In: Kalinowski, E. (Ed.) Background Complementary Hydrogeochemical Studies. SDM-Site Forsmark. SKB Report R-08-87, SKB, Stockholm, Sweden.
19) Kunimaru, T., Shibano, K., Kurikami, H. and Hara, M. (2007): Analysis of Ground Water from Boreholes, River Water and Precipitation in the Underground Research Laboratory Project. JAEA-Data/Code 2007-015, JAEA, Tokai, Japan. (in Japanese with English abstract)
20) Waber, H.N., Gimmi, T. and Smellie, J.A.T. (2009). Pore Water in the Rock Matrix. Site descriptive modelling, SDM-Site Forsmark. SKB Report R-08-105, SKB, Stockholm, Sweden. (in press)
21) Waber, H.N. and Smellie, J.A.T. (2008): Characterisation of pore water in crystalline rocks. Applied Geochemistry, 23, pp.1834-1861.
22) Gautschi, A., Ross, C. and Scholtis, A. (1993): Pore water-groundwater relationships in Jurassic shales and limestones of northern Switzerland. In: Manning, D.A.C., Hall, P.L. and Hughes C.R. (Eds) Geochemistry of Clay-Pore Fluid Interactions. Chapman & Hall, London, UK, pp.412-422.
23) M.Gascoyne (2004): Hydrogeochemistry, groundwater ages and sources of salts in a granitic batholith on the Canadian Shield, southeastern Manitoba. Applied Geochemistry, 19, pp.519-560.
24) Smellie, J.A.T., Waber, H.N. and Frape, S.K. (2003): Matrix Fluid Chemistry Experiment, Final Report. SKB Technical Report TR-03-18, SKB, Stockholm, Sweden.
25) NEA (2000): Pore-water Extraction from Argillaceous Rocks for Geochemical Characterisation. Methods and interpretations. OECD/NEA, Paris, France.
26) Charlton, B.D., Milodowski, A.E., Cave, M.R., Entwistle, D.C. and Darling, W.G. (2005): Specialist Pore-Water Characterisation in the Horonobe Boreholes HDB-9, HDB-10 and HDB-11: Final report. BGS CR 05-147, BGS, Keyworth, UK.
27) Alexander, W.R. (1985): Inorganic diagenesis in anoxic sediments of the Tamar estuary. PhD Thesis, University of Leeds, Leeds, UK.
28) Upstill-Goddard, R.C., Alexander, W.R., Elderfield, H. and Whitfield, M. (1989): Chemical diagenesis in the Tamar estuary. Contributions to Sedimentology, 16, pp.1-49.

29) Bradbury, M.H., Baeyens, B. and Alexander, W.R. (1990): Experimental Proposals for Procedures to Investigate the Water Chemistry, Sorption and Transport Properties of Marl. Nagra Technical Report NTB 90-16, Nagra, Wettingen, Switzerland.
30) Oyama, T. and Suzuki, K. (2006): Study on Investigation and Evaluation Methods of Deep Seated Sedimentary Rocks. Chemical weathering, porewater squeezing and relationships of physical properties of sedimentary rocks. CRIEPI Report: N05020, CREIPI, Tokyo, Japan.
31) Frick, U., Alexander, W.R. et al. (1992): Grimsel Test Site – The Radionuclide Migration Experiment: Overview of investigations 1985-1990. Nagra Technical Report NTB 91-04, Nagra, Wettingen, Switzerland.
32) Smellie, J., Tullborg, E.-L. et al. (2008): Explorative Analysis of Major Components and Isotopes. SDM-Site Forsmark. SKB Report R-08-84, SKB, Stockholm, Sweden.
33) Pearson, F.J., Lolcama, J.L. and Scholtis, A. (1989): Chemistry of Groundwaters in the Böttstein, Weiach, Riniken, Schafisheim, Kaisten and Leuggern Boreholes: A hydrochemically consistent data set. Nagra Technical Report NTB 86-19, Nagra, Wettingen, Switzerland.
34) SKB (2005): Hydrogeochemical Evaluation. Preliminary site description Forsmark area – version 1.2. SKB Report R-05-17, SKB, Stockholm, Sweden.
35) SKB (2006). Hydrogeochemical Evaluation. Preliminary site description Laxemar subarea – version 1.2. SKB Report R-06-12, SKB, Stockholm, Sweden.
36) SKB (2006). Hydrogeochemical Evaluation. Preliminary site description Laxemar subarea – version 2.1. SKB Report R-06-70, SKB, Stockholm, Sweden.
37) Posiva (2005): Olkiluoto Site Description 2004. Posiva Report 2005-03, Posiva, Olkiluoto, Finland.
38) Smellie, J.A.T. (Ed.) (1998): Maqarin Natural Analogue Study: Phase III. SKB Report TR-98-04, SKB, Stockholm, Sweden.
39) Iwatsuki, T., Xu, S., Mizutani, Y., Hama, K., Saegusa, H. and Nakano, K. (2001): Carbon-14 study of groundwater in the sedimentary rocks at the Tono study site, central Japan. Applied Geochemistry, 16, pp.849-859.
40) JNC (1999): Proceedings of International Workshop for the Kamaishi In Situ Experiments. JNC TN7400 99-007, JAEA, Tokai, Japan.
41) Ota, K. and Alexander, W.R. (2001): Development and testing of radionuclide transport models for fractured crystalline rock – An overview of the Nagra-JNC radionuclide retardation programme. JNC Technical Review, No. 11, JNC, Tokai, Japan, pp.119–128. (in Japanese with English abstract)
42) Pearson, F.J., Arcos, D. et al. (2003): Mont Terri Project – Geochemistry of Water in the Opalinus Clay Formation at the Mont Terri Rock Laboratory. Reports of the FOWG, Geology Series No.5, Swisstopo, Berne, Switzerland.
43) IAEA (1996): Application of Quality Assurance to Radioactive Waste Disposal Facilities. IAEA TECDOC 895, IAEA, Vienna, Austria.
44) Wittwer, C. (1986): Probenahmen und Chemische Analysen von Grundwässern aus den Sondierbohrungen. Nagra Technical Report NTB 85-49, Nagra, Wettingen, Switzerland. (in German with English abstract)

45) Nagra (1997): Geosynthese Wellenberg 1996: Ergebnisse der Untersuchungsphasen I und II. Nagra Technical Report NTB 96-01, Nagra, Wettingen, Switzerland. (in German with English abstract)
46) Shuter, E. and Teasdale, W.E. (1989): USGS Techniques of Water-Resources Investigations Reports, Book 2: Collection of Environmental Data, Chapter F1: Application of drilling, coring and sampling techniques to test holes and wells. USGS, Reston, USA.
47) Smith, D.C., Spivack, A.J., Fisk, M.R., Haveman, S.A. and Staudigel, H. (2000): Tracer-based estimates of drilling-induced microbial contamination of deep-sea crust. Geomicrobiology Journal, 17, pp.207-219.
48) CanGold (2008): CanGold Ltd QA & QC Programme, Thorn Project (http://www.cangold.ca/i/pdf/Thorn-QAQC.pdf), CanGold, Vancouver, Canada.
49) Krouse, H.H. (1980): Sulphur isotopes in our environment. In: Fritz, P. and Fontes, J.Ch. (Eds) Handbook of Environmental Isotope Geochemistry, Vol. 1, The terrestrial environment. A. Elsevier, Amsterdam, The Netherlands, pp.435-471.
50) Nagra (2002): Projekt Opalinuston: Synthese der Geowissenschaftlichen Untersuchungsergebnisse. Entsorgungsnachweis für abgebrannte Brennelemente, verglaste hochaktive sowie langlebige mittelaktive Abfälle. Nagra Report NTB 02-03, Nagra, Wettingen, Switzerland. (in German with English abstract)
51) Kai, K. and Maekawa, K. (2006): Distribution of diagenetic minerals in the neogene diatomaceous sediments of Horonobe, Hokkaido: Implication for recharge and discharge of ground water, Journal of the Geothermal Research Society of Japan, 30, pp.205-214. (in Japanese with English abstract)
52) Marui, A. (2003): Groundwater conditions along the seawater/freshwater interface on a volcanic island and a depositional area in Japan. Geological Quarterly, 47, pp.381-388.
53) Kondo, R., Tsukamoto, S., Tachibana, H., Miyairi, Y. and Yokoyama, Y. (2007): Age of glacial and periglacial landforms in northern Hokkaido, Japan, using OSL dating of fine grain quartz. Quaternary Geochronology, 2, pp.260-265.
54) Oba, T., Kato, M. et al. (1991): Paleoenvironmental changes in the Japan Sea during the last 85,000 years. Palaeo-oceanography, 6, pp.499-518.
55) Ternois, Y., Kawamura, K., Ohkouchi, N. and Keigwin, L. (2000): Alkenone sea surface temperature in the Okhotsk Sea for the last 15 kyr. Geochemical Journal, 34, pp.283-293.
56) Dingman, S.L. (1975): Hydrologic effects of frozen ground: literature review and synthesis. US Army Cold Regions Research and Engineering Laboratory (CRREL) Special Report 218, CRREL, Hanover, USA.
57) Person, M., McIntosh, J., Bense, V. and Remenda, V. (2007): Pleistocene hydrology of North America: The role of ice sheets in reorganising groundwater systems. Reviews of Geophysics, 45, RG3007, doi:10.1029/2006RG000206.
58) Nogami, M., Koaze, T. and Fukuda, M. (1980): Periglacial environment in Japan: Present and past. GeoJournal, 4, pp.125-132. (in Japanese with English abstract)
59) Miura, H. and Hirakawa, K. (1995): Origin of fossil periglacial wedge in northern Hokkaio, Japan. Jounal of Geography, 104, pp.189-224. (in Japanese with English abstract)

60) Igarashi, Y. (1996): A late glacial climatic reversion in Hokkaido, northeast Asia, inferred from the Larix pollen record. Quaternary Science Reviews, 15, pp.989-995.
61) Niizato, T., Yasue, K., Kurikami, H., Kawamura, M. and Ohi, T. (2008): Synthesizing geoscientific data into a site model for performance assessment: A study of the long-term evolution of the geological environment in and around the Horonobe URL, Hokkaido, northern Japan. Proceedings of 3rd AMIGO Workshop on "Approaches and Challenges for the Use of Geological Information for the Safety Case", OECD/NEA, April, 2008, Nancy, France, NEA, Paris, France, pp.222-234.
62) Teramoto, M., Shimada, J. and Kunimaru, T. (2008): Evidence of paleo groundwater flow regime in impermeable rocks by stable isotopes in porewaters of drilled cores. Proceedings of 36th IAH Congress "Integrating Groundwater Science and Human Well-Being", October 2008, Toyama, Japan, pp.435-440.
63) Kastner, M., Zheng, Y., Laier, T., Jenkins, W. and Ito, T. (1997): Geochemistry of fluids and flow regime in the décollement zone at the northern Barbados Ridge. In: Shipley, T.H., Ogawa, Y., Blum, P., and Bahr, J.M. (Eds.) Proceedings of the Ocean Drilling Program, Scientific Results, 156, Colleg Station, TX (Ocean Drilling Program), pp.311-320.
64) Sadofsky, S.J. and Bebout, G.E. (2004): Field and isotopic evidence for fluid mobility in the Franciscan Complex: Forearc paleohydrogeology to depths of 30 kilometers. International Geology Review, 46, pp.1053-1088.
65) Hensen, C., Wallmann, K., Schmidt, M., Ranero, C.R. and Suess, E. (2004): Fluid expulsion related to mud extrusion off Costa Rica – A window to the subducting slab. Geology, 32, pp.201-204.
66) Sakakibara, M., Umeki, M. and Cartwright, I. (2007): Isotopic evidence for channeled fluid flow in low-grade metamorphosed Jurassic accretionary complex in the Northern Chichibu belt, western Shikoku, Japan. Journal of Metamorphic Geology, 25, pp.383-400.
67) Gibson, J.J., Edwards, T.W.D. and Prowse, T.D. (1999): Pan-derived isotopic composition of atmospheric water vapour and its variability in northern Canada. Journal of Hydrology, 217, pp.55-74.
68) Baskaran, S., Ransley, T. and Brodie, R.S. (2005): Tools for assessing groundwater-surface water interactions: A case study in the Border Rivers catchment, Murray-Darling Basin. Bureau of Rural Sciences, Canberra, Australia.

Appendix 1: Data sources for Kemp et al.[6)]

Borehole	Core sample code	SEM lab code	Depth (mabh)			Formation	Petrography	Bulk Mineralogy
			Top	Bottom	Mean			
HDB-1	HDB-1/1	H717	94.35	94.45	94.40	Koetoi F.	Y	Y
HDB-1	HDB-1/4	H720	204.50	204.70	204.60	Koetoi F.	Y	Y
HDB-1	HDB-1/6	H722	313.90	314.00	313.95	Koetoi F.	Y	Y
HDB-1	HDB-1/8	H724	382.35	385.42	383.89	Koetoi F.	N	Y
HDB-1	HDB-1/10	H726	496.20	496.32	496.26	Wakkanai F.	Y	Y
HDB-1	HDB-1/12	H728	703.90	704.00	703.95	Wakkanai F.	Y	Y
HDB-2	HDB-2/1	H729	100.75	100.85	100.80	Wakkanai F.	Y	Y
HDB-2	HDB-2/3	H731	301.00	301.10	301.05	Wakkanai F.	Y	Y
HDB-2	HDB-2/4	H732	404.60	404.64	404.62	Wakkanai F.	N	Y
HDB-2	HDB-2/5	H733	498.85	498.90	498.88	Wakkanai F.	Y	Y
HDB-2	HDB-2/7	H735	601.72	601.82	601.77	Wakkanai F.	Y	Y
HDB-2	HDB-2/8	H736	705.23	705.30	705.27	Wakkanai F.	Y	Y

Y: Analysis undertaken, N: Analysis not undertaken

Appendix 2: Data from R. Arthur and W. Zhou via personal communication

No.*	Borehole	Depth	EC	Temp	pH	Eh	Na^+	K^+	Ca^{2+}	Mg^{2+}	TC	TIC	Alk	SO_4^{2-}	H_2S (*aq*)	F^-	Cl^-	NH_4^+	SiO_2 (*aq*)	Al^{3+}	∑Fe	Fe^{2+}	c.b.
		mabh	mSm^{-1}	°C		mV	mgL^{-1}	mgL^{-1}	mgL^{-1}	mgL^{-1}	mgL^{-1}	mgL^{-1}	mgL^{-1}	mgL^{-1}	mgL^{-1}	mgL^{-1}	mgL^{-1}	mgL^{-1}	mgL^{-1}	mgL^{-1}	mgL^{-1}	mgL^{-1}	mgL^{-1}	%
1pu14	HDB-1	548.00 – 563.19	2450	22.2	7.7	-	5010	174	180	111	373	360	1660	97.6	<0.1	<0.1	7330	120	100.3	<0.1	0.02	<0.01	1.4
1pu15	HDB-1	548.00 – 563.19	2560	12.4§	6.87§	-76.0§	5140	170	180	120	400	390	1740	96.7	<0.1	<0.1	7500	130	104	<0.1	2.9	<0.01	1.4
2pu11	HDB-2	334.90 – 404.90	-	19.6	8.2	-	2040	44	81	27	335	290	1170	8.7	<0.1	<0.1	2730	44	72.7	<0.1	<0.03	<0.01	-0.9
2pu12	HDB-2	334.90 – 404.90	1256.0§	12.2§	7.45§	-114.0§	3120	51	24	36	444	400	1740	2.4	<0.1	<0.1	4180	53	96.3	<0.1	0.06	0.03	-2.7
3pu14	HDB-3	160.50 – 200.45	3170.0§	14.7§	6.56§	192.5§	6900	320	220	210	582	530	2020	38	-	-	11600	380	57.8	-	0.19	0	-1
4pu24	HDB-4	281.45 – 299.53	430	15.9	7.84	-	880	21	23	10	266	250	1070	0.3	-	0.2	820	2.6	42.8	-	0.05	0.02	-5.3
4pu43	HDB-4	407.90 – 520.00	1667.0§	12.8§	6.98§	177.7§	3700	59	95	56	612	570	2140	7	-	0.4	4600	86	49.2	0.02	0.11	0.06	1.1
5pu14	HDB-5	154.05 – 180.46	42.0§	11.5§	8.82§	227.3§	86	4	0.9	0.5	53	50	200	0.5	-	0.4	16	5.4	42.8	-	0.11	0	-3.5
5pu24	HDB-5	182.05 – 250.46	84.0§	9.5§	8.58§	240.9§	180	5	2.2	1	91	86	340	2.2	-	0.4	67	6.7	40.6	0.1	0.13	0	-1.2
5pu43	HDB-5	331.22 – 402.23	1303.0§	14.0§	7.01§	221.4§	2900	46	99	46	610	580	2170	6.8	-	0.2	3250	64	42.8	0.4	2.52	0.02	1.8
6pu3	HDB-6	280.95 – 312.00	1199.0§	17.7§	7.27§	11.0§	2460	77	69	43	520	390	-	5.9	<0.1	<0.1	3050	94	55.6	0.02	0.03	0.03	16.4
6pu47	HDB-6	363.95 – 409.00	1966.0§	20.5§	6.87§	-52.6§	4220	110	140	110	573	510	-	0.2	<0.1	0.2	6300	140	51.3	<0.01	0.04	0.04	8.4
9pu1L	HDB-9	25.50 – 82.60	16.0§	16.6§	6.12§	-	22	1.8	3.9	1.1	11	9	0.8	10	<0.1	<0.1	14	0.5	44.9	0.01	-	3.9	-3.7
9pu2L	HDB-9	216.90 – 257.50	1239.0§	13.0§	6.92§	-	4200	59	84	59	639	630	54.9	6.9	<0.1	0.2	5400	87	47.1	<0.01	-	0.14	-1.6
10pu1L	HDB-10	41.33 – 59.88	1067.0§	10.3§	7.16§	-	2300	110	67	55	676	640	58.7	1	<0.1	0.3	2400	140	55.6	0.06	0.67	0.12	-2.4
10pu2L	HDB-10	445.84 – 469.89	2510.0§	14.0§	6.77§	-	5000	160	97	140	340	320	38.8	0.4	<0.1	<0.1	8100	220	53.5	<0.01	2.17	2.1	1.2

* Sample numbers: general format "*x*pu*yz*", *x*: borehole number (excluding the designation HDB-), "pu": "pumped" (i.e., groundwater), *y*: sampling event corresponding to a particular time interval and packer configuration, *z*: sample number taken in that configuration (increasing with time)

§ Measured in flow-through cells at the wellhead

Appendix 3: Drilling fluid tracer vs TOC plots for the individual boreholes

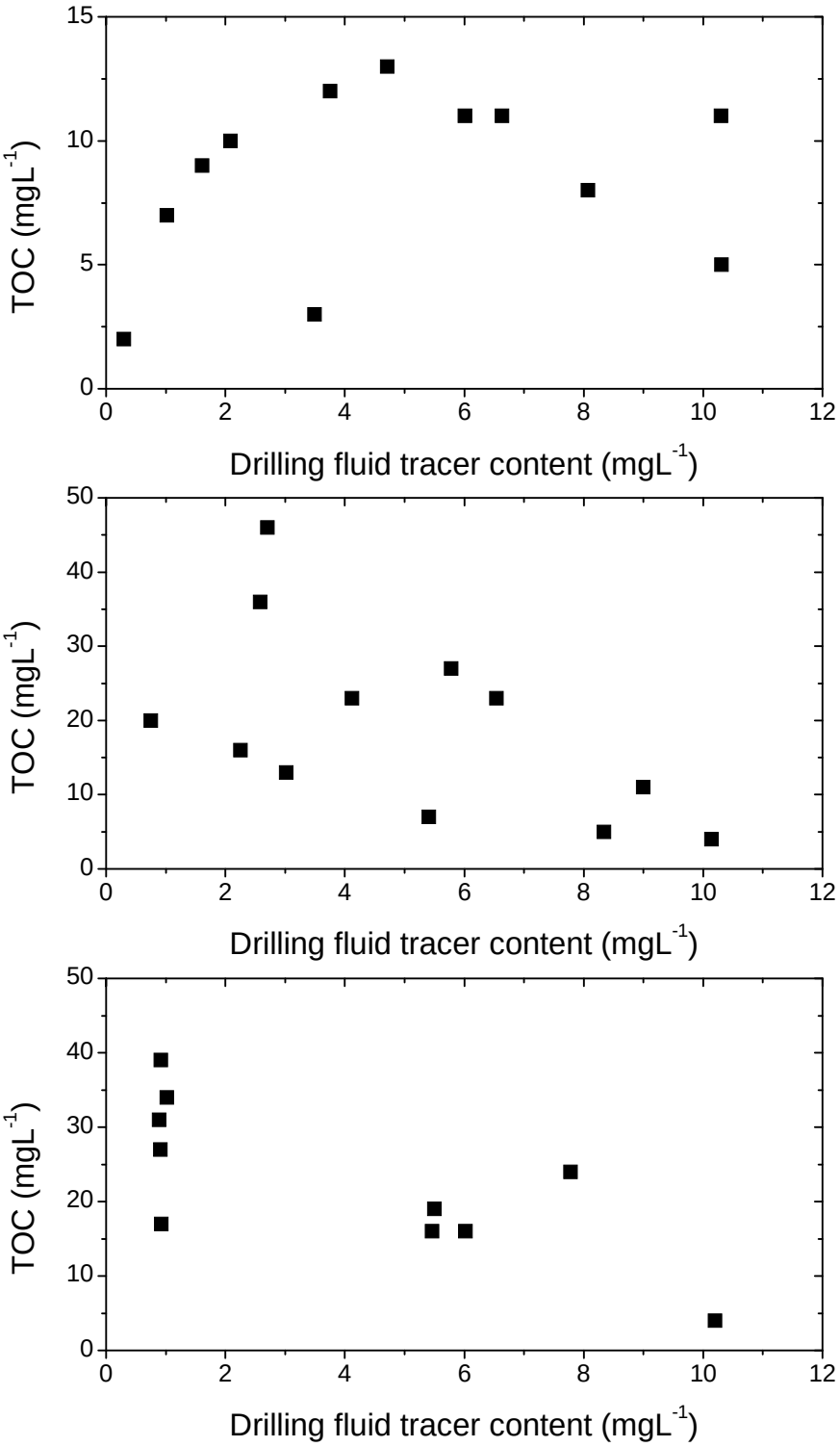

Appendix 4: Hydrochemical data from 8 groundwater samples for further interpretation

ID		9-pu-1L	9-pu-2L	10-pu-1L	10-pu-2L	11-pu-1-1	11-pu-1L	11-pu-2-1	11-pu-2L
Mid-depth	[m]	54.05	237.20	50.61	457.87	204.03	204.03	625.03	625.03
pH		6.12	6.92	7.16	6.77	7.11	7.03	-	-
EC (@25°C)	[mSm^{-1}]	15.8	1239	1067	2510	15.6	1147	35	35.5
ORP(Pt)	[mV]	-	-94.6	-217	-234	112	-216	3007	3796
ORP(Au)	[mV]	-	-71.6	-136	-147.7	83	-132	-145	-166
DO	[mgL^{-1}]	-	-	0	0	10.1	0	0.15	0.52
Tracer	[mgL^{-1}]	0.3	1.61	2.58	0.75	10.2	5.5	1.02	0.89
Tracer	[%]	3	18	29	8	113	61	11	10
Temp.	[°C]	16.6	13	10.3	14	5.1	17.5	6.2	6.2
Na^+	[mgL^{-1}]	22	4200	2300	5000	18	3300	6300	6600
K^+	[mgL^{-1}]	1.8	59	110	160	1.5	160	130	140
NH_4^+	[mgL^{-1}]	0.51	87	140	220	-	190	-	200
Li^+	[mgL^{-1}]	0.01	2.7	15	20	-	12	-	12
Ca^{2+}	[mgL^{-1}]	3.9	84	67	97	7.1	40	240	250
Mg^{2+}	[mgL^{-1}]	1.1	59	55	140	3.6	84	170	170
Sr^{2+}	[mgL^{-1}]	0.03	1.4	1.2	3.4	-	2.2	-	4.3
Se^{2-}	[mgL^{-1}]	<0.001	<0.001	0.001	<0.001	-	0.002	-	<0.001
Total-P	[mgL^{-1}]	<0.05	0.91	5.7	0.05	0.16	<0.05	<0.05	<0.05
I^-	[mgL^{-1}]	<1	15	10	33	<1	16	27	29
Mn(II)	[mgL^{-1}]	-	-	-	-	-	0.02	-	0.01
Total Mn	[mgL^{-1}]	0.16	0.07	0.02	<0.01	-	-	-	-
dissolved Si	[mgL^{-1}]	21	22	26	25	17	26	27	27
insoluble SiO_2	[mgL^{-1}]	-	-	-	-	-	-	-	-
Ti^{4+}	[mgL^{-1}]	<0.002	<0.002	<0.002	<0.002	-	<0.002	-	<0.01
Fe(III)	[mgL^{-1}]	<0.05	<0.05	0.55	0.07	<0.05	4.3	<0.05	<0.05
Fe(II)	[mgL^{-1}]	3.9	0.14	0.12	2.1	<0.05	2.6	4.1	2.3
Total-Fe	[mgL^{-1}]	0.02	0.04	0.02	0.03	0.03	0.02	0.05	0.04
Al^{3+}	[mgL^{-1}]	0.01	<0.01	0.06	<0.01	0.01	<0.01	<0.01	<0.01
F^-	[mgL^{-1}]	<0.1	0.2	0.3	<0.1	0.1	<0.1	0.2	0.1
Cl^-	[mgL^{-1}]	14	5400	2400	8100	19	5100	10000	10000
Br^-	[mgL^{-1}]	<1	34	26	83	<1	42	77	78
NO_3^-	[mgL^{-1}]	<0.1	3.9	1	0.5	-	0.3	-	0.1
NO_2^-	[mgL^{-1}]	<0.1	<0.01	<0.1	<0.1	-	<0.1	-	<0.1
SO_4^{2-}	[mgL^{-1}]	10	6.9	1	0.4	5.1	11	<0.2	<0.2
S^{2-}	[mgL^{-1}]	<0.1	<0.1	<0.1	<0.1	<0.1	<0.1	<0.1	<0.1
H_2S	[mgL^{-1}]	<0.1	<0.1	<0.1	<0.1	<0.1	<0.1	<0.1	<0.1
Total-B	[mgL^{-1}]	0.05	83	46	87	0.03	80	120	120
Total-Be	[mgL^{-1}]	<0.002	<0.002	<0.002	<0.002	-	<0.002	-	<0.01
Total-Cr	[mgL^{-1}]	<0.002	<0.002	0.003	<0.002	-	<0.002	-	<0.01
Total-Co	[mgL^{-1}]	<0.002	<0.002	<0.002	<0.002	-	<0.002	-	<0.01
Total-Ni	[mgL^{-1}]	0.003	0.014	0.004	<0.002	-	0.064	-	<0.01
HCO_3^-	[mgL^{-1}]	47	3200	3600	1100	37	1410	2100	2200
CO_3^{2-}	[mgL^{-1}]	0	0	0	0	0	0	0	0
M-Alk($CaCO_3$)	[mgL^{-1}]	0.8	54.93	58.7	38.8	0.71	30.1	43.1	43.6
P-Alk($CaCO_3$)	[mgL^{-1}]	0	0	0	0	0	0	0	0
TOC	[mgL^{-1}]	2	9	36	20	4	19	34	31
TIC	[mgL^{-1}]	9	630	640	320	9	260	460	450

Appendix 5: On-site water sampling/treatment/analysis protocols at MIU

On-site Water Sampling/Treatment/Analysis Protocols at MIU

Kunio Ota, with contribution from K Hama, T Mizuno and M Asai

This note summarises the work protocols applied to water sampling and the following treatment and analysis of water samples during borehole investigations at MIZ-1, DH-15 and 06MI03 based around the Mizunami Underground Research Laboratory (MIU). Although the whole procedures described below were not applied to a single borehole programme, the applicability of each of the procedures was more or less confirmed during these investigations.

1 Maintenance of Drilling Fluid Tracer Concentration

Background

- Necessary to evaluate the degree of groundwater contamination with drilling fluid by quantifying tracer concentrations in sampled waters periodically; for the evaluation, the drilling fluid tracer concentrations to be kept as constant as practicable (generally within ±10 %) during drilling
- Two independent tracers (normally fluorescent dyes) to be selected and used for cross-checking; for the selection of appropriate tracers, the following issues to be investigated based on the local geological and hydrochemical information available:
  a) toxicity/radioactivity
  b) cost
  c) easiness of handling/analysis
  d) stability (pH-, concentration-, temperature-dependency)
  e) sorptivity onto rock
  f) solubility in water
  g) extinction/emission wavelength coincidence (for different fluorescent dyes)
- For the definition of the drilling fluid tracer concentration following the tracer selection, the following issues to be considered:
  a) analytical detection limit (the need to identify the contamination as low as 1 %)
  b) influence of colour on BTV survey
- A rapid or significant change in the drilling fluid tracer concentrations as an indicator for exchanging the drilling fluid; work to be carried out on-site as quickly as practicable involving sampling and chemical analysis of the drilling fluid in order to take necessary actions without undesirable delay
- In case likely increase expected in drilling fluid TDS owing to interaction with cuttings and/or mixture with groundwater with higher TDS during drilling, although the drilling fluid tracer concentrations kept within the ±10 % range, drilling fluid chemistry to be maintained by means of adjusting the drilling fluid EC periodically; EC control value to be defined based on the local geological and hydrochemical information available

1.1 Adjustment of drilling fluid tracer concentration

Methodology

1) Addition of the prescribed amount of tracer to fluid (fresh water at the beginning of drilling) in the tank and mixing of the fluid sufficiently; the amount of the fluid in the tank to be calculated from fluid level readings
2) Sampling, treatment and chemical analysis of the drilling fluid on-site immediately after the mixing (see 1.2 and 1.3 for details)
3) Adjustment of the drilling fluid tracer concentration for three times or more if necessary to attain the defined tracer concentration with a permissible range of ±10 %

Timing and frequency

- Sampling and chemical analysis of the initial drilling fluid to be done before drilling
- Sampling and chemical analysis of the circulated drilling fluid to be done hourly on-site during drilling to ensure the variation of drilling fluid tracer concentrations within a permissible range of ±10 %
- In case the drilling fluid tracer concentrations moving over the ±10 % range, the drilling fluid tracer concentration to be adjusted
- As a rule, the adjustment to be done immediately before (re)starting drilling; borehole drilling to be suspended during the adjustment

Place

- Adjustment at the drilling fluid reservoir

1.2 Sampling and treatment of drilling fluid

Methodology

1) Cleaning of sample bottles by diluted nitric acid, de-ionised water and ultra pure water in the on-site laboratory
2) Bailing of the drilling fluid (or water) directly from the tank with a PE dipper
3) Washing of the cleaned sample bottles with the small amount of sampled fluid three times and filling of the bottles with the drilling fluid
4) Quick observation of the drilling fluid in the on-site laboratory; the following items to be checked and described:
   a) colour
   b) smell
   c) bubbles
   d) suspension
   e) precipitation
5) Filtration of the samples through a 0.45 μm pore sized filter immediately after sampling in the on-site laboratory; no chemical treatment to be applied for the drilling fluid
6) Labelling of the sample bottles with the following information:
   a) borehole number
   b) sample number
   c) sampling date and time
   d) sampling depth
   e) name of sampling person
   f) quick observation results
7) Storage of all the samples except for hourly collecting ones in the refrigerator in the on-site laboratory until chemical analysis (see 1.3 for details)

Timing and frequency

- Sampling of the initial drilling fluid to be done before drilling on-site
- Sampling of the circulated drilling fluid to be done hourly, daily and every 100 mabh drilling on-site; in case of continuous (24 hours) drilling, sampling to be scheduled at night and chemical analysis in the daytime
- In case of the preparation of drilling fluid with fresh water to refill the reservoir, the input water also to be sampled for both chemical analysis and storage

Place

- Sampling at the suction tank
- Treatment and storage of the samples in the on-site laboratory

Volume

- Obligatory to collect the following samples (see Table 1):
  a) 100 ml drilling fluid hourly for tracer measurement
  b) 100 ml drilling fluid daily (and input water when used) for storage (in a PE bottle)
  c) 1,000 ml drilling fluid daily (and input water when used) for major component analysis
  d) 1,000 ml drilling fluid every 100 mabh drilling for stable isotope analysis
  e) 20 litres drilling fluid every 100 mabh drilling for back-up storage (in a PE tank)

1.3 Chemical analysis of drilling fluid

Methodology

- Analytical constituents and methods listed in Table 1 for physico-chemical parameters, tracers, chemical components and isotopes

Timing and frequency

- Chemical analysis of the initial drilling fluid to be done before drilling
- Chemical analysis of the circulated drilling fluid to be done hourly, daily and every 100 mabh drilling; in case of continuous (24 hours) drilling, sampling to be scheduled at night and chemical analysis in the daytime
- In case of the preparation of additional drilling fluid with fresh water, chemical analysis of the input water is to be performed on the same day of its sampling

Place

- Measurement of physico-chemical parameters and tracer concentrations and major component analysis in the on-site laboratory
- Isotope analysis in the off-site laboratory

Quality assurance

- Charge balance to be confirmed within a permissible range of ±5 %; in case of the charge balance over the ±5 % range, reanalysis to be required; still over the ±5 % range after the reanalysis, a cause for charge imbalance to be studied to as much extent as possible
- Accuracy and precision of the analytical techniques employed to be evaluated; standard materials to be analysed regularly in the course of the sample analyses; calibration curves to be established in advance for each of the analytical campaigns
- In case the analytical results being out of trends or far inconsistent with the predicted values, reanalysis to be performed

2 Characterisation of Groundwater Chemistry

Background

- Necessary to sample *in situ* groundwater; for sampling, the concentrations of tracers and major chemical components and the physico-chemical parameters of the sampled waters to be determined periodically; sampling to be started ideally when the tracer concentrations becoming below 1 % and the physico-chemical parameters stable
- Based on the linear correlation between the concentrations of tracers and major chemical components of the sampled waters, the *in situ* (or initial) groundwater chemical composition to be back calculated by eliminating contamination with the drilling fluid

- Suitable and/or practicable sampling methods to be selected considering the following issues; advantage and disadvantage of each method to be assessed:
  a) local hydraulic/hydrochemical/geothermal conditions
  b) priority of groundwater sampling over the whole programme
  c) applicability/availability of equipment
  d) time/budget constraints
- Preferable to apply batch sampling with an air-tight bottle (*eg* MP sampler) for maintaining the *in situ* anaerobic and pressure conditions of groundwater; physico-chemical parameters to be measured *in situ* by a down-hole equipment if applicable
- Convenient to employ continuous sampling using a submersible pump during a hydraulic test campaign for sampling a large amount of groundwater quickly; however, impossible to maintain the *in situ* anaerobic and pressure conditions of groundwater
- In case of artesian conditions *in situ*, naturally flowing groundwater to be sampled directly on the surface
- Chemical analysis of the groundwater samples to be conducted soon after sampling

2.1 Continuous sampling and treatment of groundwater

Methodology

1) Attachment of a flow cell to the flow line off the hydraulic test equipment for monitoring physico-chemical parameters under anaerobic conditions at the beginning of the pumping test
2) Continuous monitoring of the physico-chemical parameters of pumped water during the pumping test; flow rates and the total volume of the pumped water are also to be continuously monitored on-site
3) Start of *in situ* groundwater sampling campaign when the tracer concentrations becoming below 1 % and the physico-chemical parameters stable
4) Cleaning of sample bottles by diluted nitric acid, de-ionised water and ultra pure water in the on-site laboratory
5) Washing of the cleaned sample bottles with the small amount of the pumped water three times and filling of the bottles with the pumped water directly from the flow line; sampling to be done at the interval defined based on flow rate, interval volume and time available
6) Chemical treatment of the samples for ^{14}C and ^{34}S analyses only in the on-site laboratory as follows;
   a) 5N-NaOH (10 ml) and 2N-$SrCl_2$ (10 ml) to be added to the sample (1,000 ml) to induce $SrCO_3$ precipitation for the ^{14}C analysis
   b) 5N-NaOH (1 ml) and 1N-$(CH_3COO)_2Zn$ (1.5 ml) to be added to the sample (1,000 ml) to induce ZnS precipitation for the ^{34}S analysis
7) Quick observation of the water samples, in the on-site laboratory, for major component analysis; the following items to be checked and described:
   a) colour
   b) smell
   c) bubbles
   d) suspension
   e) precipitation
8) Labelling of the sample bottles with the following information:
   a) borehole number
   b) sample number
   c) sampling date and time
   d) sampling depth
   e) name of sampling person
   f) quick observation results

9) Transport of the samples to the off-site laboratory in the specified manner soon after the treatment of the samples; storage of the remaining samples except for back-up ones in the refrigerator in the on-site laboratory until chemical analysis (see 2.2 for details); back-up samples to be stored up at room temperature in the on-site storage room to avoid direct sun light

Timing

- Sampling of *in situ* groundwater to be started ideally when the tracer concentrations becoming below 1 % and the physico-chemical parameters stable
- In case the tracer concentration not decreasing sufficiently or the sufficient removal of the drilling fluid not expecting within the time available for sampling owing to large contamination with the drilling fluid, sampling to be started; *in situ* groundwater chemistry to be estimated by back calculations

Place

- Batch sampling *in situ* at the test interval in the borehole
- Continuous sampling at the borehole mouse on the surface
- Treatment of the samples in the on-site laboratory
- Storage of the samples in the on-site laboratory and storage room

Volume

- Obligatory to collect the following groundwater samples:
  a) 20~50 ml for gas analysis (in a special glass bottle)
  b) 1,000 ml for major component analysis (in a PE bottle)
  c) 1,000 ml for minor component analysis (in a Teflon® bottle)
  d) 1,000 ml for H, D analysis (in a PE bottle)
  e) 1,000 ml for ^{16}O, ^{18}O analysis (in a PE bottle)
  f) 1,000 ml for ^{13}C analysis (in a glass bottle)
  g) 1,000 ml for ^{14}C analysis (in a glass bottle)
  h) 1,000 ml for ^{34}Sr analysis (in a PE bottle)
  i) 5,000 ml for ^{36}Cl analysis (in a PE bottle)
  j) 20 litres for U-series nuclides analysis (in a PE tank, if necessary)
  k) 20 litres for back-up storage (in a PE tank)

2.2 Chemical analysis of groundwater

Methodology

- Analytical constituents and methods listed in Table 1 for physico-chemical parameters, tracers, major/minor components, isotopes and gases; detailed analytical methods to be defined and documented in advance

Timing

- Measurement of physico-chemical parameters and tracer concentrations soon after sampling on-site
- Chemical analysis of the *in situ* groundwater to be done soon after the sample delivery to the off-site laboratory

Place

- Measurement of physico-chemical parameters and tracer concentrations in the on-site laboratory
- Chemical analyses for major/minor components, isotopes and gases in the off-site laboratory

Quality assurance

- Charge balance to be confirmed within a permissible range of ±5 %; in case of the charge balance over the ±5 % range, reanalysis to be required; still over the ±5 % range after the reanalysis, a cause for charge imbalance to be studied to as much extent as possible

- Accuracy and precision of the analytical techniques employed to be evaluated; standard materials to be analysed regularly in the course of the sample analyses; calibration curves to be established in advance for each of the analytical campaigns
- In case the analytical results being out of trends or far inconsistent with the predicted values, reanalysis to be performed

3 Characterisation of Surface Water Chemistry

Background

- Necessary to sample precipitation, river water and soil water as surface water for providing necessary information for local hydrochemical interpretation
- In case the river or soil water being used as the drilling fluid, sampling and chemical analysis of the water samples to be performed periodically
- Chemical analysis of the surface water samples to be conducted soon after sampling

3.1 Sampling and treatment of surface water

Methodology

1) Cleaning of sample tank and bottles by diluted nitric acid, de-ionised water and ultra pure water in the off-site laboratory
2) Collection of precipitation with the cleaned PE tank for a month; sampling to be done avoiding direct sun light
3) Installation of soil water sampling system (BAT system) into a shallow borehole; soil water to be sampled by the system
4) Washing of the cleaned sample bottles with the small amount of river or soil water three times and filling of the bottles with the water directly using a PE dipper or a BAT sampler respectively
5) Chemical treatment of the samples for ^{14}C and ^{34}S analyses only at the sampling site as follows;
   a) 5N-NaOH (10 ml) and 2N-$SrCl_2$ (10 ml) to be added to the sample (1,000 ml) to induce $SrCO_3$ precipitation for the ^{14}C analysis
   b) 5N-NaOH (1 ml) and 1N-$(CH_3COO)_2Zn$ (1.5 ml) to be added to the sample (1,000 ml) to induce ZnS precipitation for the ^{34}S analysis
6) Quick observation of the water samples, at the sampling site, for major component analysis; the following items to be checked and described:
   a) colour
   b) smell
   c) bubbles
   d) suspension
   e) precipitation
7) Labelling of the sample bottles with the following information:
   a) sampling location
   b) sample number
   c) sampling date and time
   d) name of sampling person
   e) quick observation results
8) Transport of the samples to the off-site laboratory in the specified manner soon after the treatment of the samples; storage of the remaining samples except for back-up ones in the refrigerator in the on-site laboratory until chemical analysis (see 3.2 for details); back-up samples to be stored up at room temperature in the on-site storage room to avoid direct sun light

Timing and interval

- Sampling of precipitation, river water and soil water to be done every month for characterising the seasonal variation of their chemistries
- In case of the preparation of additional drilling fluid with fresh water (*eg* river water), the input water also to be sampled for both chemical analysis and storage

Place

- Precipitation sampling on-site on the surface
- River water sampling at the defined sampling points along the river
- Batch sampling *in situ* in the shallow borehole
- Treatment of the samples at the sampling site
- Storage of the samples in the on-site laboratory and storage room

Volume

- Obligatory to collect the following groundwater samples:
  a) 1,000 ml for major component analysis (in a PE bottle)
  b) 1,000 ml for minor component analysis (in a Teflon® bottle)
  c) 1,000 ml for H, D analysis (in a PE bottle)
  d) 1,000 ml for ^{16}O, ^{18}O analysis (in a PE bottle)
  e) 1,000 ml for ^{13}C analysis (in a glass bottle)
  f) 1,000 ml for ^{14}C analysis (in a glass bottle)
  g) 1,000 ml for ^{34}Sr analysis (in a PE bottle, if necessary)
  h) 5,000 ml for ^{36}Cl analysis (in a PE bottle, if necessary)
  i) 20 litres for back-up storage (in a PE tank)

3.2 Chemical analysis of surface water

Methodology

- Analytical constituents and methods listed in Table 1 for physico-chemical parameters, major/minor components, isotopes and gases; detailed analytical methods to be defined and documented in advance

Timing and interval

- Measurement of physico-chemical parameters soon after sampling
- Chemical analysis of the surface water to be done soon after the sample delivery to the off-site laboratory

Place

- Measurement of physico-chemical parameters and tracer concentrations in the on-site laboratory
- Chemical analyses for major/minor components, isotopes and gases in the off-site laboratory

Quality assurance

- Charge balance to be confirmed within a permissible range of ±5 %; in case of the charge balance over the ±5 % range, reanalysis to be required; still over the ±5 % range after the reanalysis, a cause for charge imbalance to be studied to as much extent as possible
- Accuracy and precision of the analytical techniques employed to be evaluated; standard materials to be analysed regularly in the course of the sample analyses; calibration curves to be established in advance for each of the analytical campaigns
- In case the analytical results being out of trends or far inconsistent with the predicted values, reanalysis to be performed

Table 1: Analytical Constituents, Methods and Frequency

Constituents	Methods*	Frequency**				
		Fresh Water for Drilling Fluid	Drilling Fluid during Drilling	Outflow during Pumping	Groundwater	Surface Water
Tracers						
Uranine, Amino G Acid, Na-Naphtionate	FL	–	B	B	B	–
Physico-chemical Parameters						
pH	PR	D	A	A	A	F
Eh	PR	–	B	A	A	F
Electrical Conductivity (EC)	PR	D	A	A	A	F
Dissolved Oxygen (DO)	PR	D	B	A	A	F
Temperature	PR	D	A	A	A	F
Major Components						
Sodium (Na^+)	IC	D	D	C	F	F
Potassium (K^+)	IC	D	D	C	F	F
Ammonium (NH_4^+)	IC	–	–	–	F	F
Magnesium (Mg^{2+})	IC	D	D	C	F	F
Calcium (Ca^{2+})	IC	D	D	C	F	F
Manganese (Mn^{2+})	CM, ICP-MS	–	–	–	F	F
Total Iron (T-Fe)	CM	D	D	C	F	F
Iron (Fe^{2+})	CM	–	–	–	F	F
Aluminium (Al)	CM, ICP-MS	D	D	–	F	F
Uranium (U)	ICP-MS	–	–	–	F	F
Fluoride (F^-)	IC	D	D	C	F	F
Chloride (Cl^-)	IC	D	D	C	F	F
Bromide (Br^-)	CM	D	D	C	F	F
Iodine (I^-)	IC	D	D	C	F	F
Nitrate (NO_3^-)	IC	D	D	C	F	F
Nitrite (NO_2^-)	IC	–	–	–	F	F
Sulphate (SO_4^{2-})	IC	D	D	C	F	F
Sulphide (S^{2-})	CM	D	D	–	F	F
Phosphate (PO_4^{3-})	IC	D	D	–	F	F
Silica (H_2SiO_3)	CM	D	D	C	F	F
Alkalinity	TI	D	D	C	F	F
Total Inorganic Carbon (TIC)	IA	D	D	C	F	F
Total Organic Carbon (TOC)	IA	–	–	–	F	F
Minor Components						
Titanium (Ti)	ICP-MS	–	–	–	F	F
Cobalt (Co)	ICP-MS	–	–	–	F	F
Copper (Cu)	ICP-MS	–	–	–	F	F
Zinc (Zn)	ICP-MS	–	–	–	F	F
Strontium (Sr)	ICP-MS	–	–	–	F	F
Yttrium (Y)	ICP-MS	–	–	–	F	F
Zirconium (Zr)	ICP-MS	–	–	–	F	F
Tin (Sn)	ICP-MS	–	–	–	F	F
Caesium (Cs)	ICP-MS	–	–	–	F	F
Tungsten (W)	ICP-MS	–	–	–	F	F
Thorium (Th)	ICP-MS	–	–	–	F	F
Rare Earth Elements (REEs)	ICP-MS	–	–	–	F	F
Isotopes						
Deuterium (^2H)	MS	E	E	C	F	F
Tritium (^3H)	SC	E	E	C	F	F
Oxygen-18 (^{18}O)	MS	E	E	C	F	F
Carbon-13/-14 (^{13}C, ^{14}C)	AMS	E	E	–	F	F
Sulphur-34 (^{34}S)	AMS	–	–	–	F	(F)
Chlorine-36 (^{36}Cl)	AMS	–	–	–	F	(F)
U-series nuclides	AS	–	–	–	(F)	–
Gases						
H_2, N_2, CH_4, CO_2, He, Ar, H_2S	GC	–	–	–	F	–

*Methods
AMS: Accelerator mass spectrometry, AS: α-spectrometry, CM: Colorimetry, FL: Fluorometry, GC: Gas chromatography, IA: Infrared absorption spectrometry, IC: Ion chromatography, ICP-MS: Inductively coupled plasma mass spectrometry, MS: Mass spectrometry, PR: Measurement with a probe, SC: Scintillation counting, TI: Titration

**Frequency
A: Continuously, B: Hourly, C: Hourly ~ Daily, D: Daily, E: Every 100 mabh drilling, F: At the end of sampling

Appendix 6: Laboratory water sample treatment/analysis protocols at MIU

Laboratory Water Sample Treatment/Analysis Protocols at MIU

Kunio Ota, with contribution from M Asai

This note summarises the work protocols applied to the treatment and analysis of water samples in the laboratory during the borehole investigations based around the Mizunami Underground Research Laboratory (MIU). The applicability of the procedures described below was confirmed during these investigations.

1 Treatment of water samples

1.1 Samples for tracer measurement

Pressurise 100 ml of the water sample through a 0.45 μm membrane filter. Use the filtrate for tracer measurement. Store the remaining unfiltered water sample in the refrigerator until further measurement is required.

1.2 Samples for chemical analysis

- **Drilling fluid, input water and outflow**

Following cleaning and rinsing a 0.45 μm membrane filter, place it in a holder and pressurise 1,000 ml water sample through the filter. Use the filtrate for chemical analysis.

- **Groundwater and surface water**

Following cleaning and rinsing a 0.45 μm membrane filter, place it in a holder and pressurise 1,000 ml water sample through the filter.

For Na^+, K^+, NH_4^+, Mg^{2+}, Ca^{2+}, Mn^{2+}, Fe^{2+}, T-Fe, Al, Cl^-, Br^-, I^-, NO_3^-, NO_2^-, SO_4^{2-}, PO_4^{3-}, H_2SiO_3, TC, IC

Use 500 ml of the filtrate for analysis.

For Mn^{2+}, T-Fe, Al by ICP-MS

Draw off 100 ml of the filtrate and syringe the sub-sample into a 250 ml Teflon® bottle. Add 10 ml of HNO_3 (1+1) and swirl to mix.

For S^{2-}

Draw off 250 ml of the filtrate and syringe the sub-sample into a 300 ml PE bottle. Add 5 ml of 20 % NaOH solution and swirl to mix.

For dissolved gases

Fill completely a 20 ~ 50 ml gas-tight glass bottle with the filtrate and seal it tightly.

Following cleaning and rinsing a 0.45 μm membrane filter, place it in a holder and pressurise 1,000 ml water sample through the filter.

For F^-

Transfer the sufficient volume of the sub-sample into a 100 ml distillation flask. Heat and evaporate the sub-sample to about 30 ml. Rinse the inside wall of the flask out with 10 ml of deionised water. Heat the distillation flask to the liquid temperature of around 140 °C, generating the steam. Remove a cooler and a check valve. Rinse out the inner tube of the cooler and the inside and outside of the check valve with a small amount of deionised water. The washing is also added into the flask. Then add deionised water up to the fixed volume of 100 ml.

For Ti, Co, Cu, Zn, Sr, Y, Zr, Sn, Cs, W, Th, U

Add 1 ml of concentrated HNO_3 to 500 ml of the filtrate in a 500 ml Teflon® bottle.

2 Analysis of water samples

2.1 Tracer measurement

Uranine by fluorometry

- **Drilling fluid and outflow**

Transfer 5 ml of the filtrate into a 50 ml volumetric flask, add 5 ml of buffer solution (pH 9) and fill the flask with deionised water to the fixed volume of 50 ml using the Eppendorf® pipette. Measure the fluorescence maxima. Uranine concentration in the water sample is calculated based on a calibration curve previously established.

- **Groundwater and surface water**

Add 5 ml of buffer solution (pH 9) into a 50 ml volumetric flask and transfer 45 ml of the filtrate to the fixed volume of 50 ml using the Eppendorf® pipette. Measure the fluorescence maxima. Uranine concentration in the water sample is calculated based on a calibration curve previously established.

Amino G acid by fluorometry

- **Drilling fluid and outflow**

Transfer 1 ml of the filtrate into a 50 ml volumetric flask and fill the flask with deionised water to the fixed volume of 50 ml using the Eppendorf® pipette. Measure the fluorescence maxima. Amino G acid concentration in the water sample is derived from a calibration curve previously established.

- **Groundwater and surface water**

Fill a 50 ml of volumetric flask with 50 ml of the filtrate using the Eppendorf® pipette. Measure the fluorescence maxima. Amino G acid concentration in the water sample is derived from a calibration curve previously established.

2.2 Chemical analysis for major components

Na^+, K^+, NH_4^+, Mg^{2+}, Ca^{2+} by ion chromatography (JIS K0102 42.5, 48.3 and 49.3)

Use the filtrate for the determination of each cation concentration by ion chromatography.

Mn^{2+} by colorimetry (JIS K0102 56.1 Compliance)

Syringe the sufficient volume of the filtrate into a 50 ml colorimetric tube. Add 10 ml of H_2SO_4 (1+1), 1 ml of H_3PO_4 and KIO_4 (potassium periodate) and swirl to mix. Place the tube in a boiling water bath and heat it for 30 minutes to allow for colour development. Syringe a portion of the sub-sample into a 50 mm absorption cell. Measure the absorbance of the sample with respect to the blank at a wavelength of around 525 nm and 545 nm. Manganese concentration in the water sample is derived from a calibration curve previously established.

Mn^{2+} by ICP-MS (JIS K0102 56.1)

Draw off 30 ml of the pre-treated sub-sample from the Teflon® bottle and syringe it into a Teflon® beaker. Measure the sub-sample weight and add 300 ml of HNO_3. Heat the sub-sample for over 10 minutes and allow it to cool. Dilute with deionised water to the fixed volume of 30 ml. Measure the atomic mass numbers for the sub-sample with respect to the blank by ICP-MS. Manganese concentration in the water sample is derived from a calibration curve previously established.

Fe^{2+} by colorimetry (JIS K0101 60.1)

Syringe the sufficient volume of the filtrate into a 50 ml colorimetric tube. Add 2 ml of HCl (1+1) and 1 ml of $C_{12}H_8N_2$ (1, 10-phenanthroline) solution (2.6 g l^{-1}) and swirl to mix. Add 5 ml of CH_3COONH_4 (ammonium acetate) solution (500 g l^{-1}). Dilute with deionised water up to the marked line and leave it for about 20 minutes. Syringe a portion of the sub-sample into a 50 mm absorption cell. Measure the absorbance of the sub-sample with respect to a blank at a wavelength of 510 nm. Iron (II) concentration in the water sample is derived from a calibration curve previously established.

Total Fe by colorimetry (JIS K0101 60.1)

Syringe the sufficient volume of the filtrate into a 50 ml colorimetric tube. Add 2 ml of HCl (1+1), 0.5 ml of 10% ClH_4NO (hydroxylammonium chloride) solution and 1 ml of $C_{12}H_8N_2$ (1, 10-phenanthroline) solution (2.6 g l^{-1}) and swirl to mix. And add 5 ml of CH_3COONH_4 (ammonium acetate) solution (500 g l^{-1}). Dilute with deionised water up to the marked line and leave it for about 20 minutes. Syringe a portion of the sub-sample into a 50 mm absorption cell. Measure the absorbance of the sub-sample with respect to a blank at a wavelength of 510 nm. Total iron concentration in the water sample is derived from a calibration curve previously established.

Total Fe by ETAAS (JIS K0101 58.4)

Draw off 25 ml of the pre-treated sub-sample from the Teflon® bottle and syringe it into a Teflon® beaker. Heat the sub-sample and then allow it to cool. Dilute with deionised water to the fixed volume of 25 ml. Measure Fe by ETAAS (electrothermal atomic absorption spectrometry).

Al by colorimetry (Standard Methods of Analysis for Hygienic Chemists, 4.33.2, 2000)

Syringe the sufficient volume of the filtrate into a 50 ml colorimetric tube. Add 1 ml of 1 % $C_6H_8O_6$ (ascorbic acid) solution and 5 ml of acetate buffer. Dilute with deionised water up to 20 ml. Add 1 ml of 2 % $Na_2S_2O_3$ (sodium thiosulphate) solution and 2 ml of $C_{23}H_{13}Cl_2Na_3O_9S$ (chrome azurol S) solution. Dilute with deionised water up to 25 ml. Syringe a portion of the sub-sample into a 10 mm absorption cell within 10 minutes after the colour is developed. Measure the absorbance of the sub-sample with respect to a blank at a wavelength of 567.5 nm. Aluminium concentration in the water sample is derived from a calibration curve previously established.

Al by ICP-MS (JIS K0102 56.4)

Draw off 30 ml of the pre-treated sub-sample from the Teflon® bottle and syringe it into a Teflon® beaker. Measure the sub-sample weight and add 300 ml of HNO_3. Heat the sub-sample for over 10 minutes and allow it to cool. Dilute with deionised water to the fixed volume of 30 ml. Measure the atomic mass numbers for the sub-sample and a blank by ICP-MS. Aluminium concentration in the water sample is derived from a calibration curve previously established.

H_2SiO_3 by colorimetry (JIS K0101 44.1.2)

Syringe the sufficient volume of the filtrate into a 30 ml measurement cylinder with a stopper. Fill the cylinder with deionised water up to 30 ml. Add 0.6 ml of HCl (1+1) and 1.2 ml of $(NH_4)_6Mo_7O_{24}\cdot 4H_2O$ (ammonium molybdate tetrahydrate) solution (100 mg ml^{-1}) and swirl to mix. Leave it for about 5 minutes. Add 0.6 ml of 1% $(COOH)_2$ (oxalic acid) solution and swirl to mix. Leave it for about a minute. Add 0.6 ml of 10% $C_6H_8O_6$ (ascorbic acid) solution and swirl to mix. Leave it for about 10 minutes. Syringe a portion of the sample solution into a 10 mm absorption cell. Measure the absorbance of the sub-sample with respect to a blank at a wavelength of around 815 nm. Silica concentration in the sample is derived from a calibration curve previously established.

F^-, Cl^-, Br^-, NO_3^-, NO_2^-, SO_4^{2-} by ion chromatography (Table 6 attached to Notification No. 59 of the Ministry of the Environment, JIS K0102 35.3, 41.3, 43.1 and 43.2)

Use the filtrate for the determination of each anion concentration by ion chromatography.

F^- by colorimetry (JIS K0102.34)

i) Syringe the sufficient volume (smaller than 35 ml) of the sub-sample (NB this should contain 3.5 to 50 μg F^-) into a 50 ml volumetric flask (A).
ii) Syringe 35 ml of deionised water into another 50 ml volumetric flask (B).
iii) Add 5 ml of Alfusone® solution and 10 ml of acetone into both A and B. Dilute with deionised water up to the fixed volume of 50 ml and swirl to mix. Leave both A and B for about 1 hour. 'Solution B' is to be used as the control sample
iv) Transfer a portion of each solution into an absorption cell. Measure the absorbance of each solution with respect to the blank at a wavelength of 620 nm.
v) F^- concentration in the water sample is derived from a calibration curve previously established.

PO_4^{3-}, I^- by ion chromatography (JIS K0102 46.1.1 and 35.3)

Use the filtrate for the determination of each anion concentration by ion chromatography.

S^{2-} by colorimetry (JIS K0102 39.1)

Draw off the sufficient volume of the pre-treated sub-sample from a PE bottle and syringe it into a 50 ml colorimetric tube. Add 1 ml of H_2SO_4 (1+1) and dilute with deionised water up to 50 ml. Add 0.5 ml of $H_2NC_6H_4N(CH_3)_2$ (*N*,*N*-dimethyl-*p*-phenylenediamine) and swirl to mix. Also add 1 ml of $FeCl_3$ and swirl to mix. Leave it for a minute. Add 1.5 ml of $(NH_4)_2HPO_4$ (diammonium hydrogenphosphate) and swirl to mix. Leave it for 5 minutes. Syringe the sub-sample into a 50 ml of absorption cell. Measure the absorbance of the sample with respect to the blank at a wavelength of around 670 nm. Sulphide ion concentration in the sample is derived from a calibration curve previously established.

Alkalinity by titration (JIS K0101 13.1)

Transfer 100 ml of the sub-sample into a 200 ml beaker using a whole pipette. Place the beaker on the magnetic stirrer and gently stir it. While stirring, titrate it by adding 0.01 mol l^{-1} H_2SO_4 until pH value reaches at pH 4.8. Glass-electrode pH meter should be used. Total the whole volume of 0.01 mol l^{-1} H_2SO_4 required for the titration and calculate the alkalinity (pH 4.8) in the sample by the following equation:

Alkalinity (meq ml^{-1}) = a x f x 1/50 x 1000/v

where a: total volume of 0.01mol l^{-1} H_2SO_4 required for the titration (ml)
f: factor
v: sample volume (ml)

TC, IC by infrared absorption spectrometry (JIS K0101 20.1)

Syringe the filtrate into a TC combustion tube and measure the value. Repeat the measurement three times and calculate the average TC value. Syringe the filtrate into an IC combustion tube and measure the value. Repeat the measurement three times and calculate the average IC value. The TOC value is calculated by the following equation:

TOC = TC – IC

2.3 Chemical analysis for minor components

Ti, Co, Cu, Zn, Sn, Th, U by ICP-MS (chelating resin pre-concentration method)

Treat the sub-sample by the chelating resin pre-concentration method. Measure the sample mass and strength by optimised ICP-MS conditions. The each concentration in the sample is derived from a corresponding calibration curve previously established.

Sr, Cs, W by ICP-MS (direct sample introduction method)

Apply the direct sample introduction method to measure the sample mass and strength by ICP-MS directly. The each concentration in the sub-sample is derived from a corresponding calibration curve previously established.

2.4 Gas analysis

a) Attach gas sampling containers to a sample container

Prepare a 1 litre bulk sample container (1 litre dissolved gas collecting pressurised container) on-site. Attach two 50 ml gas sampling containers (50 ml gas sampling pressurised container) to it.

b) Evacuate inside the gas sampling containers

Connect the attached 50 ml gas sampling containers to the canister auto-cleaning system. Evacuate the containers and fill it with inert gas. Repeat 9 times to have the containers cleaned and completely evacuated.

c) Reducing pressure inside of the bulk sample container

Open the valves connected between the 1 litre bulk sample container and 50 ml gas sampling containers. Open the valve attached to the bulk sample container first to reduce the pressure inside of the bulk sample container.

d) Ultrasonic wave irradiation

Apply the ultrasonic wave irradiation to the attached 1 litre bulk sample container for 60 minutes to generate dissolved gases. Collect the gases into the 50 ml gas sampling containers.

e) Completion process

Complete collecting gas, close the valves.

f) Uninstalling the sample gas containers

Disconnect the 50 ml gas sampling containers from the 1 litre bulk sample container and separate both 50 ml gas sampling containers.

g) Adding pressure into the sample gas containers

To extract the sample from the 50 ml gas sampling containers, ensure positive pressure in the containers. Using the canister auto-cleaning system, evacuate the fluid tube. Open the valves until pressure reaches 3 atm in the 50 ml sample gas containers. For adding pressure, He and Ar gases are respectively applied to the containers.

h) H_2, He, O_2, N_2, CH_4, CO, CO_2, Ar, H_2S analysis

Using a 5 ml gas tight syringe, transfer 1 ml of the sampled gas from the gas sampling containers and inject into the gas chromatography.

2.5 Isotope analysis

a) Preparation of samples for carbon isotopes

Leave the water sample until $SrCO_3$ completely precipitates. Clean the $SrCO_3$ precipitate with CO_2 free water in the CO_2 free atmosphere and dry. Dissolve $SrCO_3$. Remove the vapour in the CO_2 with cryogens (dry ice and acetone) or liquid nitrogen. Then purify the dissolved $SrCO_3$. For the sample for $^{14}C/^{12}C$ analysis, heat the purified CO_2 and set the graphite target of the accelerator mass spectrometry. A portion of this purified CO_2 is also used for $^{13}C/^{12}C$ analysis.

b) Carbon isotope measurement

For $^{14}C/^{12}C$ analysis, transfer the sub-sample to the accelerator mass spectrometry ion source. Irradiate it on a caesium target. Alternately measure the sample and the standard substance and calculate the $^{14}C/^{12}C$ ratio. For $^{13}C/^{12}C$ analysis, alternately inject the sub-sample and the standard substance, CO_2 gas, to the accelerator mass spectrometry. Then calculate the $^{13}C/^{12}C$ ratio.

3 Others

3.1 Sample waste

Prepare sample waste tank (20 litres PE tank) in the laboratory. Collect and store the sample waste in the tank. When the tank is filled up, dispose the sample waste as an industry waste.

3.2 Countermeasure against failure of analytical equipment

When a trouble occurred to the spectrophotometer on the site, deal it with the spare equipment. In case other equipment had any problem with measurement, send the samples to the contractor’s off-site laboratory and perform chemical analyses there. Contact the equipment producer and request to fix the equipment immediately.

3.3 Quality management

Use the following check sheets, observe the all performance and manage the data quality.

装置・機器チェックシート/Work check sheet for equipment & device

確認/Confirmation		
JAEA	JV	

平成 年 月 日/____/____/____
day month year

日付/Date	1	2	3	4	5	6	7	8	9	10	11	12	13	14	15	16	17	18	19	20	21	22	23	24	25	26	27	28	29	30	31
空調/Air conditioner																															
冷蔵庫 1/Refrigerator 1																															
冷蔵庫 2/Refrigerator 2																															
超純水装置/Water purification device																															
イオンクロマトグラフ装置(陰イオン) Ion chromatograph for anions																															
イオンクロマトグラフ装置(I^-, PO_4^{3-}) Ion chromatograph for I^- and PO_4^{3-}																															
イオンクロマトグラフ装置(陽イオン) Ion chromatograph for cations																															
蛍光分光光度計 Fluorescence Spectrophotometer																															
紫外可視分光光度計 UV/Visible Spectrophotometer																															
有機炭素分析装置/TOC Analyser																															
pH 計/pH meter																															
DO 計/DO meter																															
EC 計/EC meter																															
ORP 計/ORP meter																															
確認者/Checked by																															

分析操作手順確認表（その 1）/Process check sheet for chemical analysis no 1

分析日/Analysis date:
分析者/Analyst:
試料名/Sample number:

確認/Confirmation		
JAEA	JV	

測定項目 Constituents	添加試薬・操作 Reagent & process	使用量 Amount	確認 Checked by	備考 Remarks
マンガン/Mn	硫酸(1+1)/H_2SO_4 (1+1)			
	リン酸/H_3PO_4			
	過ヨウ素酸カリウム/Potassium periodate			
	30 分加熱/Heating for 30 minutes			
全鉄/Total Fe	塩酸(1+1)/HCl (1+1)			
	10% 塩酸ヒドロキシルアンモニウム溶液 10 % Hydroxylammonium chloride solution			
	1, 10−フェナントロリン溶液(2. 6 g l^{-1}) 1, 10-Phenanthroline solution (2.6 g l^{-1})			
	酢酸アンモニウム溶液(500 g l^{-1}) Ammonium acetate solution (500 g l^{-1})			
アルミニウム/Al	1% アスコルビン酸 1 % Ascorbic acid solution			
	酢酸緩衝液/Acetate buffer			
	2% チオ硫酸ナトリウム溶液 2 % Sodium thiosulphate solution			
	クロムアズロール S/Chrome azurol S			
シリカ/Silica	塩酸(1+1)/HCl (1+1)			
	10% モリブデン酸アンモニウム溶液 10 % Ammonium molybdate tetrahydrate sol			
	1% シュウ酸/1 % Oxalic acid			
	10% アスコルビン酸 10 % Ascorbic acid solution			
アルカリ度/Alkalinity	試料量/Sample volume			
	0. 01 mol l^{-1} 硫酸/0.01 mol l^{-1} H_2SO_4			
イオンクロマトグラフ (陽イオン) IC for cations	試料ろ過/Sample filtration			
	注入量/Injection volume			
	ベースラインの安定/Stability of baseline			
イオンクロマトグラフ (陰イオン) IC for anions	試料ろ過/Sample filtration			
	注入量/Injection volume			
	ベースラインの安定/Stability of baseline			

分析操作手順確認表（その 2）/Process check sheet for chemical analysis no 2

分析日/Analysis date:
分析者/Analyst:
試料名/Sample number:

確認/Confirmation		
JAEA	JV	

測定項目 Constituents	添加試薬・操作 Reagent & process	使用量 Amount	確認 Checked by	備考 Remarks
二価鉄/Fe^{2+}	加圧ろ過/Pressurised filtration			
	塩酸(1+1)/HCl (1+1)			
	1,10-フェナントロリン溶液(2.6 g l^{-1}) 1, 10-Phenanthroline solution (2.6 g l^{-1})			
	酢酸アンモニウム溶液(500 g l^{-1}) Ammonium acetate solution (500 g l^{-1})			
硫化物/S^{2-}	加圧ろ過/Pressurised filtration			
	水酸化ナトリウム溶液/NaOH solution			
	硫酸(1+1)/H_2SO_4 (1+1)			
	N,N-ジメチル-p-フェニレンジアミン *N*,*N*-Dimethyl-*p*-phenylenediamine			
	塩化鉄(Ⅲ)/$FeCl_3$			
	リン酸水素ニアンモニウム Diammonium hydrogenphosphate			
	標定/Standardisation			
イオンクロマトグラフ (I^-, PO_4^{3-}) IC for I^- and PO_4^{3-}	試料ろ過/Sample filtration			
	注入量/Injection volume			
	ベースラインの安定/Stability of baseline			
外部委託試料 Samples to off-site lab	同位体分析試料 Samples for isotope analysis			

This is a blank page.

国際単位系（SI）

表１．SI 基本単位

基本量	SI 基本単位	
	名称	記号
長さ	メートル	m
質量	キログラム	kg
時間	秒	s
電流	アンペア	A
熱力学温度	ケルビン	K
物質量	モル	mol
光度	カンデラ	cd

表２．基本単位を用いて表されるSI組立単位の例

組立量	SI 基本単位	
	名称	記号
面積	平方メートル	m^2
体積	立法メートル	m^3
速さ，速度	メートル毎秒	m/s
加速度	メートル毎秒毎秒	m/s^2
波数	毎メートル	m^{-1}
密度，質量密度	キログラム毎立方メートル	kg/m^3
面積密度	キログラム毎平方メートル	kg/m^2
比体積	立方メートル毎キログラム	m^3/kg
電流密度	アンペア毎平方メートル	A/m^2
磁界の強さ	アンペア毎メートル	A/m
量濃度(a)，濃度	モル毎立方メートル	mol/m^3
質量濃度	キログラム毎立法メートル	kg/m^3
輝度	カンデラ毎平方メートル	cd/m^2
屈折率(b)	（数字の） 1	1
比透磁率(b)	（数字の） 1	1

(a) 量濃度（amount concentration）は臨床化学の分野では物質濃度（substance concentration）ともよばれる。
(b) これらは無次元量あるいは次元１をもつ量であるが、そのことを表す単位記号である数字の１は通常は表記しない。

表３．固有の名称と記号で表されるSI組立単位

組立量	SI 組立単位			
	名称	記号	他のSI単位による表し方	SI基本単位による表し方
平面角	ラジアン(b)	rad	1 (b)	m/m
立体角	ステラジアン(b)	sr(c)	1 (b)	m^2/m^2
周波数	ヘルツ(d)	Hz		s^{-1}
力	ニュートン	N		m kg s^{-2}
圧力，応力	パスカル	Pa	N/m^2	m^{-1} kg s^{-2}
エネルギー，仕事，熱量	ジュール	J	N m	m^2 kg s^{-2}
仕事率，工率，放射束	ワット	W	J/s	m^2 kg s^{-3}
電荷，電気量	クーロン	C		s A
電位差（電圧），起電力	ボルト	V	W/A	m^2 kg s^{-3} A^{-1}
静電容量	ファラド	F	C/V	m^{-2} kg^{-1} s^4 A^2
電気抵抗	オーム	Ω	V/A	m^2 kg s^{-3} A^{-2}
コンダクタンス	ジーメンス	S	A/V	m^{-2} kg^{-1} s^3 A^2
磁束	ウエーバ	Wb	Vs	m^2 kg s^{-2} A^{-1}
磁束密度	テスラ	T	Wb/m^2	kg s^{-2} A^{-1}
インダクタンス	ヘンリー	H	Wb/A	m^2 kg s^{-2} A^{-2}
セルシウス温度	セルシウス度(e)	℃		K
光束	ルーメン	lm	cd sr(c)	cd
照度	ルクス	lx	lm/m^2	m^{-2} cd
放射性核種の放射能(f)	ベクレル(d)	Bq		s^{-1}
吸収線量，比エネルギー分与，カーマ	グレイ	Gy	J/kg	m^2 s^{-2}
線量当量，周辺線量当量，方向性線量当量，個人線量当量	シーベルト(g)	Sv	J/kg	m^2 s^{-2}
酸素活性	カタール	kat		s^{-1} mol

(a)SI接頭語は固有の名称と記号を持つ組立単位と組み合わせても使用できる。しかし接頭語を付した単位はもはやコヒーレントではない。
(b)ラジアンとステラジアンは数字の１に対する単位の特別な名称で、量についての情報をつたえるために使われる。実際には、使用する時には記号rad及びsrが用いられるが、習慣として組立単位としての記号である数字の１は明示されない。
(c)測光学ではステラジアンという名称と記号srを単位の表し方の中に、そのまま維持している。
(d)ヘルツは周期現象についてのみ、ベクレルは放射性核種の統計的過程についてのみ使用される。
(e)セルシウス度はケルビンの特別な名称で、セルシウス温度を表すために使用される。セルシウス度とケルビンの単位の大きさは同一である。したがって、温度差や温度間隔を表す数値はどちらの単位で表しても同じである。
(f)放射性核種の放射能（activity referred to a radionuclide）は、しばしば誤った用語で"radioactivity"と記される。
(g)単位シーベルト（PV,2002,70,205）についてはCIPM勧告2（CI-2002）を参照。

表４．単位の中に固有の名称と記号を含むSI組立単位の例

組立量	SI 組立単位		
	名称	記号	SI 基本単位による表し方
粘度	パスカル秒	Pa s	m^{-1} kg s^{-1}
力のモーメント	ニュートンメートル	N m	m^2 kg s^{-2}
表面張力	ニュートン毎メートル	N/m	kg s^{-2}
角速度	ラジアン毎秒	rad/s	m m^{-1} s^{-1}=s^{-1}
角加速度	ラジアン毎秒毎秒	rad/s^2	m m^{-1} s^{-2}=s^{-2}
熱流密度，放射照度	ワット毎平方メートル	W/m^2	kg s^{-3}
熱容量，エントロピー	ジュール毎ケルビン	J/K	m^2 kg s^{-2} K^{-1}
比熱容量，比エントロピー	ジュール毎キログラム毎ケルビン	J/(kg K)	m^2 s^{-2} K^{-1}
比エネルギー	ジュール毎キログラム	J/kg	m^2 s^{-2}
熱伝導率	ワット毎メートル毎ケルビン	W/(m K)	m kg s^{-3} K^{-1}
体積エネルギー	ジュール毎立方メートル	J/m^3	m^{-1} kg s^{-2}
電界の強さ	ボルト毎メートル	V/m	m kg s^{-3} A^{-1}
電荷密度	クーロン毎立方メートル	C/m^3	m^{-3} sA
表面電荷	クーロン毎平方メートル	C/m^2	m^{-2} sA
電束密度，電気変位	クーロン毎平方メートル	C/m^2	m^{-2} sA
誘電率	ファラド毎メートル	F/m	m^{-3} kg^{-1} s^4 A^2
透磁率	ヘンリー毎メートル	H/m	m kg s^{-2} A^{-2}
モルエネルギー	ジュール毎モル	J/mol	m^2 kg s^{-2} mol^{-1}
モルエントロピー，モル熱容量	ジュール毎モル毎ケルビン	J/(mol K)	m^2 kg s^{-2} K^{-1} mol^{-1}
照射線量（X線及びγ線）	クーロン毎キログラム	C/kg	kg^{-1} sA
吸収線量率	グレイ毎秒	Gy/s	m^2 s^{-3}
放射強度	ワット毎ステラジアン	W/sr	m^4 m^{-2} kg s^{-3}=m^2 kg s^{-3}
放射輝度	ワット毎平方メートル毎ステラジアン	$W/(m^2$ sr)	m^2 m^{-2} kg s^{-3}=kg s^{-3}
酵素活性濃度	カタール毎立方メートル	kat/m^3	m^{-3} s^{-1} mol

表５．SI 接頭語

乗数	接頭語	記号	乗数	接頭語	記号
10^{24}	ヨタ	Y	10^{-1}	デシ	d
10^{21}	ゼタ	Z	10^{-2}	センチ	c
10^{18}	エクサ	E	10^{-3}	ミリ	m
10^{15}	ペタ	P	10^{-6}	マイクロ	μ
10^{12}	テラ	T	10^{-9}	ナノ	n
10^9	ギガ	G	10^{-12}	ピコ	p
10^6	メガ	M	10^{-15}	フェムト	f
10^3	キロ	k	10^{-18}	アト	a
10^2	ヘクト	h	10^{-21}	ゼプト	z
10^1	デカ	da	10^{-24}	ヨクト	y

表６．SIに属さないが、SIと併用される単位

名称	記号	SI 単位による値
分	min	1 min=60s
時	h	1h =60 min=3600 s
日	d	1 d=24 h=86 400 s
度	°	1°=(π/180) rad
分	’	1’=(1/60)°=(π/10800) rad
秒	”	1”=(1/60)’=(π/648000) rad
ヘクタール	ha	$1ha=1hm^2=10^4m^2$
リットル	L, l	$1L=11=1dm^3=10^3cm^3=10^{-3}m^3$
トン	t	$1t=10^3$ kg

表７．SIに属さないが、SIと併用される単位で、SI単位で表される数値が実験的に得られるもの

名称	記号	SI 単位で表される数値
電子ボルト	eV	$1eV=1.602\ 176\ 53(14)\times10^{-19}J$
ダルトン	Da	$1Da=1.660\ 538\ 86(28)\times10^{-27}kg$
統一原子質量単位	u	1u=1 Da
天文単位	ua	$1ua=1.495\ 978\ 706\ 91(6)\times10^{11}m$

表８．SIに属さないが、SIと併用されるその他の単位

名称	記号	SI 単位で表される数値
バール	bar	1 bar=0.1MPa=100kPa=10^5Pa
水銀柱ミリメートル	mmHg	1mmHg=133.322Pa
オングストローム	Å	1 Å=0.1nm=100pm=10^{-10}m
海里	M	1 M=1852m
バーン	b	$1\ b=100fm^2=(10^{-12}cm)2=10^{-28}m^2$
ノット	kn	1 kn=(1852/3600)m/s
ネーパ	Np	SI単位との数値的な関係は、対数量の定義に依存。
ベル	B	
デジベル	dB	

表９．固有の名称をもつCGS組立単位

名称	記号	SI 単位で表される数値
エルグ	erg	$1\ erg=10^{-7}$ J
ダイン	dyn	$1\ dyn=10^{-5}$N
ポアズ	P	1 P=1 dyn s cm^{-2}=0.1Pa s
ストークス	St	1 St =$1cm^2$ s^{-1}=$10^{-4}m^2$ s^{-1}
スチルブ	sb	1 sb =1cd cm^{-2}=10^4cd m^{-2}
フォト	ph	1 ph=1cd sr cm^{-2} 10^4lx
ガル	Gal	1 Gal =1cm s^{-2}=$10^{-2}ms^{-2}$
マクスウェル	Mx	1 Mx = 1G cm^2=10^{-8}Wb
ガウス	G	1 G =1Mx cm^{-2} =10^{-4}T
エルステッド(c)	Oe	1 Oe ≙ $(10^3/4\pi)$A m^{-1}

(c) ３元系のCGS単位系とSIでは直接比較できないため、等号「 ≙ 」は対応関係を示すものである。

表10．SIに属さないその他の単位の例

名称	記号	SI 単位で表される数値
キュリー	Ci	$1\ Ci=3.7\times10^{10}Bq$
レントゲン	R	$1\ R=2.58\times10^{-4}C/kg$
ラド	rad	$1\ rad=1cGy=10^{-2}Gy$
レム	rem	$1\ rem=1\ cSv=10^{-2}Sv$
ガンマ	γ	1γ=1 nT=10-9T
フェルミ		1フェルミ=1 fm=10-15m
メートル系カラット		1メートル系カラット = 200 mg = 2×10-4kg
トル	Torr	1 Torr = (101 325/760) Pa
標準大気圧	atm	1 atm = 101 325 Pa
カロリー	cal	1cal=4.1858J（「15℃」カロリー），4.1868J（「IT」カロリー）4.184J（「熱化学」カロリー）
ミクロン	μ	1 μ =1μm=10^{-6}m

（第8版，2006年改訂）

この印刷物は再生紙を使用しています